INTERNATIONAL JOURNAL FOR NUMERICAL METHODS IN ENGINEERING
Int. J. Numer. Meth. Engng 2011; **86**:1225–1276
Published online 7 April 2011 in Wiley Online Library (wileyonlinelibrary.com). DOI: 10.1002/nme.3127

Variational principles in dissipative electro-magneto-mechanics: A framework for the macro-modeling of functional materials

C. Miehe*,†, D. Rosato and B. Kiefer

Institute of Applied Mechanics, Chair I, University of Stuttgart, 70550 Stuttgart, Pfaffenwaldring 7, Germany

SUMMARY

This paper presents a general framework for the macroscopic, continuum-based formulation and numerical implementation of dissipative functional materials with electro-magneto-mechanical couplings based on *incremental variational principles*. We focus on quasi-static problems, where mechanical inertia effects and time-dependent electro-magnetic couplings are *a priori* neglected and a time-dependence enters the formulation only through a possible rate-dependent dissipative material response. The underlying variational structure of non-reversible coupled processes is related to a canonical constitutive modeling approach, often addressed to so-called standard dissipative materials. It is shown to have enormous consequences with respect to all aspects of the continuum-based modeling in macroscopic electro-magneto-mechanics. At first, the *local constitutive modeling* of the coupled dissipative response, i.e. stress, electric and magnetic fields versus strain, electric displacement and magnetic induction, is shown to be variational based, governed by incremental minimization and saddle-point principles. Next, the implications on the formulation of *boundary-value problems* are addressed, which appear in energy-based formulations as minimization principles and in enthalpy-based formulations in the form of saddle-point principles. Furthermore, the *material stability* of dissipative electro-magneto-mechanics on the macroscopic level is defined based on the convexity/concavity of incremental potentials. We provide a comprehensive outline of alternative variational structures and discuss details of their computational implementation, such as formulation of constitutive update algorithms and finite element solvers. From the viewpoint of constitutive modeling, including the understanding of the stability in coupled electro-magneto-mechanics, an *energy-based formulation* is shown to be the canonical setting. From the viewpoint of the computational convenience, an *enthalpy-based formulation* is the most convenient setting. A numerical investigation of a multiferroic composite demonstrates perspectives of the proposed framework with regard to the future design of new functional materials. Copyright © 2011 John Wiley & Sons, Ltd.

Received 1 October 2010; Revised 15 December 2010; Accepted 15 December 2010

KEY WORDS: variational methods; functional materials; multiferroic composites; electro-mechanics; magneto-mechanics; constitutive update algorithms; finite element methods for coupled problems

1. INTRODUCTION

The goal of this work is to outline a variational-based framework for dissipative functional materials with electro-magneto-mechanical couplings. The proposed *incremental variational structure* for quasi-static response serves as a unified guide to the theoretical formulation and numerical implementation of continuum problems in electro-magneto-mechanics on a macroscopic level. We develop compact constitutive statements based on *local* variational principles, which govern representative evolutions and update algorithms of internal variables. As a consequence, incremental

*Correspondence to: C. Miehe, Institute of Applied Mechanics, Chair I, University of Stuttgart, 70550 Stuttgart, Pfaffenwaldring 7, Germany.
†E-mail: christian.miehe@mechbau.uni-stuttgart.de

Copyright © 2011 John Wiley & Sons, Ltd.

boundary-value problems in quasi-static, dissipative electro-magneto-mechanics and associated finite element discretization appear in the form of compact *global* variational statements. The *macroscopic incremental stability* of coupled electro-magneto-mechanical problems is defined in terms of these variational concepts.

1.1. Modeling approaches to dissipative functional materials

The motivation for the presented work is the recent emergence of materials that possess strong electro-magneto-mechanical coupling and the resulting need for advanced constitutive modeling of such effects. These materials are often referred to as *active (or smart) materials*, i.e they exhibit coupling between mechanical output and non-mechanical input, or *(multi-)functional materials*, when they exhibit a structural and at least one additional functional property. The unique properties of multi-functional materials can be utilized in many technological applications such as the design of compact, high energy density actuators and smart structures, sensors (including chemical and bio-hazard sensors), biomedical devices, biomimetics (bionics), energy harvesting, and health monitoring and self-healing. Classical examples of *electro-mechanical coupling* are piezoelectricity and the higher order effect of electrostriction. In ferroelectric ceramics (e.g. $BiTiO_3$, PZT) one observes a highly non-linear and dissipative response with hysteresis effects caused by the switching of polarized domains on the microscale. Ferroelectrics have successfully been used in common rail systems with piezofuel injection for diesel engines and micro-positioning in printers and optical devices. Polymers whose properties or shape are controllable by electric input are known as electro-active polymers (EAP). These are used, for example, as bio-mimetic actuators, often termed 'artificial muscles' (see e.g. Bar-Cohen [1]). Materials exhibiting *magneto-mechanical coupling* include piezomagnetic (e.g. $CoFe_2O_4$) and magnetostrictive materials (e.g. Galfenol, Terfenol-D). So-called 'giant magnetostriction' is observed in ferromagnetic shape memory alloys (FSMA, i.e. Ni–Mn–Ga, Fe–Pd, Co–Ni–Al), in which, similar to the coupling mechanism in ferroelectrics, the non-linear, hysteretic macro-response is caused by the reorientation of martensitic variants and the motion of magnetic domain walls on the microscale. It is further interesting to note that composites of the abovementioned materials can possess *full electro-magneto-mechanical* coupling properties that their individual constituents do not. An example is the three-phase electro-magneto-elastic composite proposed by Lee *et al*. [2]. In this composite, piezoelectric and piezomagnetic particles are arranged in a patterned microstructure inside an elastic matrix. It is observed that the effective properties of such a composite show static electromagnetic coupling, which can be attributed to the mechanical interaction of the piezoelectric and piezomagnetic phases through the elastic matrix. The recent interest focuses on the construction of new, so-called *multiferroic composites* with strong magnetic–electric (ME) coupling, see for example Fiebig [3], Eerenstein *et al*. [4] or Nan *et al.* [5]. Section 6 of this work outlines a numerical study of such a composite.

The complex behavior of the materials described above necessitates not only the design of adequate material models, but also the formulation and solution of fully coupled boundary-value problems, especially in the context of technological applications. Theoretical frameworks for the *mechanics of electro-magnetic continua* combine extended versions of the classical balance equations of continuum mechanics with the Maxwell equations of electro-magnetics. Such frameworks have been proposed in fully relativistic versions as well as semi-relativistic approximations (where terms with factor $\dot{x}/c^2$ are neglected, and c is the speed of light in vacuo) and non-relativistic approximations (where all terms with factor $1/c^2$ are neglected). Two main aspects define these theories: (i) in the dynamic case, the transformation relations between electro-magnetic fields observed in a fixed (laboratory) frame and the effective fields observed in a (rest) frame attached to a moving material point; (ii) the modeling of field matter interactions that the body experiences when subjected to electromagnetic fields. These interactions are taken into account in the form of additional body forces, body couples and energy sources of electromagnetic nature. The three types of coupling between mechanics and electro-magnetics are thus (i) constitutive coupling effects, (ii) field matter interactions with resulting contributions in the mechanical balance equations and (iii) the geometry of deformation of the electro-magnetic domain. Pioneering work in the field of the mechanics of electromagnetic continua has been conducted by Landau and Lifshitz [6],

Copyright © 2011 John Wiley & Sons, Ltd.

DOI: 10.1002/nme

Guggenheim [7, 8], Tiersten [9], Tiersten and Tsai [10], Brown [11], Penfield and Haus [12], Coleman dill [13, 14], Truesdell and Toupin [15], Pao and Hutter [16], Hutter, Van de ven and ursescu [17], Eringen and Maugin [18–20], Maugin [21], Nowacki [22] and Kovetz [23], among others. A broad spectrum of *continuum-based material models* exhibiting electro-mechanical or magneto-mechanical coupling effects described above can be found in the literature. The recent book of Smith [24] gives an overview. The constitutive formulation of *linear piezoelectricity* is fairly standard, see for example Nowacki [22] or Ikeda [25] for reviews. The modeling of complex constitutive response of *dissipative ferro-electricity* has been addressed by Maugin and co-workers, see Bassiouny *et al*. [26–29], and in the last decade by Cocks and McMeeking [30], Kamlah and Tsakmakis [31], Kamlah and Böhle [32], Kamlah and Wang [33], Landis [34, 35], Huber and Fleck [36], McMeeking and Landis [37], Schröder and Romanowski [38], Klinkel [39], Zhang and Bhattacharya [40, 41], Su and Landis [42], Schrade *et al*. [43], among others. Models for non-linear and *hysteretic magnetostriction* have been proposed by Smith *et al.* [44], Linnemann and Klinkel [45]. Constitutive models that address the strongly magneto-mechanically coupled non-linear and hysteretic response of *ferromagnetic shape memory alloys* have been proposed by James and Wuttig [46], O'handley [47], Likhachev and Ullakko [48], Hirsinger and Lexcellent [49] and Kiefer and Lagoudas [50].

Some of the earliest work regarding the *numerical analysis* of piezoelectric problems was published by Allik and Hughes [51]. A review of piezoelectric finite element modeling is found in [52]. Geometrically linear and non-linear piezoelectric shell elements have been developed, see e.g. Klinkel and Wagner [53] and the references therein. Finite element analyses of electromechanically coupled problems for ferroelectric ceramics has for example been presented by Kamlah *et al*. [54], Schroeder and Romanowski [38], Elhadrouz *et al.* [55]. Su and Landis [42] and Schrade *et al*. [43] used coupled finite element analysis to address meso-scale problems such as ferroelectric domain evolution and pinning. Furthermore, Landis [56] and Semenov *et al*. [57] implemented vector-valued electric potential formulations as an alternative approach to the standard scalar-valued potential approach for coupled electro-mechanical problems. A hybrid finite element scheme for non-linear electromechanical problems was proposed by Ghandi and Hagood [58]. A formulation of return mapping algorithms and consistent tangents in ferro-electricity was outlined in Semenov *et al*. [59].

However, an embedding of the abovementioned continuum models, associated incremental update algorithms and finite element formulations into variational principles for dissipative solids is missing in the literature.

1.2. Incremental variational principles for a macro-modeling

This work focuses on the purely phenomenological modeling of functional materials on the macroscopic level. This covers essentially internal variable approaches to complex macroscopic hystereses effects, but excludes microscopic phase field or energy relaxation approaches to electric and magnetic domain motion, such as considered in Zhang and Bhattacharya [40] or Desimone and James [60], which are based on extended gradient-type theories including non-convex potentials. In contrast to *absolute* energy minimization concepts used in those formulations, we focus on *rate-type, incremental* variational principles. The key aspect of this work is a comprehensive outline of alternative *incremental variational principles in dissipative electro-magneto-mechanics*. The underlying variational structure of non-reversible coupled processes is related to a canonical constitutive modeling approach, often addressed to the standard dissipative materials. These are governed by only two scalar constitutive functions: the energy storage and the dissipation functions. The field equations of this class of dissipative solids may be obtained as the Euler equations of suitable defined *rate-type incremental variational principles*. We refer to the treatments of plasticity by Simó and Honein [61], Ortiz and Stainier [62], Miehe [63] and Carstensen, hackl and Mielke [64]. In the recent works of Miehe *et al.* [63, 65, 66], a variational framework for the mechanical response of solids with threshold-type dissipation functions was outlined and applied to variational-based definitions of homogenization and relaxation of dissipative solids. These variational principles may be considered as the canonically compact formulations of the boundary-value problems for

Copyright © 2011 John Wiley & Sons, Ltd.

DOI: 10.1002/nme

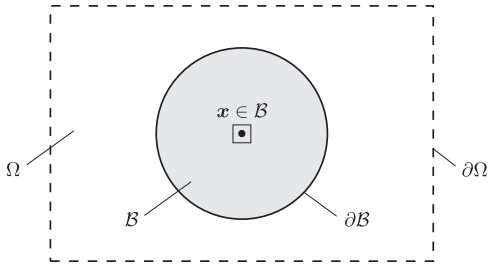

Figure 1. Local and global solid domains embedded into free space. Let $\Omega \subset \mathscr{R}^3$ denote a vacuum free space box and $\mathscr{B} \subset \Omega$ be the domain occupied by the solid. Sections 2 and 3 outline a *local*, purely macroscopic constitutive modeling of the *superimposed response* of the free space with embedded solid matter, associated with a typical volume element at $\boldsymbol{x} \in \mathscr{B}$, see Figures 2, 3 and results in Boxes 1, 2, 3. Sections 4 and 5 consider *global* variational formulations of the IBVP of quasi-static, dissipative electro-magneto-mechanics, associated with the domain $\mathscr{B}$, see Figure 5 and results in Boxes 4, 5.

standard dissipative solids such as those defined in the purely mechanical context in Biot [67], Ziegler [68], Germain [69] and Halphen and Nguyen [70]. A first steps toward the generalization of the variational principles to ferroelectrics is outlined in Mielke and Timofte [71]. This work extends these concepts from mechanics to fully coupled electro-magneto-mechanics. To this end, we focus on *quasi-static problems*, where mechanical inertia effects and time-dependent electro-magnetic couplings are *a priori* neglected and the time-dependence enters the formulation only through a possible rate-dependent (viscous) response. The dissipation is described by internal variables. The treatment is restricted to a *local dissipative response*, where only the internal variables itself enter the constitutive equations and not their gradients. As a consequence, the constitutive evolution of the internal variables appears in the form of ordinary differential equations. This allows a *decoupling* of the proposed incremental variational structure into a sequence of local and global optimizations of the involved functionals. Based on this decoupling, related to the local and global domains depicted in Figure 1, the main result of the work is the construction of the

- *Local variational principles in Boxes* 1, 2, 3, which determine the response at a point of the continuum in terms of constitutive incremental potentials, and
- *Global variational principles in Boxes* 4, 5, which govern the incremental boundary-value problem of the coupled problem based on condensed incremental potentials.

This variational structure has enormous consequences with respect to all aspects of the continuum-based modeling and the associated numerical implementation. On the theoretical side, the underlying variational principles focus the modeling on the construction of *incremental potentials*, which combine energetic and dissipative effects. On the computational side, the above decoupling dictates the structure of the algorithmic implementation of dissipative models in electro-magneto-mechanics by a *two-step procedure*. The first step is related to a *local constitutive update*, defined in terms of the above local variational principle. The outcome is a condensed or reduced incremental potential with respect to the unit volume. This enters into a second step a global variational problem, which is typically solved by a *global finite element method*. This variational-based two-step cycling then governs a typical iterative solution process of the non-linear incremental problem. Owing to the inherent potential structure, the *coupled problem is symmetric* with respect to the involved fields. This feature is highly attractive with regard to the numerical implementation and is considered to be the canonical formulation of dissipative electro-magneto-mechanics. Furthermore, the macroscopic material stability of incremental problems in coupled electro-magneto-mechanics can be defined based on the convexity of condensed or reduced potentials. This extends definitions of material stability for purely mechanical problems, outlined for example in Hill [72], Petryk [73], Nguyen [74], Miehe and Lambrecht [75], Miehe *et al.* [66], to coupled electro-magneto-mechanics. This variational-based definition of

- *Material stability* for fully coupled electro-magneto-mechanical processes based on the convexity/concavity of the condensed potentials in Boxes 2, 3

Copyright © 2011 John Wiley & Sons, Ltd.

DOI: 10.1002/nme

is an important concern of this work. The variational principles may be represented in alternative forms. The canonical form is based on the energy storage functions and provides a *minimization structure*. The primary local constitutive variables in this setting are the strains, the electric displacements and the magnetic induction. An alternative setting uses a partial Legendre transformation with respect to the electro-mechanical slots and results in a mixed energy–enthalpy formulation that provides a *saddle-point structure*. This setting is more convenient with respect to numerical implementations, because the involved primary constitutive variables, i.e. the strains, electric and magnetic fields, are in a straightforward manner related to the gradients of displacements, electric and magnetic potential fields. This is of particular importance with respect to a simple definition of boundary conditions. An important aspect of the paper is to point out the physical and geometric nature of these alternative formulations, in what follows referred to as the

- *Energy-based setting* with a canonical physically based arrangement of dual variables, providing a minimization structure of principles in Boxes 1, 2, 3, and the
- *Enthalpy-based setting* with a convenient geometry-based arrangement of dual variables, providing a saddle-point structure of the principles in Boxes 1, 2, 3.

A stable electro-magneto-mechanical response is then defined by a *convex* incremental potential in the energy-based setting, and a *convex–concave* potential in the enthalpy-based setting as depicted in Figure 4. This treatment also provides a new variational-based view on the recent treatments of ferro-electricity by Landis [56], Semenov *et al.* [57] and Semenov *et al.*, [59] in terms of vector potentials. The constitutive modeling of the evolution of internal variables in dissipative electro-magneto-mechanics can be based on *threshold, yield or switching functions*. The dissipation functions are then defined by a *principle of maximum dissipation*, a standard terminology in plasticity theory as outlined for example in Hill [76], Maugin [77] and Han and reddy [78]. Within this spirit, we develop *extended incremental variational principles* of electro-magneto-mechanics, which also include the *driving forces* dual to the internal variables. They are of particular importance for the practical formulations. This results in variational principles for

- *Rate-independent dissipative mechanisms* based on the introduction of a Lagrange parameter accounting for exact threshold constraints in Box 2, and
- *Rate-dependent dissipative mechanisms* based on a viscous setting that penalizes effective driving forces above the threshold in Box 3.

The latter approach is due to its smoothness particularly convenient for numerical implementation. The proposed variational-based update algorithms, summarized in Boxes 2 and 3, extend general return schemes of elasto-(visco)-plasticity and visco-plasticity, such as reviewed in Simó [79], Simó and Hughes [80] and Armero and perez-foguet [81], from mechanics to fully coupled electro-magneto-mechanics. They recast the recent work on electro-mechanics of Semenov, Liskowsky & Balke [59] into a consistent variational framework. The proposed algorithmic setting, including generalized return mappings and associated consistent tangents, is *fully governed by the proposed incremental potentials* and its first and second derivatives.

The comprehensive treatment provides a framework for the construction of variational-based models in electro-magneto-mechanics. The paper is organized according to the above items by first focusing in Sections 2 and 3 on the *local* constitutive response, and considering in a second part in Sections 4 and 5 the variational nature of *global* boundary-value problems. The treatment is accompanied by the construction of model problems, which illustrate the features of the general developments. Sections 2 and 3 develop the energy- and enthalpy-based formulations for the local constitutive response. We introduce a representation of the constitutive expressions in terms of generalized stress- and strain-arrays, which recast the set of constitutive equations in a uniquely compact form. Particular aspects are the construction of (i) *energy-based variational principles* in Section 2, which provide the canonical constitutive minimization structure in dissipative electro-magneto-mechanics, and (ii) the *enthalpy-based variational principles* in Section 3, yielding the most convenient fit to conventional formulations of boundary-value problems. The associated *incremental potentials* are summarized in Box 1. We also address particular features related to the

Copyright © 2011 John Wiley & Sons, Ltd.

DOI: 10.1002/nme

constitutive modeling in dissipative electro-magneto-mechanics. These are a conceptual treatment of the (i) *free-space-problem*, see Figure 1, providing a rational approach for the modeling of matter embedded into the free space, the definition of the (ii) *material stability* of the coupled electro-magneto-mechanical process based on variational statements, and the design of particular variational structures for rate-independent and rate-dependent responses in terms of (iii) *threshold*, *yield* or *switching functions*.

The second part of the work is concerned with the design of global variational principles in dissipative electro-magneto-mechanics, see Figure 5 for a visualization. We first summarize in Section 4 the governing equations and recast them into a compact notation by assembling the displacement, electric and magnetic potential fields in a generalized displacement array. This notation results in an extremely compact representation of the mechanical equilibrium and Maxwell equations for the quasi-static problem. We then outline in Section 5 particular variational principles associated with a conventional (i) *enthalpy-based setting* and the non-conventional (ii) *energy-based setting*. The latter needs the design of *Lagrange-type*, *penalty-type* or *vector-potential-type variational structures*. The formulations use locally the incremental potentials per unit volume defined in the foregoing Sections 2 and 3. We start with an outline of the enthalpy-based setting, providing a saddle-point structure of the global variational principle. This formulation is straightforward, uses the displacement, electric and magnetic potentials as the primary fields and yields as the *Euler equations* the quasi-static forms of the balance of momentum coupled with the first and third Maxwell equations at a discrete time, including the Neumann conditions for the stresses, the electric displacement and the magnetic induction. We then consider alternative realizations of an energy-based variational structure in coupled electro-magneto-mechanics. In the Lagrange-type setting, the Lagrange parameters turn out to be the electric and magnetic potentials. The Euler equations then include the definitions for the electric and magnetic fields at the current time. The penalty-type setting incorporates these relationships for finite penalty parameters in an approximate manner. We also comment on the related vector potential formulation. A difficulty in all energy-based formulations is the formulation of the boundary conditions and the extended set of primary variables, which makes this setting inconvenient for numerical implementations.

The full *global–local* variational setting of coupled electro-magneto-mechanics is summarized in Box 4. Box 5 contains the reduced global principles based on the locally condensed or reduced incremental potentials. We also point out details of the finite element implementation, focusing on the enthalpy-based saddle-point principle and the penalty-type energy-based minimization principle. The proposed representations provide a comprehensive outline of alternative variational structures in dissipative electro-magneto-mechanics. From the viewpoint of constitutive modeling, including the understanding of the stability in coupled electro-magneto-mechanics, the *energy-based formulation* is considered to be the canonical setting. From the viewpoint of computational convenience, the *enthalpy-based formulation* is the most convenient setting. A numerical investigation of a multiferroic composite with full electro-magneto-mechanical coupling in Section 6 demonstrates perspectives of the proposed framework with regard to the future design of new functional materials.

2. ENERGY-BASED CONSTITUTIVE VARIATIONAL PRINCIPLES

We start our consideration by focusing on a typical point of the continuum as depicted in Figure 1. The key aspect is an *energy*-based formulation of the local dissipative response in electro-magneto-mechanics by constitutive variational principles.

2.1. Introduction of local variables in electro-magneto-mechanics

We focus on the local volume element in Figure 2 cut out of the continuum visualized in Figure 1, which undergoes an electro-magneto-mechanical loading. Consider the interval $[0,t] \in \mathscr{R}_+$ of the process time with initial value 0 and the current value t. Let

$$W_0^t := \int_0^t \mathscr{P}\, \mathrm{d}\tau \tag{1}$$

Copyright © 2011 John Wiley & Sons, Ltd.

DOI: 10.1002/nme

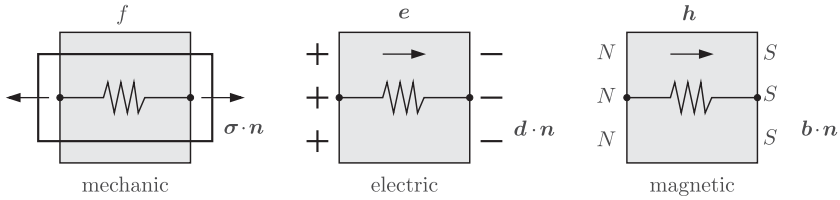

Figure 2. Dual constitutive variables in non-dissipative electro-magneto-mechanics. (i) On the mechanical side, the deformation tensor $\boldsymbol{f}$ is dual to the stress tensor $\boldsymbol{\sigma}$. (ii) The electric field vector $\boldsymbol{e}$ corresponds to the electric displacement $\boldsymbol{d}$. (iii) The magnetic field vector $\boldsymbol{h}$ is dual to the magnetic induction $\boldsymbol{b}$. From the viewpoint of physics, $\mathfrak{s} := \{\boldsymbol{\sigma}, \boldsymbol{e}, \boldsymbol{h}\}$ are *forces* which drive the *reactions* $\mathfrak{f} := \{\boldsymbol{f}, \boldsymbol{d}, \boldsymbol{b}\}$. From the viewpoint of geometry, $\mathfrak{s}' := \{\boldsymbol{\sigma}, -\boldsymbol{d}, -\boldsymbol{b}\}$ are *vectors* (contra-variant objects) and $\mathfrak{f}' := \{\boldsymbol{f}, \boldsymbol{e}, \boldsymbol{h}\}$ *co-vectors* (co-variant objects). The spring indicates an energy storage mechanism, characterizing for example non-dissipative piezoelectricity, electrostriction, piezomagnetism or magnetostriction.

be the work done per unit volume to the material element within this process. Here,

$$\underbrace{\mathscr{P}}_{\text{total}} := \underbrace{\boldsymbol{\sigma} : \dot{\boldsymbol{f}}}_{\text{mechanic}} + \underbrace{\boldsymbol{e} \cdot \dot{\boldsymbol{d}}}_{\text{electric}} + \underbrace{\boldsymbol{h} \cdot \dot{\boldsymbol{b}}}_{\text{magnetic}} \tag{2}$$

is the *canonical electro-magnet-mechanical power* per unit volume of the continuum, see e.g. Novacki [22, p. 107] with regard to the electro-magnetic terms. This power expression defines at a local level dual variables in electro-magneto-mechanics. $\boldsymbol{\sigma} \in \mathscr{R}^{d \times d}$ is the total electro-magneto-mechanical stress tensor, $\boldsymbol{e} \in \mathscr{R}^d$ and $\boldsymbol{h} \in \mathscr{R}^d$ the electric and magnetic field vectors, respectively. These variables are considered as *external forces*. They drive the *external reactions* of the volume element, i.e. the deformation tensor $\boldsymbol{f} \in \mathscr{R}^{d \times d}$, the electric displacement vector $\boldsymbol{d} \in \mathscr{R}^d$ and the magnetic induction vector $\boldsymbol{b} \in \mathscr{R}^d$. Here, $d \in [1, 2, 3]$ is the spatial dimension of the problem under consideration. The dot $(\dot{\cdot}) := \mathrm{d}(\cdot)/\mathrm{d}t$ indicates the derivative by time. Note that, for reasons which become clear in the subsequent treatment, we introduced the total stress and deformation $\boldsymbol{\sigma}$ and $\boldsymbol{f}$ as general second-order tensors.

With regard to a compact representation of the electro-magneto-mechanical actions depicted in Figure 2, we introduce for the coupled problem the dual arrays

$$\boxed{\mathfrak{s} := [\boldsymbol{\sigma}, \boldsymbol{e}, \boldsymbol{h}]^{\mathrm{T}} \quad \text{and} \quad \mathfrak{f} := [\boldsymbol{f}, \boldsymbol{d}, \boldsymbol{b}]^{\mathrm{T}}} \tag{3}$$

with $\{\mathfrak{s}, \mathfrak{f}\} \in \mathscr{R}^{d \times d+2d}$, in the subsequent treatment referred to as the *generalized stress* and *generalized deformation* of electro-magneto-mechanics. With this notation at hand, we write the power expression (2) in the compact form

$$\mathscr{P} = \mathfrak{s} \cdot \dot{\mathfrak{f}}. \tag{4}$$

Here, the dot denotes a generalized inner product in the $\mathscr{R}^{d \times d+2d}$ that produces a scalar according to definition (2). Expressions (2) and (4) are the starting points for the constitutive modeling of local dissipative processes in electro-magneto-mechanics.[‡]

[‡]*Remark on the Macroscopic Modeling Concept.* The electric displacement $\boldsymbol{d}$ and the magnetic induction $\boldsymbol{b}$ include superimposed effects of the free space and the embedded solid matter as depicted in Figure 1. This is characterized by the *constitutive* decompositions

$$\boldsymbol{d} = \varepsilon_0 \boldsymbol{e} + \boldsymbol{p} \quad \text{with } \boldsymbol{b} = \mu_0 (\boldsymbol{h} + \boldsymbol{m}) \tag{5}$$

into free space contributions and the *electric polarization* $\boldsymbol{p}$ and *magnetization* $\boldsymbol{m}$ of the solid, respectively. Here, ε_0 and μ_0 are the electric permittivity and the magnetic permeability of the vacuum, respectively. The total stress $\boldsymbol{\sigma}$ is assumed to include electro-magnetic-mechanical interaction effects, for example based on the *two-dipole model*

Copyright © 2011 John Wiley & Sons, Ltd.

DOI: 10.1002/nme

2.2. Canonical energy-based formulation of non-dissipative response

2.2.1. Free energy function. Let us first consider a non-dissipative electro-magneto-mechanical response associated with the spring in Figure 2. This type of reversible material response characterizes phenomena of *piezoelectricity, electrostriction, piezomagnetism* or *magnetostriction*. The key property of this type of material response is the path-independence of the work done to the material element defined in (1). This property may be expressed by the statement

$$\underbrace{W_0^t}_{\text{work}} = \underbrace{\hat{\psi}(t) - \hat{\psi}(0)}_{\text{stored}}, \tag{7}$$

where $\hat{\psi}(t)$ is the free energy stored in the material element at time t. It is assumed that this energy storage depends exclusively on the current state of generalized strain $\mathfrak{f}(t)$, i.e

$$\hat{\psi}(t) = \psi(\mathfrak{f}(t)), \tag{8}$$

where $\psi : \mathscr{R}^{d\times d+2d} \to \mathscr{R}$ is the *free energy function*. This constitutive function describes the internal energy storage in the electro-magneto-mechanical loaded solid material element depicted in Figure 2, *including the free space background*, with respect to the unit volume in terms of the generalized deformation $\mathfrak{f}$ introduced in (3). The above expression simply states that the work done to the material element in the time interval $[0, t]$ is fully stored in the material and the free space background. With definition (1), we may recast (7) into the rate form

$$\mathscr{P} = \frac{\mathrm{d}}{\mathrm{d}t}\psi(\mathfrak{f}(t)). \tag{9}$$

2.2.2. Constitutively defined forces. Insertion of (4) gives an identity that must be satisfied for all possible fluxes $\dot{\mathfrak{f}}$, i.e. $\mathfrak{s}\cdot\dot{\mathfrak{f}} = \partial_{\mathfrak{f}}\psi\cdot\dot{\mathfrak{f}}$, yielding the potential constitutive equation

$$\boxed{\mathfrak{s}(t) = \partial_{\mathfrak{f}}\psi(\mathfrak{f}(t))} \tag{10}$$

which defines the current generalized stress in terms of the generalized strain. Equation (10) consists of the three coupled parts

$$\boldsymbol{\sigma} = \partial_f\psi(\boldsymbol{f},\boldsymbol{d},\boldsymbol{b}), \quad \boldsymbol{e} = \partial_d\psi(\boldsymbol{f},\boldsymbol{d},\boldsymbol{b}), \quad \boldsymbol{h} = \partial_b\psi(\boldsymbol{f},\boldsymbol{d},\boldsymbol{b}), \tag{11}$$

---

suggested by Pao and Hutter [16]. Then, the total stress includes the purely mechanical Cauchy stress and an additional contribution

$$\boldsymbol{\sigma} = \boldsymbol{\sigma}^C + \boldsymbol{\sigma}^M \quad \text{with } \boldsymbol{\sigma}^M := \boldsymbol{e}\otimes\boldsymbol{d} + \boldsymbol{h}\otimes\boldsymbol{b} - \tfrac{1}{2}(\varepsilon_0|\boldsymbol{e}|^2 + \mu_0|\boldsymbol{h}|^2)\mathbf{1} \tag{6}$$

often called the Maxwell stress. The latter provides micro-mechanically motivated, *constitutively* defined electro-magnetic body forces $\gamma^{em} := \operatorname{div}\boldsymbol{\sigma}^M$ and couples $\boldsymbol{l}^{em} := \operatorname{axial}[\operatorname{skew}\boldsymbol{\sigma}^M]$ in the macroscopic balance of linear and angular momentums, respectively. The resulting macroscopic terms $\gamma^{em} = \bar{\rho}^e\boldsymbol{e} + \bar{\boldsymbol{j}}\times\mu_0\boldsymbol{h} + \nabla\boldsymbol{e}\cdot\boldsymbol{p} + \mu_0\nabla\boldsymbol{h}\cdot\boldsymbol{m}$ and $\boldsymbol{l}^{em} = \boldsymbol{p}\times\boldsymbol{e} + \mu_0\boldsymbol{m}\times\boldsymbol{h}$ of the two-dipole model include mechanical macro-actions resulting from the *homogenization of Lorentz-type forces* on discrete electric and magnetic micro-dipoles.

In the subsequent treatment, we perform a *two-step constitutive modeling concept*. The first step is a *purely macroscopic constitutive modeling* of the generalized stress variables $\mathfrak{s} := [\boldsymbol{\sigma}, \boldsymbol{e}, \boldsymbol{h}]^{\mathrm{T}}$ in terms of the generalized deformation variables $\mathfrak{f} := [\boldsymbol{f}, \boldsymbol{d}, \boldsymbol{b}]^{\mathrm{T}}$. This covers the superimposed response of the free space with embedded solid matter, defining directly the total stress $\boldsymbol{\sigma}$, the electric displacement $\boldsymbol{d}$ and the magnetic induction $\boldsymbol{b}$. The second step is concerned with the decomposition of these quantities into free space and solid matter contributions, as well as the definition of the electro-magnetic body forces. It is governed by *additional micro-mechanically based constitutive assumptions*, such as the above equations (5) and (6). Note that, for given overall quantities $\mathfrak{f}$ and $\mathfrak{s}$ of the superimposed problem, these equations determine the electric solid polarization $\boldsymbol{p}$, the solid magnetization $\boldsymbol{m}$ as well as the Maxwell and Cauchy stresses $\boldsymbol{\sigma}^M$ and $\boldsymbol{\sigma}^C$. We view this as a micro-mechanical post-processing step. Clearly, our treatment focuses on the first purely macroscopic modeling step. Note that this focus circumvents *a priori* the difficulty of the lack of experimental data for electro-magnetic body force actions. This problem is shifted to the second modeling step that is strongly hypothetical in nature.

Copyright © 2011 John Wiley & Sons, Ltd.

DOI: 10.1002/nme

which constitute the dependencies of the total stress tensor, the electric and magnetic field vectors on the deformation tensor, the electric displacement and the magnetic flux vectors. Equation (10) is the key constitutive expression in reversible electro-magneto-mechanics.

2.2.3. Normalization and objectivity. We assume the zero energy level and a zero natural state at zero generalized deformation $\mathfrak{f}=\mathbf{0}$. This is ensured by the *normalization constraints*

$$\psi(\mathbf{0})=0 \quad \text{and} \quad \partial_{\mathfrak{f}}\psi(\mathbf{0})=\mathbf{0} \tag{12}$$

on the free energy function ψ. Furthermore, the energetic state must be invariant with respect to arbitrary rotations of the material volume element. In the small strain theory, infinitesimal rotations are characterized by skew second-order tensors. Hence, we postulate the *objectivity constraint* $\psi(\boldsymbol{f}+\boldsymbol{w},\boldsymbol{e},\boldsymbol{h})=\psi(\boldsymbol{f},\boldsymbol{e},\boldsymbol{h})$ for all $\boldsymbol{w}\in Skw(3):=\{\boldsymbol{w}\in\mathscr{R}^{d\times d}|\boldsymbol{w}=-\boldsymbol{w}^{\mathrm{T}}\}$ on the free energy function. This is *a priori* satisfied by a reduced form $\tilde{\psi}$ of the free energy function

$$\psi(\boldsymbol{f},\boldsymbol{d},\boldsymbol{b})=\tilde{\psi}(\boldsymbol{\varepsilon},\boldsymbol{d},\boldsymbol{b}) \quad \text{with} \quad \boldsymbol{\varepsilon}:=\tfrac{1}{2}(\boldsymbol{f}+\boldsymbol{f}^{\mathrm{T}}) \tag{13}$$

which depends on the symmetric part $\boldsymbol{\varepsilon}\in Sym(3)$ of the deformation tensor $\boldsymbol{f}$, i.e. the classical small-strain tensor.[§]

2.2.4. Stable constitutive response. We focus on a *unique constitutive behavior*, in what follows denoted as a stable electro-magneto-mechanical response. This is characterized by bifurcation- and limit-point-free relationship between the generalized stress and the generalized deformation. For

[§] *Representation of Energy Function for Non-Dissipative Response.* ψ may be a general non-linear function of the generalized deformation $\mathfrak{f}$, which satisfies (12), (13) and (22). For objective, *isotropic* response with

$$\psi(\boldsymbol{Q}\boldsymbol{\varepsilon}\boldsymbol{Q}^{\mathrm{T}},\boldsymbol{Q}\boldsymbol{d},\boldsymbol{Q}\boldsymbol{b})=\psi(\boldsymbol{f},\boldsymbol{d},\boldsymbol{b}) \quad \text{for all } \boldsymbol{Q}\in SO(3) \tag{14}$$

one has the standard representation based on the coupled invariants of the three variables $\boldsymbol{\varepsilon}$, $\boldsymbol{d}$ and $\boldsymbol{b}$

$$\begin{aligned}\psi(\mathfrak{f}) = \psi_{\mathrm{iso}}(&\mathrm{tr}\,\boldsymbol{\varepsilon},\mathrm{tr}\,\boldsymbol{\varepsilon}^2,\mathrm{tr}\,\boldsymbol{\varepsilon}^3,\mathrm{tr}\,\boldsymbol{d}\otimes\boldsymbol{d},\mathrm{tr}\,\boldsymbol{b}\otimes\boldsymbol{b},\mathrm{tr}\,\boldsymbol{\varepsilon}(\boldsymbol{d}\otimes\boldsymbol{d}),\mathrm{tr}\,\boldsymbol{\varepsilon}^2(\boldsymbol{d}\otimes\boldsymbol{d}),\\ &\mathrm{tr}\,\boldsymbol{\varepsilon}(\boldsymbol{b}\otimes\boldsymbol{b}),\mathrm{tr}\,\boldsymbol{\varepsilon}^2(\boldsymbol{b}\otimes\boldsymbol{b}),\mathrm{tr}\,\boldsymbol{\varepsilon}(\boldsymbol{d}\otimes\boldsymbol{b}),\mathrm{tr}\,\boldsymbol{\varepsilon}^2(\boldsymbol{d}\otimes\boldsymbol{b}),\mathrm{tr}\,\boldsymbol{d}\otimes\boldsymbol{b})\end{aligned} \tag{15}$$

see for example Boehler [82, p. 37] Such isotropic representation can be a basis for the formulation of *electrostrictive* or *magnetostrictive* response. Observe that a quadratic free energy function for *linear* response cannot have electro-mechanical or magneto-mechanical couplings. Representations of anisotropic response become more complex, where the free energy may be modeled by taking into account additional structural tensors. For the important case of *coupled transversely isotropic response*

$$\psi(\boldsymbol{Q}\boldsymbol{\varepsilon}\boldsymbol{Q}^{\mathrm{T}},\boldsymbol{Q}\boldsymbol{d},\boldsymbol{Q}\boldsymbol{b})=\psi(\boldsymbol{f},\boldsymbol{d},\boldsymbol{b}) \quad \text{for all } \boldsymbol{Q}\in\mathscr{G}_{\mathrm{tra}}:=\{\boldsymbol{Q}\subset\mathscr{O}(3)|\boldsymbol{Q}\boldsymbol{a}=\boldsymbol{a}\}. \tag{16}$$

ψ depends on a *constant structural director vector* $\boldsymbol{a}$ with $|\boldsymbol{a}|=1$. We then have the representation

$$\begin{aligned}\psi(\mathfrak{f};\boldsymbol{a}) = \psi_{\mathrm{tra}}(&\mathrm{tr}\,\boldsymbol{\varepsilon},\mathrm{tr}\,\boldsymbol{\varepsilon}^2,\mathrm{tr}\,\boldsymbol{\varepsilon}^3,\mathrm{tr}\,\boldsymbol{d}\otimes\boldsymbol{d},\mathrm{tr}\,\boldsymbol{b}\otimes\boldsymbol{b},\mathrm{tr}\,\boldsymbol{\varepsilon}(\boldsymbol{d}\otimes\boldsymbol{d}),\mathrm{tr}\,\boldsymbol{\varepsilon}^2(\boldsymbol{d}\otimes\boldsymbol{d}),\\ &\mathrm{tr}\,\boldsymbol{\varepsilon}(\boldsymbol{b}\otimes\boldsymbol{b}),\mathrm{tr}\,\boldsymbol{\varepsilon}^2(\boldsymbol{b}\otimes\boldsymbol{b}),\mathrm{tr}\,\boldsymbol{\varepsilon}(\boldsymbol{d}\otimes\boldsymbol{b}),\mathrm{tr}\,\boldsymbol{\varepsilon}^2(\boldsymbol{d}\otimes\boldsymbol{b}),\mathrm{tr}\,\boldsymbol{d}\otimes\boldsymbol{b},\\ &\mathrm{tr}\,\boldsymbol{\varepsilon}(\boldsymbol{a}\otimes\boldsymbol{a}),\mathrm{tr}\,\boldsymbol{\varepsilon}^2(\boldsymbol{a}\otimes\boldsymbol{a}),\mathrm{tr}\,\boldsymbol{\varepsilon}(\boldsymbol{d}\otimes\boldsymbol{a}),\mathrm{tr}\,\boldsymbol{\varepsilon}^2(\boldsymbol{d}\otimes\boldsymbol{a}),\\ &\mathrm{tr}\,\boldsymbol{\varepsilon}(\boldsymbol{b}\otimes\boldsymbol{a}),\mathrm{tr}\,\boldsymbol{\varepsilon}^2(\boldsymbol{b}\otimes\boldsymbol{a}),\mathrm{tr}\,\boldsymbol{d}\otimes\boldsymbol{a},\mathrm{tr}\,\boldsymbol{b}\otimes\boldsymbol{a})\end{aligned} \tag{17}$$

suitable for *piezoelectric* or *piezomagnetic response*, where the director $\boldsymbol{a}$ represents an electric polarization or a magnetization, respectively. A simple objective model function for *linear piezoelectricity* has the form

$$\begin{aligned}\psi(\mathfrak{f};\boldsymbol{a}) = \mu\,\mathrm{tr}[\boldsymbol{\varepsilon}^2]+\lambda\,\mathrm{tr}^2[\boldsymbol{\varepsilon}]/2-\{&\alpha_0\,\mathrm{tr}[\boldsymbol{\varepsilon}(\boldsymbol{a}\otimes\boldsymbol{a})]\mathrm{tr}[\boldsymbol{a}\otimes\boldsymbol{d}]\\ &+\alpha_\perp\mathrm{tr}[\boldsymbol{\varepsilon}]\mathrm{tr}[\boldsymbol{a}\otimes\boldsymbol{d}]+\alpha_=\mathrm{tr}[\boldsymbol{\varepsilon}(\boldsymbol{a}\otimes\boldsymbol{d})]\}+\sigma\mathrm{tr}[\boldsymbol{d}\otimes\boldsymbol{d}]/2\end{aligned} \tag{18}$$

with positive mechanical Lame parameters μ and λ, positive electric susceptibility σ and three transversely isotropic, electro-mechanical coupling parameters $\alpha_\parallel$, $\alpha_=$, α_0.

Copyright © 2011 John Wiley & Sons, Ltd.

DOI: 10.1002/nme

smooth response, this demand can be expressed by the constraint on what we call the second-order work

$$\mathscr{S} := \dot{\mathfrak{s}} \cdot \dot{\mathfrak{f}} \geqslant 0 \quad \text{for all } \dot{\mathfrak{f}} \neq \mathbf{0}. \tag{19}$$

It characterizes a stable material response such that an increase in the generalized strain produces an increase in the generalized stress. Taking into account the constitutive expression (11) for the thermodynamic force, we may recast (19) into the form

$$\mathscr{S} = \dot{\mathfrak{f}} \cdot \partial^2_{\mathfrak{f}\mathfrak{f}} \psi(\mathfrak{f}) \cdot \dot{\mathfrak{f}} \geqslant 0 \quad \text{for all } \dot{\mathfrak{f}} \neq \mathbf{0}, \tag{20}$$

enforcing the positive definiteness of the coupled electro-magneto-mechanical moduli

$$\mathfrak{c} := \partial^2_{\mathfrak{f}\mathfrak{f}} \psi(\mathfrak{f}) = \begin{bmatrix} \partial^2_{\boldsymbol{f}\boldsymbol{f}}\psi & \partial^2_{\boldsymbol{f}\boldsymbol{d}}\psi & \partial^2_{\boldsymbol{f}\boldsymbol{b}}\psi \\ \partial^2_{\boldsymbol{d}\boldsymbol{f}}\psi & \partial^2_{\boldsymbol{d}\boldsymbol{d}}\psi & \partial^2_{\boldsymbol{d}\boldsymbol{b}}\psi \\ \partial^2_{\boldsymbol{b}\boldsymbol{f}}\psi & \partial^2_{\boldsymbol{b}\boldsymbol{d}}\psi & \partial^2_{\boldsymbol{b}\boldsymbol{b}}\psi \end{bmatrix}. \tag{21}$$

This is achieved for a *convex free energy function* ψ with the property

$$\alpha\psi(\mathfrak{f}_1) + (1-\alpha)\psi(\mathfrak{f}_2) \geqslant \psi(\alpha\mathfrak{f}_1 + (1-\alpha)\mathfrak{f}_2) \tag{22}$$

with $\alpha \in [0, 1]$, which provides a further constraint to the construction of this key constitutive function. A convex free energy function of the generalized strain $\boldsymbol{f}$ defined in (3) ensures *uniqueness* of the local electro-magneto-mechanical loading process, see Figure 4(a) for a visualization.

2.2.5. Incremental constitutive minimization principle. The above outlined constitutive equation (10) can be related to an incremental (rate-type) constitutive minimization principle as follows. Consider a finite time increment $\tau := t - t_n$ and introduce the potential $\pi^\tau := \int_{t_n}^t [\dot{\psi} - \mathscr{P}] \mathrm{d}t$ with the algorithmic representation

$$\underbrace{\pi^\tau(\mathfrak{f})}_{\text{potential}} := \underbrace{\psi(\mathfrak{f}) - \psi(\mathfrak{f}_n)}_{\text{stored}} - \underbrace{\mathfrak{s} \cdot (\mathfrak{f} - \mathfrak{f}_n)}_{\text{ext.load}}. \tag{23}$$

The potential π^τ contains the difference between incremental energy storage and incremental external load done to the electro-magneto-mechanical volume element depicted in Figure 2. It is a function of the current generalized strain $\mathfrak{f} := \mathfrak{f}(t)$ at time t and refers to the *fixed value* $\mathfrak{f}_n := \mathfrak{f}(t_n)$ at time t_n. Note that the incremental load is defined in an implicit format in terms of the generalized stress $\mathfrak{s} := \mathfrak{s}(t)$ at time t. Then, for a given external load $\mathfrak{s}$ of the volume element depicted in Figure 2, the associated generalized strain is defined by the *constitutive minimization principle*

$$\boxed{\mathfrak{f} = \operatorname{Arg}\left\{\inf_{\mathfrak{f}} \pi^\tau(\mathfrak{f})\right\} = \operatorname{Arg}\left\{\inf_{\boldsymbol{f}}\inf_{\boldsymbol{d}}\inf_{\boldsymbol{b}} \pi^\tau(\boldsymbol{f}, \boldsymbol{d}, \boldsymbol{b})\right\}.} \tag{24}$$

The Euler equation of this variational principle is the constitutive equation (10), which defines for a given generalized stress $\mathfrak{s}$ the generalized strain $\mathfrak{f}$. This relationship is unique if the incremental potential π^τ is *convex*, which follows for a stable electro-magneto-mechanical response from the convexity (22) of the energy function ψ.

2.3. Canonical energy-based formulation of dissipative response

2.3.1. Dissipation. We now focus on dissipative electro-magneto-mechanical material response, characterized by non-reversible local mechanisms as depicted in Figure 3. This is typically associated with ferroelectric and ferromagnetic hystereses effects accompanied by so-called remanent *electric and magnetic polarization effects*. From the viewpoint of local material modeling, the

Copyright © 2011 John Wiley & Sons, Ltd.

DOI: 10.1002/nme

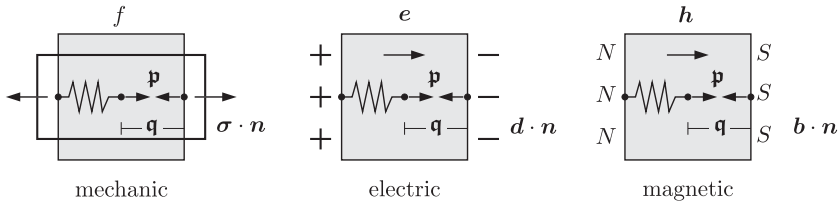

Figure 3. Dual constitutive variables in dissipative electro-magneto-mechanics. Additional to the *external forces* $\mathfrak{s} := \{\boldsymbol{\sigma}, \boldsymbol{e}, \boldsymbol{h}\}$ and the dual *external reactions* $\mathfrak{f} := \{\boldsymbol{f}, \boldsymbol{d}, \boldsymbol{b}\}$ acting on the volume element, we consider the *internal variables* $\mathfrak{q}$ and their dual *internal driving forces* $\mathfrak{p}$. While the energy storage is symbolized by the spring, the internal variables $\mathfrak{q}$ model dissipative internal mechanisms, for example poling vectors and remanent strains in ferroelectricity or ferromagnetism.

work done to the material element defined in (1) is in this case not fully stored in the material. Thus, condition (7) must be extended to

$$\underbrace{W_0^t}_{\text{work}} = \underbrace{\hat{\psi}(t) - \hat{\psi}(0)}_{\text{stored}} + \underbrace{D_0^t}_{\text{dissipated}}, \tag{25}$$

where

$$D_0^t := \int_0^t \mathscr{D} \mathrm{d}\tau \geqslant 0 \tag{26}$$

is the part of the electro-magneto-mechanical work done to the material element that dissipates into heat. Statement (26) is a mechanical version of the second law of thermodynamics and states a *positive dissipation* $\mathscr{D} \geqslant 0$ for arbitrary processes. From (25), we conclude that (9) needs to be extended to

$$\mathscr{P} = \frac{\mathrm{d}}{\mathrm{d}t}\hat{\psi} + \mathscr{D}. \tag{27}$$

It is then clear from the representation (4) of the electro-magnetic-mechanical power that the energy storage $\hat{\psi}$ cannot only be a function of the generalized deformation $\mathfrak{f}(t)$ as for the non-dissipative response (8).

2.3.2. Free energy function. A classical approach to the constitutive modeling of dissipative material response is the *concept of internal variables*. Here, the free energy function $\psi : \mathscr{R}^{d\times d+2d+m} \to \mathscr{R}$ is assumed to depend *additionally* on a generalized internal variable vector $\mathfrak{q} \in \mathscr{R}^m$ that contains m scalar entries

$$\hat{\psi}(t) = \psi(\mathfrak{f}(t), \mathfrak{q}(t)). \tag{28}$$

Typical internal variables are mechanic, electric or magnetic in nature, such as for example plastic strains, remanent electric polarizations or remanent magnetization. The assumed dependence of the free energy on internal variables then *defines* for given external power $\mathscr{P}$ the dissipation by

$$\mathscr{D} := \mathscr{P} - \frac{\mathrm{d}}{\mathrm{d}t}\psi(\mathfrak{f}(t), \mathfrak{q}(t)) \geqslant 0. \tag{29}$$

2.3.3. Constitutively defined forces. Writing this with (4) in the form $\mathscr{D} = [\mathfrak{s} - \partial_{\mathfrak{f}}\psi] \cdot \dot{\mathfrak{f}} - \partial_{\mathfrak{q}}\psi \cdot \dot{\mathfrak{q}} \geqslant 0$, a standard argument of dissipative material modeling identifies the generalized stresses $\mathfrak{s}$ and the internal forces $\mathfrak{p}$ dual to $\mathfrak{q}$ by

$$\boxed{\mathfrak{s} = \partial_{\mathfrak{f}}\psi(\mathfrak{f}, \mathfrak{q}) \quad \text{and} \quad \mathfrak{p} := -\partial_{\mathfrak{q}}\psi(\mathfrak{f}, \mathfrak{q}).} \tag{30}$$

Copyright © 2011 John Wiley & Sons, Ltd.

DOI: 10.1002/nme

With the definition $(30)_2$ at hand, the dissipation appears

$$\mathscr{D} = \mathfrak{p} \cdot \dot{\mathfrak{q}} \geqslant 0 \tag{31}$$

as an inner product of *dissipative driving forces* $\mathfrak{p}$ and *dissipative fluxes* $\dot{\mathfrak{q}}$. This power statement can be interpreted such that the dissipative forces $\mathfrak{p}$ drive the evolution $\dot{\mathfrak{q}}$ of the internal variables as visualized in Figure 3.[¶]

2.3.4. Dissipation function and evolution of internal variables. The critical point in the modeling of dissipative material response is the construction of constitutive evolution equations for the internal variables. This is achieved in a canonical format by introduction of a *dissipation function* $\phi : \mathscr{R}^m \to \mathscr{R}$, which determines per definition the driving forces $\mathfrak{p}$ in terms of the rates $\dot{\mathfrak{q}}$ of the internal variables by

$$\boxed{\mathfrak{p} \in \partial_{\dot{\mathfrak{q}}} \phi(\dot{\mathfrak{q}}).} \tag{38}$$

The dissipation function may be non-smooth, in particular in rate-independent dissipative processes. Thus, the operator $\partial_{\dot{\mathfrak{q}}}(\cdot)$ in (38) is understood to be a sub-gradient, representing a set. For smooth

[¶]*Representation of Energy Function for Dissipative Response.* A typical example is the representation of the free energy function in *ferro-electricity*, which uses the *electric polarization vector* $\boldsymbol{p}$ and the symmetric *remanent strain tensor* $\boldsymbol{\varepsilon}^r$ as internal variables. Let $\boldsymbol{\pi}$ and $\boldsymbol{\sigma}^r$ denote the variables dual to $\boldsymbol{p}$ and $\boldsymbol{\varepsilon}^r$, respectively. Thus we have in ferroelectricity

$$\mathfrak{q} := \{\boldsymbol{p}, \boldsymbol{\varepsilon}^r\} \in \mathscr{R}^{3+6} \quad \text{and} \quad \mathfrak{p} := \{\boldsymbol{\pi}, \boldsymbol{\sigma}^r\} \in \mathscr{R}^{3+6}. \tag{32}$$

The free energy is usually assumed to be additively decomposed into a *piezoelectric part* and a *polarization part* according to

$$\psi(\mathfrak{f}, \mathfrak{q}) = \psi_{\text{pie}}(\mathfrak{f}, \mathfrak{q}) + \psi_{\text{pol}}(\mathfrak{q}), \tag{33}$$

see for example Bassiouny *et al*. [26] and Landis [34]. The first part may be based on the simple *linear* piezoelectric representation (18), yielding

$$\begin{aligned}\psi_{pie}(\mathfrak{f}, \mathfrak{q}) = {} & \mu \operatorname{tr}[(\boldsymbol{\varepsilon} - \boldsymbol{\varepsilon}^r)^2] + \lambda \operatorname{tr}^2[\boldsymbol{\varepsilon} - \boldsymbol{\varepsilon}^r]/2 - (p/p_s)\{\alpha_0 \operatorname{tr}[(\boldsymbol{\varepsilon} - \boldsymbol{\varepsilon}^r)(\boldsymbol{a} \otimes \boldsymbol{a})] \operatorname{tr}[\boldsymbol{a} \otimes (\boldsymbol{d} - \boldsymbol{p})] \\ & + \alpha_\perp \operatorname{tr}[\boldsymbol{\varepsilon} - \boldsymbol{\varepsilon}^r] \operatorname{tr}[\boldsymbol{a} \otimes (\boldsymbol{d} - \boldsymbol{p})] + \alpha_= \operatorname{tr}[(\boldsymbol{\varepsilon} - \boldsymbol{\varepsilon}^r)(\boldsymbol{a} \otimes (\boldsymbol{d} - \boldsymbol{p}))]\} + \sigma \operatorname{tr}[(\boldsymbol{d} - \boldsymbol{p}) \otimes (\boldsymbol{d} - \boldsymbol{p})]/2,\end{aligned} \tag{34}$$

where $p := |\boldsymbol{p}|$ is the amount of polarization and $\boldsymbol{a} := \boldsymbol{p}/|\boldsymbol{p}|$ the polarization director. Note that (34) is obtained by replacing $\boldsymbol{\varepsilon}$ and $\boldsymbol{d}$ in (18) by the *reversible* contributions $\boldsymbol{\varepsilon} - \boldsymbol{\varepsilon}^r$ and $\boldsymbol{d} - \boldsymbol{p}$. The scalar factor (p/p_s) controls the increase in the electromechanical coupling with increasing amount of polarization, where p_s is a material parameter that describes a saturated polarization state. A simpler representation is obtained by a *kinematic assumption*

$$\boldsymbol{\varepsilon}^r = \hat{\boldsymbol{\varepsilon}}^r(\boldsymbol{p}) = \frac{3}{2} \varepsilon_s^r \frac{p}{p_s} \operatorname{dev}[\boldsymbol{a} \otimes \boldsymbol{a}], \tag{35}$$

see Kamlah [83] or McMeeking and Landis [37], which makes the remanent strain $\boldsymbol{\varepsilon}^r$ dependent on the polarization vector $\boldsymbol{p}$. Here, the material parameter ε_s^r characterizes a maximum possible remanent strain at saturated polarization. Note that such an assumption reduces the internal state (32) to

$$\mathfrak{q} := \{\boldsymbol{p}\} \in \mathscr{R}^3 \quad \text{and} \quad \mathfrak{p} := \{\boldsymbol{\pi}\} \in \mathscr{R}^3, \tag{36}$$

where $\boldsymbol{\pi}$ is now an *effective internal force* that drives the polarization *and* the remanent strain. The polarization part in (33) describes a *back electric field effect* similar to the back stress in the plasticity theory, which governs the hysteresis under cyclic electromechanical loading. A typical function has the form

$$\psi_{pol}(\mathfrak{q}) = -h_0 p_s^2 \left[\ln\left(1 - \frac{p}{p_s}\right) + \frac{p}{p_s} \right], \tag{37}$$

see Huber and Fleck [36], with material parameter h_0, which provides a saturation-type kinematic hardening response. Owing to additive split (33) of the free energy function, the effective internal force appears in the typical additive split $\boldsymbol{\pi} = \boldsymbol{\pi}_{\text{pie}} - \boldsymbol{\pi}_{\text{pol}}$ with a back contribution due to the poling, where $\boldsymbol{\pi}_{\text{pie}}$ is a function of the electric field $\boldsymbol{e}$ *and* the stress $\boldsymbol{\sigma}$.

Copyright © 2011 John Wiley & Sons, Ltd.

DOI: 10.1002/nme

dissipation functions, $\partial_{\dot{\mathbf{q}}}(\cdot)$ is the standard derivative and we simply have $\mathbf{p}=\partial_{\dot{\mathbf{q}}}\phi(\dot{\mathbf{q}})$. Note carefully that Equation (38) determines along with a *suitable initial condition* the evolution of the internal variables. This becomes clear by combining $(30)_2$ and (38) with the so-called Biot equation

$$\mathbf{0}\in\partial_{\mathbf{q}}\psi(\mathbf{f},\mathbf{q})+\partial_{\dot{\mathbf{q}}}\phi(\dot{\mathbf{q}}) \quad \text{with } \mathbf{q}(0)=\mathbf{q}_0. \tag{39}$$

The choice of concrete dissipation functions is constrained by the demand (31) of positive dissipation. This thermodynamic constraint is *a priori* satisfied for *normalized*, *positive* dissipation functions with

$$\phi(\mathbf{0})=0 \quad \text{and} \quad \phi(\dot{\mathbf{q}})\geqslant 0, \tag{40}$$

which are *convex*, i.e.

$$\alpha\phi(\dot{\mathbf{q}}_1)+(1-\alpha)\phi(\dot{\mathbf{q}}_2)\geqslant\phi(\alpha\dot{\mathbf{q}}_1+(1-\alpha)\dot{\mathbf{q}}_2) \tag{41}$$

for $\alpha\in[0,1]$. Depending on particular applications, the dissipation function may be assumed to be *positively homogeneous of the degree p*

$$\phi(\alpha\dot{\mathbf{q}})=\alpha^p\phi(\dot{\mathbf{q}}) \quad \text{for } \alpha>0. \tag{42}$$

An important case is $p=1$ that characterizes rate-independent response. Then, differentiation of (42) with respect to α gives $\partial_{\dot{\mathbf{q}}}\phi(\dot{\mathbf{q}})\cdot\dot{\mathbf{q}}=\phi(\dot{\mathbf{q}})$, which identifies for the rate-independent case the dissipation to be $\mathscr{D}=\phi(\dot{\mathbf{q}})\geqslant 0$ to be identical with the dissipation function. A Legendre–Fenchel transformation defines the *dual dissipation function* $\phi^*:\mathscr{R}^m\to\mathscr{R}$

$$\phi^*(\mathbf{p}):=\sup_{\dot{\mathbf{q}}}[\mathbf{p}\cdot\dot{\mathbf{q}}-\phi(\dot{\mathbf{q}})], \tag{43}$$

which is a function of the internal forces $\mathbf{p}$. The dual dissipation function defines directly the evolution of the internal variables by

$$\dot{\mathbf{q}}\in\partial_{\dot{\mathbf{q}}}\phi^*(\mathbf{p}) \tag{44}$$

dual to (38), degenerating for smooth response to $\dot{\mathbf{q}}=\partial_{\dot{\mathbf{q}}}\phi^*(\mathbf{p})$.

2.3.5. Incremental constitutive minimization principle. The above outlined constitutive equations (30) and (38) can be related to an incremental (rate-type) constitutive minimization principle, which extends the principle (24) to *dissipative* electro-magneto-mechanics. To this end, we consider again a finite time increment $\tau:=t-t_n$ and introduce the potential $\pi_d^\tau:=\int_{t_n}^t[\dot{\psi}+\mathscr{D}-\mathscr{P}]\mathrm{d}t$ with the algorithmic representation

$$\underbrace{\pi_d^\tau(\mathbf{f},\mathbf{q})}_{\text{potential}}:=\underbrace{\psi(\mathbf{f},\mathbf{q})-\psi(\mathbf{f}_n,\mathbf{q}_n)}_{\text{stored}}+\underbrace{\tau\phi([\mathbf{q}-\mathbf{q}_n]/\tau)}_{dissipated}-\underbrace{\mathfrak{s}\cdot(\mathbf{f}-\mathbf{f}_n)}_{\text{ext.load}}. \tag{45}$$

The potential π_d^τ contains the difference between the algorithmic expression for the incremental internal work potential

$$w(\mathbf{f},\mathbf{q}):=\psi(\mathbf{f},\mathbf{q})-\psi(\mathbf{f}_n,\mathbf{q}_n)+\tau\phi([\mathbf{q}-\mathbf{q}_n]/\tau) \tag{46}$$

consisting of a stored and a dissipated part, and the incremental external load done to the electro-magneto-mechanical volume element depicted in Figure 3. It is a function of the current generalized strain $\mathbf{f}:=\mathbf{f}(t)$ and the internal variables $\mathbf{q}:=\mathbf{q}(t)$ at time t and refers to the *given values* $\mathbf{f}_n:=\mathbf{f}(t_n)$ and $\mathbf{q}_n:=\mathbf{q}(t_n)$ at time t_n. Note that this function approximates the incremental dissipation based on the algorithm $\dot{\mathbf{q}}=(\mathbf{q}-\mathbf{q}_n)/\tau$, defining a *constant rate* of internal variables within the interval $[t_n,t]$. Furthermore, observe that the incremental load is defined in an implicit format in terms of the generalized stress $\mathfrak{s}:=\mathfrak{s}(t)$ at time t. Then, for a given external load $\mathfrak{s}$ of the volume element

Copyright © 2011 John Wiley & Sons, Ltd.

DOI: 10.1002/nme

depicted in Figure 3, the current generalized strains *and* internal variables are defined by the *constitutive minimization principle*

$$\boxed{(\mathfrak{f},\mathfrak{q})=\operatorname{Arg}\left\{\inf_{\mathfrak{f},\mathfrak{q}}\pi_d^\tau(\mathfrak{f},\mathfrak{q})\right\}=\operatorname{Arg}\left\{\inf_{\boldsymbol{f}}\inf_{\boldsymbol{d}}\inf_{\boldsymbol{b}}\inf_{\mathfrak{q}}\pi_d^\tau(\boldsymbol{f},\boldsymbol{d},\boldsymbol{b},\mathfrak{q})\right\}.} \tag{47}$$

The solution of this constitutive minimization principle is obtained within *two steps*, which correspond to typical algorithmic procedures in computational inelasticity with a *local* constitutive response. In a *first solution step*, π_d^τ in (45) is optimized for a *given* generalized deformation $\mathfrak{f}$ with respect to the current internal variables

$$(S1):\quad \mathfrak{q}=\operatorname{Arg}\left\{\inf_{\mathfrak{q}} w(\mathfrak{f},\mathfrak{q})\right\}. \tag{48}$$

This partial minimization defines a *reduced or condensed incremental work potential*

$$w_{\mathrm{red}}(\mathfrak{f})=\inf_{\mathfrak{q}} w(\mathfrak{f},\mathfrak{q}). \tag{49}$$

The Euler equation of (49) provides a *time-discrete* algorithmic form

$$\mathbf{0}\in\partial_{\mathfrak{q}}\psi(\mathfrak{f},\mathfrak{q})+\partial_{\dot{\mathfrak{q}}}\phi([\mathfrak{q}-\mathfrak{q}_n]/\tau) \tag{50}$$

of the Biot equation (39). Hence, the minimization problem (49) determines for given internal state $\mathfrak{q}_n$ at time t_n the current internal state $\mathfrak{q}$ at time t. With the reduced incremental work potential $w_{\mathrm{red}}(\mathfrak{f})$ defined in (49) at hand, we get the reduced potential function

$$\underbrace{\pi_{d,\mathrm{red}}^\tau(\mathfrak{f})}_{\text{potential}}:=\underbrace{w_{\mathrm{red}}(\mathfrak{f})}_{\text{int.work}}-\underbrace{\mathfrak{s}\cdot(\mathfrak{f}-\mathfrak{f}_n)}_{\text{ext.load}} \tag{51}$$

similar to the non-dissipative formulation (23). Hence, a *second solution step*, governed by the minimization principle

$$(S2):\quad \mathfrak{f}=\operatorname{Arg}\left\{\inf_{\mathfrak{f}}\pi_{d,\mathrm{red}}^\tau(\mathfrak{f})\right\}=\operatorname{Arg}\left\{\inf_{\boldsymbol{f}}\inf_{\boldsymbol{d}}\inf_{\boldsymbol{b}}\pi_{d,\mathrm{red}}^\tau(\boldsymbol{f},\boldsymbol{d},\boldsymbol{b})\right\} \tag{52}$$

similar to (24), defines for given generalized stress $\mathfrak{s}$ the generalized strain $\mathfrak{f}$. The Euler equation of this incremental variational principle

$$\mathfrak{s}=\partial_{\mathfrak{f}} w_{\mathrm{red}}(\mathfrak{f}) \tag{53}$$

has the same structure as the non-dissipative formulation (10), when the energy function $\psi(\mathfrak{f})$ is replaced by the incremental work potential $w_{\mathrm{red}}(\mathfrak{f})$ defined in (49). This relationship is unique if the incremental work potential $w_{\mathrm{red}}(\mathfrak{f})$ is *convex*, which follows for a stable electro-magneto-mechanical response form the convexity (22) of the energy function ψ *and* the convexity (41) of the dissipation function ϕ. This is a basic feature of the above outlined standard dissipative electro-magneto-mechanical media, where the evolution of the internal variables has the above outlined extremum property. The variational-based incremental constitutive structure is the basic foundation for the formulation of variational principles for the boundary-value problems in Section 5. Note that the incremental variational structure allows to write the coupled electro-magneto-mechanical tangent moduli at the current time t as the second derivative

$$\mathfrak{c}:=\partial_{\mathfrak{f}}\mathfrak{s}=\partial^2_{\mathfrak{f}\mathfrak{f}} w_{\mathrm{red}}(\mathfrak{f}) \tag{54}$$

of the reduced work potential. Hence, the incremental constitutive representation for a dissipative response is in full analogy to the non-dissipative response (10), if the free energy function $\psi(\mathfrak{f})$ is replaced by the incremental work potential $w_{\mathrm{red}}(\mathfrak{f})$. The key equations of the energy-based constitutive structure are summarized in Box 1.

Copyright © 2011 John Wiley & Sons, Ltd.

DOI: 10.1002/nme

Box 1: Constitutive equations in dissipative electro-magneto-mechanics.

1. *Dual Variables.* Forces and reactions in local electro-magneto-mechanics are

$$\left.\begin{array}{rl} \text{stress tensor} & \boldsymbol{\sigma} \\ \text{electric field vector} & \boldsymbol{e} \\ \text{magnetic field vector} & \boldsymbol{h} \\ \text{dissipative force array} & \mathfrak{p} \end{array}\right\} \quad \text{and} \quad \left\{\begin{array}{ll} \boldsymbol{f} & \text{deformation tensor} \\ \boldsymbol{d} & \text{electric displacement vector} \\ \boldsymbol{b} & \text{magnetic induction vector} \\ \mathfrak{q} & \text{internal variable array} \end{array}\right.$$

2. *Energy-based Formulation.* The *physically defined* generalized variables

$$\mathfrak{s} := [\boldsymbol{\sigma}, \boldsymbol{e}, \boldsymbol{h}]^{\mathrm{T}} \quad \text{and} \quad \mathfrak{f} := [\boldsymbol{f}, \boldsymbol{d}, \boldsymbol{b}]^{\mathrm{T}}$$

are related via *convex* energy and dissipation functions ψ and ϕ by

$$\mathfrak{s} = \partial_{\mathfrak{f}} \psi(\mathfrak{f}, \mathfrak{q}) \quad \text{with } \mathfrak{p} := -\partial_{\mathfrak{q}} \psi(\mathfrak{f}, \mathfrak{q}) \in \partial_{\dot{\mathfrak{q}}} \phi(\dot{\mathfrak{q}})$$

and initial condition $\mathfrak{q}(0) = \mathfrak{q}_0$ for internal variables. These are the Euler equations of an incremental constitutive *minimization principle*

$$\boxed{(\mathfrak{f}, \mathfrak{q}) = \operatorname{Arg}\left\{ \inf_{\boldsymbol{f}} \inf_{\boldsymbol{d}} \inf_{\boldsymbol{b}} \inf_{\mathfrak{q}} \pi_d^\tau(\boldsymbol{f}, \boldsymbol{d}, \boldsymbol{b}, \mathfrak{q}) \right\}}.$$

$$\pi_d^\tau(\mathfrak{f}, \mathfrak{q}) := \psi(\mathfrak{f}, \mathfrak{q}) - \psi(\mathfrak{f}_n, \mathfrak{q}_n) + \tau \phi([\mathfrak{q} - \mathfrak{q}_n]/\tau) - \mathfrak{s} \cdot (\mathfrak{f} - \mathfrak{f}_n).$$

3. *Enthalpy-based Formulation.* The *geometrically defined* generalized variables

$$\mathfrak{s}' := [\boldsymbol{\sigma}, -\boldsymbol{d}, -\boldsymbol{b}]^{\mathrm{T}} \quad \text{and } \mathfrak{f}' := [\boldsymbol{f}, \boldsymbol{e}, \boldsymbol{h}]^{\mathrm{T}}$$

are related via *convex–concave* enthalpy and *convex* dissipation functions ψ' and ϕ

$$\mathfrak{s}' = \partial_{\mathfrak{f}'} \psi'(\mathfrak{f}', \mathfrak{q}) \quad \text{with } \mathfrak{p} := -\partial_{\mathfrak{q}} \psi'(\mathfrak{f}', \mathfrak{q}) \in \partial_{\dot{\mathfrak{q}}} \phi(\dot{\mathfrak{q}})$$

and initial condition $\mathfrak{q}(0) = \mathfrak{q}_0$ for internal variables. These are the Euler equations of an incremental constitutive *saddle-point principle*

$$\boxed{(\mathfrak{f}', \mathfrak{q}) = \operatorname{Arg}\left\{ \inf_{\boldsymbol{f}} \sup_{\boldsymbol{e}} \sup_{\boldsymbol{h}} \inf_{\mathfrak{q}} \pi_d'^\tau(\boldsymbol{f}, \boldsymbol{e}, \boldsymbol{h}, \mathfrak{q}) \right\}}.$$

$$\pi_d'^\tau(\mathfrak{f}', \mathfrak{q}) := \psi'(\mathfrak{f}', \mathfrak{q}) - \psi'(\mathfrak{f}_n', \mathfrak{q}_n) + \tau \phi([\mathfrak{q} - \mathfrak{q}_n]/\tau) - \mathfrak{s}' \cdot (\mathfrak{f}' - \mathfrak{f}_n').$$

2.3.6. Incrementally stable dissipative material response. With the above closed-form representation (54) of the tangent moduli at hand, we define an incrementally stable dissipative electro-magneto-mechanical response as follows. Consider at the current time t in analogy to (19) the incremental second-order work

$$\mathscr{S} := \Delta\mathfrak{s} \cdot \Delta\mathfrak{f} \geqslant 0 \quad \text{for all } \Delta\mathfrak{f} \neq \mathbf{0}. \tag{55}$$

It characterizes an incrementally stable dissipative response such that an increase in the generalized strain produces an increase in the generalized stress. Taking into account the linear increment of the generalized stresses $\Delta\mathfrak{s} = \mathfrak{c} \cdot \Delta\mathfrak{f}$, we obtain

$$\mathscr{S} := \Delta\mathfrak{f} \cdot \mathfrak{c} \cdot \Delta\mathfrak{f} \geqslant 0 \quad \text{for all } \Delta\mathfrak{f} \neq \mathbf{0} \tag{56}$$

Copyright © 2011 John Wiley & Sons, Ltd.

DOI: 10.1002/nme

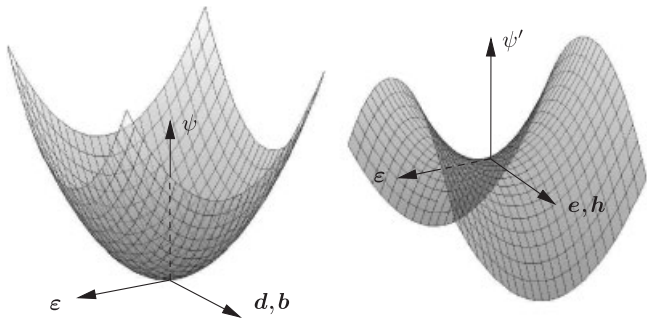

(a) Energy Formulation (b) Enthalpy Formulation

Figure 4. Minimum and saddle-point structure of constitutive variational problems: (a) *Energy-based setting* $\psi(\boldsymbol{\varepsilon}, \boldsymbol{d}, \boldsymbol{b}, \cdot)$ with a canonical physically based arrangement of dual variables provides a minimization structure and (b) *Enthalpy-based setting* $\psi'(\boldsymbol{\varepsilon}, \boldsymbol{e}, \boldsymbol{h}, \cdot)$ with a convenient geometry-based arrangement of dual variables has a saddle-point structure.

enforcing the *positive definiteness* of the coupled electro-magneto-mechanical tangent moduli $\mathbf{c}$ at the current time t. This extends the stability condition (20) from the non-dissipative to the incrementally dissipative response. Because the tangent moduli are obtained via (54) as the second derivative of the incremental work potential w_{red}, we have

$$\mathscr{S}^{\tau} := \Delta\mathfrak{f} \cdot \partial^2_{\mathfrak{f}\mathfrak{f}} w_{\text{red}}(\mathfrak{f}) \cdot \Delta\mathfrak{f} \geqslant 0 \quad \text{for all } \Delta\mathfrak{f} \neq \mathbf{0} \tag{57}$$

enforcing the *incremental work potential* w_{red} *to be locally convex*, as visualized in Figure 4(a). This is ensured for models with convex free energy and dissipation functions ψ and ϕ, see (22) and (41). It guarantees the uniqueness of the dissipative electro-magneto-mechanical loading process.

2.4. Rate-independent formulation based on threshold functions

2.4.1. A class of rate-independent dissipation functions. In practical engineering applications, rate-independent dissipation functions are often modeled by the so-called *concept of maximum dissipation*, a terminology that can be traced back to the plasticity theory, see for example Hill [76], Maugin [77] and Han and reddy [78]. Here, the dissipation function is defined by the constrained maximum problem

$$\phi(\dot{\mathbf{q}}) = \sup_{\mathfrak{p} \in \mathbb{E}} \mathfrak{p} \cdot \dot{\mathbf{q}}, \tag{58}$$

where $\mathbb{E}$ models a *reversible domain* in the space of the driving forces $\mathfrak{p}$

$$\mathbb{E} := \{\mathfrak{p} \in \mathscr{R}^m \,|\, f(\mathfrak{p}) \leqslant c\} \tag{59}$$

in terms of a *threshold, yield or switching function* $f : \mathscr{R}^m \to \mathscr{R}$, which is positive $f(\mathfrak{p}) \geqslant 0$, normalized $f(\mathbf{0}) = 0$, convex and positively homogeneous of the order one $f(\alpha\mathfrak{p}) = \alpha f(\mathfrak{p})$ for $\alpha > 0$. The *threshold value* $c > 0$ bounds in combination with a particular choice of the function f the driving force $\mathfrak{p}$. The constrained maximum problem (58) can be solved by a Lagrange method

$$\phi(\dot{\mathbf{q}}) = \sup_{\mathfrak{p}, \lambda \geqslant 0} [\mathfrak{p} \cdot \dot{\mathbf{q}} - \lambda(f(\mathfrak{p}) - c)] \tag{60}$$

yielding as necessary conditions of the form

$$\boxed{\dot{\mathbf{q}} = \lambda \partial_{\mathfrak{p}} f(\mathfrak{p})} \tag{61}$$

for the evolution of the internal variables along with the loading–unloading conditions

$$\lambda \geqslant 0, \quad f(\mathfrak{p}) \leqslant c, \quad \lambda(f(\mathfrak{p}) - c) = 0. \tag{62}$$

Copyright © 2011 John Wiley & Sons, Ltd.

DOI: 10.1002/nme

The latter determine the non-smooth dissipative response by the yield or switching function f, which is in this type of modeling the basic constitutive function besides the free energy function. Note that insertion of (61) into (60) identifies the image of the dissipation function to be the simple expression $\mathscr{D}=\phi(\dot{\mathbf{q}})=c\lambda\geqslant 0$. (61) combined with (62) is a specific form of (44) for rate-independent response governed by a switching function f.[‖]

2.4.2. Incremental constitutive saddle-point principle. For rate-independent dissipative processes with reversible ranges $\mathbb{E}$ defined in (59) based on switching functions f, we modify the principle (49) by inserting the specific dissipation function (60). This yields the algorithmic form

$$\boxed{w_{\mathrm{red}}(\mathbf{f})=\inf_{\mathbf{q}}\sup_{\mathbf{p},\gamma\geqslant 0}\tilde{w}(\mathbf{f},\mathbf{q},\mathbf{p},\gamma)} \tag{64}$$

in terms of a modified algorithmic expression for the incremental electro-magneto-mechanical work (46), reading

$$\tilde{w}(\mathbf{f},\mathbf{q},\mathbf{p},\gamma)=\psi(\mathbf{f},\mathbf{q})-\psi(\mathbf{f}_n,\mathbf{q}_n)+\mathbf{p}\cdot[\mathbf{q}-\mathbf{q}_n]-\gamma(f(\mathbf{p})-c). \tag{65}$$

Here, $\gamma:=\lambda\tau$ is the Lagrange parameter associated with the increment $[t_n,t]$. In this expression, the increment of dissipated internal work is formulated in terms of the driving force $\mathbf{p}$. The last Lagrange term ensures the consistence *for the case of loading* $\gamma>0$, where the internal variable develops within the current time step. Box 2 summarizes the key structure of the constitutive formulation.

2.4.3. Update algorithm for dissipative variables. The necessary condition of the constitutive variational principle (64) for the case of loading $\gamma>0$ yield

$$\tilde{\boldsymbol{r}}:=\begin{bmatrix}\partial_{\mathbf{q}}\tilde{w}\\ \partial_{\mathbf{p}}\tilde{w}\\ \partial_{\gamma}\tilde{w}\end{bmatrix}=\begin{bmatrix}\partial_{\mathbf{q}}\psi+\mathbf{p}\\ \mathbf{q}-\mathbf{q}_n-\gamma\partial_{\mathbf{p}}f\\ -f+c\end{bmatrix}=\mathbf{0} \tag{66}$$

the algorithmic versions of the internal force definition $(30)_2$ and the evolution equation (61) along with the discrete version

$$\gamma\geqslant 0,\quad f(\mathbf{p})\leqslant c,\quad \gamma(f(\mathbf{p})-c)=0 \tag{67}$$

of the loading–unloading conditions (62). Owing to the assumed convexity of the switching function f, the decision of incremental accumulation of the internal variables can be based on its trial value f^{trial}. *Driven* by the current generalized deformation $\mathbf{f}$, the incremental response is for

$$f^{\mathrm{trial}}:=f(\mathbf{p}^{\mathrm{trial}})=f(-\partial_{\mathbf{q}}\psi(\mathbf{f},\mathbf{q}_n))\leqslant c \tag{68}$$

non-dissipative, i.e. $\gamma=0$ and $\mathbf{q}=\mathbf{q}_n$. For $f^{\mathrm{trial}}>c$, we face an incremental step with a change in the internal variable state. Then, the non-linear system (66) is solved at *given* generalized deformation $\mathbf{f}$ by a local Newton-type algorithm for the current variables $\tilde{\boldsymbol{v}}:=\{\mathbf{q},\mathbf{p},\gamma\}$ at time t

$$\tilde{\boldsymbol{v}}\Leftarrow\tilde{\boldsymbol{v}}-\tilde{\boldsymbol{a}}^{-1}\tilde{\boldsymbol{r}} \tag{69}$$

[‖]*Representation of Switching Function.* A typical example of an *isotropic* switching function is simply the norm of the dissipative driving force $\mathbf{p}$, i.e.

$$f(\mathbf{p})=|\mathbf{p}|:=(\mathbf{p}\cdot\mathbf{p})^{1/2}, \tag{63}$$

which is for example suitable when combined with the reduced dissipative model of ferroelectricity based on (33)–(37). Alternative representations of switching functions for ferroelectricity are outlined in Bassiouny *et al.* [26], Huber and Fleck [36] and Landis [34].

Copyright © 2011 John Wiley & Sons, Ltd.

DOI: 10.1002/nme

Box 2: Constitutive updates for rate-independent response.

1. *Energy-based Formulation.* Driven by the mechanical deformation $\boldsymbol{f}$, the electric displacement $\boldsymbol{d}$ and the magnetic induction $\boldsymbol{b}$ at the current time t, i.e. for *given*

$$\mathfrak{f} := [\boldsymbol{f}(\boldsymbol{x},t), \boldsymbol{d}(\boldsymbol{x},t), \boldsymbol{b}(\boldsymbol{x},t)]^{\mathrm{T}} \quad \text{and} \quad \mathfrak{q}_n = \mathfrak{q}(\boldsymbol{x},t_n)$$

the update of the internal variables $\mathfrak{q}$, forces $\mathfrak{p}$ and parameter γ, governed by *convex* energy and switching functions ψ and f, defines the incremental work potential

$$\boxed{w_{\mathrm{red}}(\mathfrak{f}) = \inf_{\mathfrak{q}} \sup_{\mathfrak{p},\gamma\geqslant 0} \tilde{w}(\mathfrak{f},\mathfrak{q},\mathfrak{p},\gamma)}.$$

$$\tilde{w}(\mathfrak{f},\mathfrak{q},\mathfrak{p},\gamma) := \psi(\mathfrak{f},\mathfrak{q}) - \psi(\mathfrak{f}_n,\mathfrak{q}_n) + \mathfrak{p}\cdot[\mathfrak{q}-\mathfrak{q}_n] - \gamma(f(\mathfrak{p})-c).$$

Equations (66)–(72) outline the necessary algorithmic steps.

2. *Enthalpy-based Formulation.* Driven by the mechanical deformation $\boldsymbol{f}$, the electric field $\boldsymbol{e}$ and the magnetic field $\boldsymbol{h}$ at the current time t, i.e. for *given*

$$\mathfrak{f}' := [\boldsymbol{f}(\boldsymbol{x},t), \boldsymbol{e}(\boldsymbol{x},t), \boldsymbol{h}(\boldsymbol{x},t)]^{\mathrm{T}} \quad \text{and} \quad \mathfrak{q}_n = \mathfrak{q}(\boldsymbol{x},t_n)$$

the update of the internal variables $\mathfrak{q}$, forces $\mathfrak{p}$ and parameter γ, governed by *convex–concave* energy and *convex* switching functions ψ' and f, defines the incremental work potential

$$\boxed{w'_{\mathrm{red}}(\mathfrak{f}') := \inf_{\mathfrak{q}} \sup_{\mathfrak{p},\gamma\geqslant 0} \tilde{w}'(\mathfrak{f}',\mathfrak{q},\mathfrak{p},\gamma).}$$

$$\tilde{w}'(\mathfrak{f}',\mathfrak{q},\mathfrak{p},\gamma) = \psi'(\mathfrak{f}',\mathfrak{q}) - \psi'(\mathfrak{f}'_n,\mathfrak{q}_n) + \mathfrak{p}\cdot[\mathfrak{q}-\mathfrak{q}_n] - \gamma(f(\mathfrak{p})-c).$$

Equations (112)–(114) outline the necessary algorithmic steps.

until convergence is achieved in the sense $|\tilde{\boldsymbol{r}}| < \mathrm{tol}$. Here, the tangent matrix of the Newton iteration has the form

$$\tilde{\boldsymbol{a}} := \begin{bmatrix} \partial^2_{\mathfrak{q}\mathfrak{q}}\tilde{w} & \partial^2_{\mathfrak{q}\mathfrak{p}}\tilde{w} & \partial^2_{\mathfrak{q}\gamma}\tilde{w} \\ \partial^2_{\mathfrak{p}\mathfrak{q}}\tilde{w} & \partial^2_{\mathfrak{p}\mathfrak{p}}\tilde{w} & \partial^2_{\mathfrak{p}\gamma}\tilde{w} \\ \partial^2_{\gamma\mathfrak{q}}\tilde{w} & \partial^2_{\gamma\mathfrak{p}}\tilde{w} & \partial^2_{\gamma\gamma}\tilde{w} \end{bmatrix} = \begin{bmatrix} \partial^2_{\mathfrak{q}\mathfrak{q}}\psi & \mathbf{1} & \mathbf{0} \\ \mathbf{1} & -\gamma\partial^2_{\mathfrak{p}\mathfrak{p}}f & -\partial_{\mathfrak{p}}f \\ \mathbf{0} & -\partial_{\mathfrak{p}}f & \mathbf{0} \end{bmatrix}. \tag{70}$$

Then, evaluation of the potential equations (53) and (54) finally gives the generalized stresses and the moduli at the current time t

$$\mathfrak{s} := \partial_{\mathfrak{f}} w_{\mathrm{red}} = \partial_{\mathfrak{f}}\psi \quad \text{and} \quad \mathfrak{c} := \partial^2_{\mathfrak{f}\mathfrak{f}} w_{\mathrm{red}} = \partial^2_{\mathfrak{f}\mathfrak{f}}\psi - s \begin{bmatrix} \partial^2_{\mathfrak{f}\mathfrak{q}}\psi \\ \mathbf{0} \\ \mathbf{0} \end{bmatrix}^{\mathrm{T}} \tilde{\boldsymbol{a}}^{-1} \begin{bmatrix} \partial^2_{\mathfrak{q}\mathfrak{f}}\psi \\ \mathbf{0} \\ \mathbf{0} \end{bmatrix} \tag{71}$$

of the coupled problem in terms of a dissipative loading flag

$$s := \begin{cases} 1 & \text{for } f^{\mathrm{trial}} > c, \\ 0 & \text{otherwise.} \end{cases} \tag{72}$$

Copyright © 2011 John Wiley & Sons, Ltd.

DOI: 10.1002/nme

Note that the second part in $(71)_2$ characterizes the softening of the fully coupled electro-magneto-mechanical tangent moduli due to the evolution of internal variables. The moduli are *symmetric* due to the underlying variational structure.

2.5. Rate-dependent formulation based on threshold functions

2.5.1. A class of rate-dependent dissipation functions. A rate-dependent class of dissipation functions with reversible range $\mathbb{E}$ governed by the above introduced switching function f is obtained by an approximate penalty-type solution of the maximum problem (58)

$$\phi(\dot{\mathbf{q}}) = \sup_{\mathfrak{p}} \left[\mathfrak{p} \cdot \dot{\mathbf{q}} - \frac{c}{\eta(m+1)} \langle f(\mathfrak{p})/c - 1 \rangle^{m+1} \right] \tag{73}$$

where the constants $\eta > 0$ and $m > 0$ are interpreted as material parameters associated with the viscosity of the dissipative electro-magneto-mechanical process. $\langle x \rangle = \frac{1}{2}(x + |x|)$ is the ramp function expressed by the McAuley bracket. The necessary condition of (73) provides the non-linear evolution equation

$$\boxed{\dot{\mathbf{q}} = \frac{1}{\eta} \langle f(\mathfrak{p})/c - 1 \rangle^{m} \partial_{\mathfrak{p}} f(\mathfrak{p})} \,. \tag{74}$$

in terms of a dimensionless, driving internal *over-force* $\langle f(\mathfrak{p})/c - 1 \rangle$. The structure of this evolution equation is borrowed from Perzyna-type visco-plasticity, see Perzyna [84]. This *smooth* evolution equation may be directly obtained from (44) based on the dual dissipation function

$$\phi^*(\mathfrak{p}) = \frac{c}{\eta(m+1)} \langle f(\mathfrak{p})/c - 1 \rangle^{m+1}, \tag{75}$$

which follows immediately from (73), if the penalty-type variational principle is interpreted as a Legendre–Fenchel transformation. For $\eta \to 0$ we obtain in the limit the rate-independent form (61) combined with (62).

2.5.2. Incremental constitutive saddle-point principle. For the rate-dependent dissipative processes with reversible range $\mathbb{E}$ defined in (59) based on switching functions f, we modify the principle (49) by inserting the specific dissipation function (73). This yields the representation

$$\boxed{w_{\mathrm{red}}(\mathfrak{f}) = \inf_{\mathfrak{q}} \sup_{\mathfrak{p}} \overline{w}(\mathfrak{f}, \mathfrak{q}, \mathfrak{p})} \tag{76}$$

in terms of a modified algorithmic expression for the incremental electro-magneto-mechanical work (46), defined by

$$\overline{w}(\mathfrak{f}, \mathfrak{q}, \mathfrak{p}) = \psi(\mathfrak{f}, \mathfrak{q}) - \psi(\mathfrak{f}_n, \mathfrak{q}_n) + \mathfrak{p} \cdot [\mathfrak{q} - \mathfrak{q}_n] - \frac{c\tau}{\eta(m+1)} \langle f(\mathfrak{p})/c - 1 \rangle^{m+1}. \tag{77}$$

Similar to (65), the increment of dissipated internal work is formulated in terms of the driving force $\mathfrak{p}$. The last term may be interpreted as a penalty term with penalty parameter $1/\eta$, which ensures approximatively the consistency of the rate-independent theory. Box 3 summarizes the structure of this constitutive setting.

2.5.3. Update algorithm for dissipative variables. The necessary condition of the constitutive variational principle (76) yields

$$\bar{\boldsymbol{r}} := \begin{bmatrix} \partial_{\mathfrak{q}} \overline{w} \\ \partial_{\mathfrak{p}} \overline{w} \end{bmatrix} = \begin{bmatrix} \partial_{\mathfrak{q}} \psi + \mathfrak{p} \\ \mathfrak{q} - \mathfrak{q}_n - \dfrac{\tau}{\eta} \langle f/c - 1 \rangle^{m} \partial_{\mathfrak{p}} f \end{bmatrix} = \mathbf{0} \tag{78}$$

Copyright © 2011 John Wiley & Sons, Ltd.

DOI: 10.1002/nme

Box 3: Constitutive updates for rate-dependent response.

1. *Energy-based Formulation.* Driven by the mechanical deformation $\boldsymbol{f}$, the electric displacement $\boldsymbol{d}$ and the magnetic induction $\boldsymbol{b}$ at the current time t, i.e. for *given*

$$\mathfrak{f} := [\boldsymbol{f}(\boldsymbol{x},t), \boldsymbol{d}(\boldsymbol{x},t), \boldsymbol{b}(\boldsymbol{x},t)]^{\mathrm{T}} \quad \text{and} \quad \mathfrak{q}_n = \mathfrak{q}(\boldsymbol{x},t_n)$$

the update of the internal variables $\mathfrak{q}$ and forces $\mathfrak{p}$, governed by *convex* energy and switching functions ψ and f, defines the incremental internal work potential

$$\boxed{w_{\mathrm{red}}(\mathfrak{f}) = \inf_{\mathfrak{q}} \sup_{\mathfrak{p}} \overline{w}(\mathfrak{f},\mathfrak{q},\mathfrak{p}).}$$

$$\overline{w}(\mathfrak{f},\mathfrak{q},\mathfrak{p}) := \psi(\mathfrak{f},\mathfrak{q}) - \psi(\mathfrak{f}_n,\mathfrak{q}_n) + \mathfrak{p}\cdot[\mathfrak{q}-\mathfrak{q}_n] - \frac{c\tau}{\eta(m+1)}\langle f(\mathfrak{p})/c - 1\rangle^{m+1}.$$

Equations (78)–(81) outline the necessary algorithmic steps.

2. *Enthalpy-based Formulation.* Driven by the mechanical deformation $\boldsymbol{f}$, the electric field $\boldsymbol{e}$ and the magnetic field $\boldsymbol{h}$ at the current time t, i.e. for *given*

$$\mathfrak{f}' := [\boldsymbol{f}(\boldsymbol{x},t), \boldsymbol{e}(\boldsymbol{x},t), \boldsymbol{h}(\boldsymbol{x},t)]^{\mathrm{T}} \quad \text{and} \quad \mathfrak{q}_n = \mathfrak{q}(\boldsymbol{x},t_n)$$

the update of the internal variables $\mathfrak{q}$ and forces $\mathfrak{p}$, governed by *convex–concave* enthalpy and *convex* switching functions ψ' and f, defines the incremental internal work potential

$$\boxed{w'_{\mathrm{red}}(\mathfrak{f}') = \inf_{\mathfrak{q}} \sup_{\mathfrak{p}} \overline{w}'(\mathfrak{f},\mathfrak{q},\mathfrak{p}).}$$

$$\overline{w}'(\mathfrak{f}',\mathfrak{q},\mathfrak{p}) := \psi'(\mathfrak{f}',\mathfrak{q}) - \psi'(\mathfrak{f}'_n,\mathfrak{q}_n) + \mathfrak{p}\cdot[\mathfrak{q}-\mathfrak{q}_n] - \frac{c\tau}{\eta(m+1)}\langle f(\mathfrak{p})/c - 1\rangle^{m+1}.$$

Equations (117)–(119) outline the necessary algorithmic steps.

the algorithmic versions of the internal force definition $(30)_2$ and the viscous evolution equation (74). The above non-linear system can be solved at *given* generalized deformation $\mathfrak{f}$ by a local Newton-type algorithm for the current variables $\overline{\boldsymbol{v}} := \{\mathfrak{q},\mathfrak{p}\}$

$$\overline{\boldsymbol{v}} \Leftarrow \overline{\boldsymbol{v}} - \overline{\boldsymbol{a}}^{-1}\overline{\boldsymbol{r}} \tag{79}$$

until convergence $|\overline{\boldsymbol{r}}| < tol$. The tangent matrix of the Newton iteration has the form

$$\overline{\boldsymbol{a}} := \begin{bmatrix} \partial^2_{\mathfrak{q}\mathfrak{q}}\overline{w} & \partial^2_{\mathfrak{q}\mathfrak{p}}\overline{w} \\ \partial^2_{\mathfrak{p}\mathfrak{q}}\overline{w} & \partial^2_{\mathfrak{p}\mathfrak{p}}\overline{w} \end{bmatrix} = \begin{bmatrix} \partial^2_{\mathfrak{q}\mathfrak{q}}\psi & \mathbf{1} \\ \mathbf{1} & -\dfrac{m\tau}{c\eta}\langle f/c-1\rangle^{m-1}\partial_{\mathfrak{p}} f \otimes \partial_{\mathfrak{p}} f - \dfrac{\tau}{\eta}\langle f/c-1\rangle^{m}\partial^2_{\mathfrak{p}\mathfrak{p}} f \end{bmatrix}. \tag{80}$$

The evaluation of the potential equations (53) and (54) then gives the generalized stresses and moduli at the current time t

$$\mathfrak{s} := \partial_{\mathfrak{f}} w_{\mathrm{red}} = \partial_{\mathfrak{f}}\psi \quad \text{and} \quad \mathfrak{c} := \partial^2_{\mathfrak{f}\mathfrak{f}} w_{\mathrm{red}} = \partial^2_{\mathfrak{f}\mathfrak{f}}\psi - \begin{bmatrix} \partial^2_{\mathfrak{f}\mathfrak{q}}\psi \\ \mathbf{0} \end{bmatrix}^{\mathrm{T}} \overline{\boldsymbol{a}}^{-1} \begin{bmatrix} \partial^2_{\mathfrak{q}\mathfrak{f}}\psi \\ \mathbf{0} \end{bmatrix}, \tag{81}$$

where the second term in $(81)_2$ is the softening of the *symmetric*, fully coupled tangent moduli due to the evolution of internal variables.

Copyright © 2011 John Wiley & Sons, Ltd.

DOI: 10.1002/nme

3. ENTHALPY-BASED CONSTITUTIVE VARIATIONAL PRINCIPLES

We now outline variational formulations of an *enthalpy*-based setting of the local dissipative response in electro-magneto-mechanics, again focusing on a local point of the continuum as depicted in Figure 1.

3.1. Energy–Enthalpy Formulation of Non-dissipative Response

3.1.1. Change of electro-magnetic primary variables. The above outlined energy-based constitutive setting with the *physically based definition* (3) of generalized stress and deformation, which assembles *forces* $\mathfrak{s}$ and *reactions* $\mathfrak{f}$, is not consistent with the straightforward formulations of coupled electro-magneto-mechanical boundary-value problems outlined in Section 4. In this context, the simplest way is to consider the electric and magnetic field strengths $\boldsymbol{e}$ and $\boldsymbol{h}$ as independent variables that determine the electric displacement $\boldsymbol{d}$ and the magnetic induction $\boldsymbol{b}$ by constitutive functions. Such a formulation is related to a *new geometry-based definition* of generalized stress and deformation, which assemble the *vectors* and *co-vectors*

$$\boxed{\mathfrak{s}' := [\boldsymbol{\sigma}, -\boldsymbol{d}, -\boldsymbol{b}]^{\mathrm{T}} \quad \text{and} \quad \mathfrak{f}' := [\boldsymbol{f}, \boldsymbol{e}, \boldsymbol{h}]^{\mathrm{T}}} \tag{82}$$

acting on the local volume element depicted in Figure 2, with $\{\mathfrak{s}', \mathfrak{f}'\} \in \mathscr{R}^{d\times d+2d}$. Observe that the electro-magnetic slots are simply interchanged.

3.1.2. Constitutively defined modified forces. The associated constitutive potential which links these variables is provided by what we denote in what follows as the *mixed energy–enthalpy function* $\psi' : \mathscr{R}^{d\times d+2d} \to \mathscr{R}$. It is obtained from the free energy function ψ by the Legendre transformation

$$\psi'(\boldsymbol{f}, \boldsymbol{e}, \boldsymbol{h}) := \inf_{\boldsymbol{d},\boldsymbol{b}} [\psi(\boldsymbol{f}, \boldsymbol{d}, \boldsymbol{b}) - \boldsymbol{e}\cdot\boldsymbol{d} - \boldsymbol{h}\cdot\boldsymbol{b}] \tag{83}$$

with respect to the electro-magnetic slots. From this definition, we conclude the potential relationship

$$\boxed{\mathfrak{s}'(t) = \partial_{\mathfrak{f}'}\psi'(\mathfrak{f}'(t))} \tag{84}$$

which defines the modified generalized stress in terms of the modified generalized strain. It is dual to (10) with regard to the electro-magnetic slots and consists of the three coupled parts

$$\boldsymbol{\sigma} = \partial_{\boldsymbol{f}}\psi'(\boldsymbol{f}, \boldsymbol{e}, \boldsymbol{h}), \quad \boldsymbol{d} = -\partial_{\boldsymbol{e}}\psi'(\boldsymbol{f}, \boldsymbol{e}, \boldsymbol{h}), \quad \boldsymbol{b} = -\partial_{\boldsymbol{h}}\psi'(\boldsymbol{f}, \boldsymbol{e}, \boldsymbol{h}), \tag{85}$$

which constitute the dependencies of the total stress tensor, the electric displacement and the magnetic induction vectors on the deformation tensor, the electric and magnetic field strengths, respectively. Associated with the mixed energy–enthalpy function ψ', we may define the modified electro-magneto-mechanical power

$$\mathscr{P}' := \mathscr{P} - \frac{\mathrm{d}}{\mathrm{d}t}[\boldsymbol{e}\cdot\boldsymbol{d} + \boldsymbol{h}\cdot\boldsymbol{b}] = \mathfrak{s}'\cdot\dot{\mathfrak{f}}' \tag{86}$$

with the explicit representation

$$\underbrace{\mathscr{P}'}_{\text{total}} = \underbrace{\boldsymbol{\sigma}:\dot{\boldsymbol{f}}}_{\text{mechanic}} - \underbrace{\boldsymbol{d}\cdot\dot{\boldsymbol{e}}}_{\text{electric}} - \underbrace{\boldsymbol{b}\cdot\dot{\boldsymbol{h}}}_{\text{magnetic}} \tag{87}$$

As a consequence, the constitutive potential relationship (84) for non-dissipative response may be obtained from the power argument $\mathscr{P}' = (\mathrm{d}/\mathrm{d}t)\psi'(\mathfrak{f}'(t))$, yielding $\mathfrak{s}'\cdot\dot{\mathfrak{f}}' = \partial_{\mathfrak{f}'}\psi'\cdot\dot{\mathfrak{f}}'$, which must be satisfied for all possible rates $\dot{\mathfrak{f}}'$. The mixed energy–enthalpy is assumed to satisfy *normalization*

Copyright © 2011 John Wiley & Sons, Ltd.

DOI: 10.1002/nme

constraints $\psi'(\mathbf{0})=0$ and $\partial_{\mathfrak{f}'}\psi'(\mathbf{0})=\mathbf{0}$ in analogy to (12), and must be *objective* satisfying the reduced form

$$\psi'(\boldsymbol{f},\boldsymbol{e},\boldsymbol{h})=\tilde{\psi}'(\boldsymbol{\varepsilon},\boldsymbol{e},\boldsymbol{h}) \quad \text{with } \boldsymbol{\varepsilon}:=\tfrac{1}{2}(\boldsymbol{f}+\boldsymbol{f}^{\mathrm{T}}) \tag{88}$$

similar to (13). These conditions are automatically satisfied if ψ' is computed from ψ via the transformation (83).

3.1.3. Stable constitutive response. A stable electro-magneto-mechanical response was shown to be related to a convex free energy function ψ. Note carefully that, due to the *partial* Legendre transformation (83), which affects only the electro-magnetic slots and leaves the mechanical slot unchanged, the resulting mixed energy–enthalpy function ψ' *is a convex–concave saddle-point function* as depicted in Figure 4(b). We refer to Rockafellar [85] for further details on the mathematics of convex analysis. Thus we have, induced by (22), the properties

$$\alpha\psi'(\boldsymbol{f}_1,\boldsymbol{e},\boldsymbol{h})+(1-\alpha)\psi'(\boldsymbol{f}_2,\boldsymbol{e},\boldsymbol{h})\geqslant\psi'(\alpha\boldsymbol{f}_1+(1-\alpha)\boldsymbol{f}_2,\boldsymbol{e},\boldsymbol{h}) \tag{89}$$

for the mechanical slot but

$$\alpha\psi'(\boldsymbol{f},[\boldsymbol{e},\boldsymbol{h}]_1^{\mathrm{T}})+(1-\alpha)\psi'(\boldsymbol{f},[\boldsymbol{e},\boldsymbol{h}]_2^{\mathrm{T}})\leqslant\psi'(\boldsymbol{f},\alpha[\boldsymbol{e},\boldsymbol{h}]_1^{\mathrm{T}}+(1-\alpha)[\boldsymbol{e},\boldsymbol{h}]_2^{\mathrm{T}}) \tag{90}$$

for the electro-magnetic slots with $\alpha\in[0,1]$. As a consequence of the convex–concave property of ψ', the modified second-order work expression

$$\mathscr{S}':=\dot{\mathfrak{f}}'\cdot\mathfrak{c}'\cdot\dot{\mathfrak{f}}' \tag{91}$$

is *not positive* for arbitrary $\dot{\mathfrak{f}}'\neq\mathbf{0}$, because the electro-magneto-mechanical moduli associated with the mixed energy–enthalpy representation

$$\mathfrak{c}':=\partial^2_{\mathfrak{f}'\mathfrak{f}'}\psi'(\mathfrak{f}')=\begin{bmatrix}\partial^2_{\boldsymbol{ff}}\psi' & \partial^2_{\boldsymbol{fe}}\psi' & \partial^2_{\boldsymbol{fh}}\psi'\\ \partial^2_{\boldsymbol{ef}}\psi' & \partial^2_{\boldsymbol{ee}}\psi' & \partial^2_{\boldsymbol{eh}}\psi'\\ \partial^2_{\boldsymbol{hf}}\psi' & \partial^2_{\boldsymbol{he}}\psi' & \partial^2_{\boldsymbol{hh}}\psi'\end{bmatrix} \tag{92}$$

are *not positive definite*. A convex–concave mixed energy–enthalpy function ψ' of the generalized strain $\mathfrak{f}'$ ensures uniqueness of the local electro-magneto-mechanical loading process. The conditions (89) and (90) provide constraints for a *direct* modeling of the mixed energy–enthalpy function, but are automatically satisfied if ψ' is computed from ψ via the transformation (83).

3.1.4. Incremental constitutive saddle-point principle. The above outlined constitutive equation (84) can be related to an incremental constitutive stationary principle as follows. Consider a typical time increment $\tau:=t-t_n$ and introduce the potential $\pi'^{\tau}:=\int_{t_n}^{t}[\dot{\psi}'-\mathscr{P}']\mathrm{d}t$ with the algorithmic approximation

$$\underbrace{\pi'^{\tau}(\mathfrak{f}')}_{\text{potential}}:=\underbrace{\psi'(\mathfrak{f}')-\psi'(\mathfrak{f}'_n)}_{\text{storage}}-\underbrace{\mathfrak{s}'\cdot(\mathfrak{f}'-\mathfrak{f}'_n)}_{\text{ext. load}} \tag{93}$$

in analogy to (23). This potential is now formulated in terms of the incremental mixed energy–enthalpy function and the increment of the modified power (86). It is a function of the current generalized strain $\mathfrak{f}':=\mathfrak{f}'(t)$ at time t and refers to the *fixed-value* $\mathfrak{f}'_n:=\mathfrak{f}'(t_n)$ at time t_n. Note that the incremental load is defined in an implicit format in terms of the generalized stress $\mathfrak{s}':=\mathfrak{s}'(t)$ at time t. For a given external load $\mathfrak{s}'$ of the volume element depicted in Figure 2, the associated generalized strain is defined by the *constitutive stationary principle*

$$\boxed{\mathfrak{f}'=\operatorname{Arg}\left\{\operatorname*{stat}_{\mathfrak{f}'}\pi'^{\tau}(\mathfrak{f}')\right\}=\operatorname{Arg}\left\{\inf_{\boldsymbol{f}}\sup_{\boldsymbol{e}}\sup_{\boldsymbol{h}}\pi'^{\tau}(\boldsymbol{f},\boldsymbol{e},\boldsymbol{h})\right\}.} \tag{94}$$

Copyright © 2011 John Wiley & Sons, Ltd.

DOI: 10.1002/nme

The Euler equation of this variational principle is the constitutive equation (84), which defines for a given generalized stress $\mathfrak{s}'$ the generalized strain $\mathfrak{f}'$. This relationship is unique if the incremental potential π'^{τ} is *convex–concave*, which follows for a stable electro-magneto-mechanical response from the convexity and concavity properties (89) and (90) of the mixed energy–enthalpy function ψ'.

3.2. Mixed Energy–Enthalpy-Based Formulation of Dissipative Response

3.2.1. Constitutive equations. For dissipative electro-magneto-mechanical material processes, the decomposition of the work done to a material element into energetically stored and dissipated contribution was defined in (25). With the mixed energy–enthalpy ψ' defined by the Legendre transformation (83) and the associated power expression $\mathscr{P}'$ defined in (86), the energy-based decomposition (27) of the power $\mathscr{P}$ is recast into the energy–enthalpy-based decomposition

$$\mathscr{P}' = \frac{\mathrm{d}}{\mathrm{d}t}\psi' + \mathscr{D} \tag{95}$$

of the modified power $\mathscr{P}'$. Assuming a mixed energy–enthalpy function $\psi' : \mathscr{R}^{d\times d+2d+m} \to \mathscr{R}$ depending on the generalized strain $\mathfrak{f}'$ and a generalized internal variable vector $\mathfrak{q} \in \mathscr{R}^m$, we define the dissipation in analogy to (29) by

$$\mathscr{D} := \mathscr{P}' - \frac{\mathrm{d}}{\mathrm{d}t}\psi'(\mathfrak{f}'(t), \mathfrak{q}(t)) \geqslant 0. \tag{96}$$

Writing this with (86) in the form $\mathscr{D} = [\mathfrak{s}' - \partial_{\mathfrak{f}'}\psi'] \cdot \dot{\mathfrak{f}}' - \partial_{\mathfrak{q}}\psi' \cdot \dot{\mathfrak{q}} \geqslant 0$, a standard argument identifies the generalized stresses $\mathfrak{s}'$ and the internal forces $\mathfrak{p}$ dual to $\mathfrak{q}$ by

$$\boxed{\mathfrak{s}' = \partial_{\mathfrak{f}'}\psi'(\mathfrak{f}', \mathfrak{q}) \quad \text{and} \quad \mathfrak{p} = -\partial_{\mathfrak{q}}\psi'(\mathfrak{f}', \mathfrak{q}).} \tag{97}$$

The dissipation then appears again in the form (31) as an inner product of *dissipative driving forces* $\mathfrak{p}$ and *dissipative fluxes* $\dot{\mathfrak{q}}$. The constitutive modeling of the evolution $\dot{\mathfrak{q}}$ of the internal variables is for the mixed energy–enthalpy formulation *identical* to the energy-based formulation and exclusively governed by the dissipation function ϕ as outlined in Section 2.3, see Equation (38). As a consequence, the evolution of the internal variable is determined by the *modification* of the Biot equation (39)

$$\mathbf{0} \in \partial_{\mathfrak{q}}\psi'(\mathfrak{f}', \mathfrak{q}) + \partial_{\dot{\mathfrak{q}}}\phi(\dot{\mathfrak{q}}) \quad \text{with } \mathfrak{q}(0) = \mathfrak{q}_0 \tag{98}$$

formulated by the above definition of the driving force $\mathfrak{p}$ in terms of the mixed energy–enthalpy function ψ'.

3.2.2. Incremental constitutive saddle-point principle. The above constitutive equations (97) and (38) can be related to an incremental constitutive *stationary* principle, which is conceptually in line with the minimization principle (47) outlined in Section 2.3. We consider again a time increment $\tau := t - t_n$ and introduce the potential $\pi'^{\tau}_d := \int_{t_n}^{t} [\dot{\psi}' + \mathscr{D} - \mathscr{P}']\mathrm{d}t$ with the algorithmic approximation

$$\underbrace{\pi'^{\tau}_d(\mathfrak{f}', \mathfrak{q})}_{\text{potential}} := \underbrace{\psi'(\mathfrak{f}', \mathfrak{q}) - \psi'(\mathfrak{f}'_n, \mathfrak{q}_n)}_{\text{stored}} + \underbrace{\tau\phi([\mathfrak{q} - \mathfrak{q}_n]/\tau)}_{\text{dissipated}} - \underbrace{\mathfrak{s}' \cdot (\mathfrak{f}' - \mathfrak{f}'_n)}_{\text{ext.load}}. \tag{99}$$

It contains the difference between the algorithmic expression for a *modified* internal work potential

$$w'(\mathfrak{f}', \mathfrak{q}) := \psi'(\mathfrak{f}', \mathfrak{q}) - \psi'(\mathfrak{f}'_n, \mathfrak{q}_n) + \tau\phi([\mathfrak{q} - \mathfrak{q}_n]/\tau) \tag{100}$$

consisting of a stored and a dissipated part, and the incremental external load done to the electro-magneto-mechanical volume element depicted in Figure 3. It is a function of the current generalized strain $\mathfrak{f}' := \mathfrak{f}'(t)$ and internal variables $\mathfrak{q} := \mathfrak{q}(t)$ at time t and refers to the *fixed-value* $\mathfrak{f}'_n := \mathfrak{f}'(t_n)$

Copyright © 2011 John Wiley & Sons, Ltd.

DOI: 10.1002/nme

and $\mathfrak{q}_n := \mathfrak{q}(t_n)$ at time t_n. Note that this function approximates the incremental dissipation based on the algorithm $\dot{\mathfrak{q}} = (\mathfrak{q} - \mathfrak{q}_n)/\tau$, defining a *constant rate* of internal variables within the interval $[t_n, t]$. Again, observe that the incremental load is defined in an implicit format in terms of the generalized stress $\mathfrak{s}' := \mathfrak{s}'(t)$ at time t. Then, for a given external load $\mathfrak{s}'$ of the volume element depicted in Figure 3, the current generalized strains *and* internal variables are defined by the *constitutive saddle-point principle*

$$\boxed{(\mathfrak{f}', \mathfrak{q}) = \operatorname{Arg}\left\{\operatorname*{stat}_{\mathfrak{f}', \mathfrak{q}} \pi_d'^{\tau}(\mathfrak{f}', \mathfrak{q})\right\} = \operatorname{Arg}\left\{\inf_{\boldsymbol{f}} \sup_{\boldsymbol{e}} \sup_{\boldsymbol{h}} \inf_{\mathfrak{q}} \pi_d'^{\tau}(\boldsymbol{f}, \boldsymbol{e}, \boldsymbol{h}, \mathfrak{q})\right\}.} \tag{101}$$

The solution of this constitutive stationary principle is obtained within *two steps* in full analogy to Section 2.3, corresponding to typical algorithmic procedures in computational inelasticity with a *local* constitutive response. In a *first solution step*, $\pi_d'^{\tau}$ in (99) is optimized with respect to the current internal variables

$$(S1): \quad \mathfrak{q} = \operatorname{Arg}\left\{\inf_{\mathfrak{q}} w'(\mathfrak{f}', \mathfrak{q})\right\} \tag{102}$$

and defines the reduced or condensed incremental work potential

$$w'_{\mathrm{red}}(\mathfrak{f}') = \inf_{\mathfrak{q}} w'(\mathfrak{f}', \mathfrak{q}). \tag{103}$$

The Euler equation of (103) provides the time-discrete form

$$\mathbf{0} \in \partial_{\mathfrak{q}} \psi'(\mathfrak{f}', \mathfrak{q}) + \partial_{\dot{\mathfrak{q}}} \phi([\mathfrak{q} - \mathfrak{q}_n]/\tau) \tag{104}$$

of the modified Biot equation (98). Hence, the stationary problem (103) determines for the given internal state $\mathfrak{q}_n$ at time t_n the current internal state $\mathfrak{q}$ at time t. With the reduced *modified* work potential $w'(\mathfrak{f}')$ defined in (103) at hand, we get the reduced function

$$\underbrace{\pi'^{\tau}_{d,\mathrm{red}}(\mathfrak{f}')}_{\text{potential}} := \underbrace{w'_{\mathrm{red}}(\mathfrak{f}')}_{\text{int.work}} - \underbrace{\mathfrak{s}' \cdot (\mathfrak{f}' - \mathfrak{f}'_n)}_{\text{ext.load}} \tag{105}$$

similar to the non-dissipative formulation (93). Hence, the *second solution step*, governed by the stationary principle

$$(S2): \quad \mathfrak{f}' = \operatorname{Arg}\left\{\operatorname*{stat}_{\mathfrak{f}'} \pi'^{\tau}_{d,\mathrm{red}}(\mathfrak{f}')\right\} = \operatorname{Arg}\left\{\inf_{\boldsymbol{f}} \sup_{\boldsymbol{e}} \sup_{\boldsymbol{h}} \pi'^{\tau}_{d,\mathrm{red}}(\boldsymbol{f}, \boldsymbol{e}, \boldsymbol{h})\right\} \tag{106}$$

similar to (94) defines for the given generalized stress $\mathfrak{s}'$ the generalized strain $\mathfrak{f}'$. The Euler equation of this incremental variational principle

$$\mathfrak{s}' = \partial_{\mathfrak{f}'} w'_{\mathrm{red}}(\mathfrak{f}') \tag{107}$$

has the same structure as the non-dissipative formulation (84), when the energy function $\psi'(\mathfrak{f}')$ is replaced by the reduced work potential $w'_{\mathrm{red}}(\mathfrak{f}')$ defined in (103). This relationship is unique if the reduced work potential $w'_{\mathrm{red}}(\mathfrak{f}')$ is *convex–concave*, which follows for a stable electro-magneto-mechanical response form a convex–concave mixed energy–enthalpy function ψ' *and* the convexity (41) of the dissipation function ϕ. Note that the incremental variational structure allows to write the coupled electro-magneto-mechanical tangent moduli at the current time t as the second derivative

$$\mathfrak{c}'^{\tau} = \partial^2_{\mathfrak{f}'\mathfrak{f}'} w'^{\tau}_{\mathrm{red}}(\mathfrak{f}') \tag{108}$$

of the incremental work potential. Thus the *incremental* constitutive representation for a dissipative response is in full analogy to the non-dissipative response (84), if the mixed energy–enthalpy function $\psi'(\mathfrak{f}')$ is replaced by the reduced work potential $w'_{\mathrm{red}}(\mathfrak{f}')$.

Copyright © 2011 John Wiley & Sons, Ltd.

DOI: 10.1002/nme

3.2.3. Stable incremental response. For stable dissipative response, the tangent moduli defined in (108) are *not positive definite*. The second-order work expression associated with the mixed energy–enthalpy formulation

$$\mathscr{S}' := \Delta\mathfrak{f}' \cdot \mathfrak{c}' \cdot \Delta\mathfrak{f}' = \Delta\mathfrak{f}' \cdot \partial^2_{\mathfrak{f}'\mathfrak{f}'} w'_{\text{red}}(\mathfrak{f}') \cdot \Delta\mathfrak{f}' \tag{109}$$

is not positive for general $\Delta\mathfrak{f}' \neq \mathbf{0}$. The *incremental potential* w'_{red} *is locally convex–concave* for a stable, dissipative response as the mixed energy–enthalpy ψ' for reversible processes, see (92) and Figure 4(b).

3.3. Rate-independent formulation based on threshold functions

For rate-independent dissipative processes with reversible ranges $\mathbb{E}$ defined in (59) based on switching functions f, we modify the principle (103) by inserting the specific dissipation function (60). This yields the algorithmic form

$$\boxed{w'_{\text{red}}(\mathfrak{f}') = \inf_{\mathfrak{q}} \sup_{\mathfrak{p},\gamma\geqslant 0} \tilde{w}'(\mathfrak{f}', \mathfrak{q}, \mathfrak{p}, \gamma)} \tag{110}$$

in terms of the algorithmic expression for a modified incremental work

$$\tilde{w}'(\mathfrak{f}', \mathfrak{q}, \mathfrak{p}, \gamma) = \psi'(\mathfrak{f}', \mathfrak{q}) - \psi'(\mathfrak{f}'_n, \mathfrak{q}_n) + \mathfrak{p} \cdot [\mathfrak{q} - \mathfrak{q}_n] - \gamma(f(\mathfrak{p}) - c). \tag{111}$$

The Euler equations for the case of loading $\gamma > 0$

$$\tilde{\boldsymbol{r}}' := \begin{bmatrix} \partial_{\mathfrak{q}}\tilde{w}' \\ \partial_{\mathfrak{p}}\tilde{w}' \\ \partial_{\gamma}\tilde{w}' \end{bmatrix} = \begin{bmatrix} \partial_{\mathfrak{q}}\psi' + \mathfrak{p} \\ \mathfrak{q} - \mathfrak{q}_n - \gamma\partial_{\mathfrak{p}} f \\ -f + c \end{bmatrix} = \mathbf{0} \tag{112}$$

are in full analogy to (66) and can be solved at *given* generalized deformation $\mathfrak{f}'$ by local Newton-updates $\tilde{\boldsymbol{v}} \Leftarrow \tilde{\boldsymbol{v}} - \tilde{\boldsymbol{a}}'^{-1}\tilde{\boldsymbol{r}}'$ for the variables $\tilde{\boldsymbol{v}} := \{\mathfrak{q}, \mathfrak{p}, \gamma\}$. The tangent matrix of the Newton iteration has the form

$$\tilde{\boldsymbol{a}}' := \begin{bmatrix} \partial^2_{\mathfrak{q}\mathfrak{q}}\tilde{w}' & \partial^2_{\mathfrak{q}\mathfrak{p}}\tilde{w}' & \partial^2_{\mathfrak{q}\gamma}\tilde{w}' \\ \partial^2_{\mathfrak{p}\mathfrak{q}}\tilde{w}' & \partial^2_{\mathfrak{p}\mathfrak{p}}\tilde{w}' & \partial^2_{\mathfrak{p}\gamma}\tilde{w}' \\ \partial^2_{\gamma\mathfrak{q}}\tilde{w}' & \partial^2_{\gamma\mathfrak{p}}\tilde{w}' & \partial^2_{\gamma\gamma}\tilde{w}' \end{bmatrix} = \begin{bmatrix} \partial^2_{\mathfrak{q}\mathfrak{q}}\psi' & \mathbf{1} & \mathbf{0} \\ \mathbf{1} & -\gamma\partial^2_{\mathfrak{p}\mathfrak{p}} f & -\partial_{\mathfrak{p}} f \\ \mathbf{0} & -\partial_{\mathfrak{p}} f & \mathbf{0} \end{bmatrix} \tag{113}$$

in full analogy to (70), and also governs the closed-form representation of the coupled electro-magneto-mechanical tangent operator defined in (108). Then, evaluation of the potential equations (107) and (108) finally gives the generalized stresses and the moduli

$$\mathfrak{s}'^{\tau} := \partial_{\mathfrak{f}'} w'^{\tau}_{\text{red}} = \partial_{\mathfrak{f}'}\psi' \quad \text{and} \quad \mathfrak{c}'^{\tau} := \partial^2_{\mathfrak{f}'\mathfrak{f}'} w'^{\tau}_{\text{red}} = \partial^2_{\mathfrak{f}'\mathfrak{f}'}\psi' - s \begin{bmatrix} \partial^2_{\mathfrak{f}'\mathfrak{q}}\psi' \\ \mathbf{0} \\ \mathbf{0} \end{bmatrix}^{\mathrm{T}} \tilde{\boldsymbol{a}}'^{-1} \begin{bmatrix} \partial^2_{\mathfrak{q}\mathfrak{f}'}\psi' \\ \mathbf{0} \\ \mathbf{0} \end{bmatrix} \tag{114}$$

in terms of a dissipative loading flag s defined in (72).

Copyright © 2011 John Wiley & Sons, Ltd.

DOI: 10.1002/nme

3.4. Rate-dependent formulation based on threshold functions

For the rate-dependent dissipative processes with reversible range $\mathbb{E}$ defined in (59) based on switching functions f, we modify the principle (103) by insertion of the specific dissipation function (73). This yields the algorithmic form

$$\boxed{w'_{\rm red}(\mathfrak{f}') = \inf_{\mathfrak{q}} \sup_{\mathfrak{p}} \overline{w}'(\mathfrak{f}, \mathfrak{q}, \mathfrak{p})} \tag{115}$$

in terms of the algorithmic expression for the modified incremental electro-magneto-mechanical work

$$\overline{w}'(\mathfrak{f}', \mathfrak{q}, \mathfrak{p}) = \psi'(\mathfrak{f}', \mathfrak{q}) - \psi(\mathfrak{f}'_n, \mathfrak{q}_n) + \mathfrak{p}\cdot[\mathfrak{q}-\mathfrak{q}_n] - \frac{c\tau}{\eta(m+1)}\langle f(\mathfrak{p})/c-1\rangle^{m+1}. \tag{116}$$

The necessary conditions

$$\overline{\boldsymbol{r}}' := \begin{bmatrix} \partial_{\mathfrak{q}}\overline{w}' \\ \partial_{\mathfrak{p}}\overline{w}' \end{bmatrix} = \begin{bmatrix} \partial_{\mathfrak{q}}\psi' + \mathfrak{p} \\ \mathfrak{p} - \mathfrak{q}_n - \dfrac{\tau}{\eta}\langle f/c-1\rangle^m \partial_{\mathfrak{p}} f \end{bmatrix} = \mathbf{0} \tag{117}$$

are in full analogy to (78) and can be solved at *given* generalized deformation $\mathfrak{f}'$ by local Newton-updates $\overline{\boldsymbol{v}} \Leftarrow \overline{\boldsymbol{v}} - \overline{\boldsymbol{a}}'^{-1}\overline{\boldsymbol{r}}'$ for the variables $\overline{\boldsymbol{v}} := \{\mathfrak{q}, \mathfrak{p}\}$ at the current time t. The tangent matrix of the Newton iteration has the form

$$\overline{\boldsymbol{a}}' := \begin{bmatrix} \partial^2_{\mathfrak{q}\mathfrak{q}}\overline{w}' & \partial^2_{\mathfrak{q}\mathfrak{p}}\overline{w}' \\ \partial^2_{\mathfrak{p}\mathfrak{q}}\overline{w}' & \partial^2_{\mathfrak{p}\mathfrak{p}}\overline{w}' \end{bmatrix} = \begin{bmatrix} \partial^2_{\mathfrak{q}\mathfrak{q}}\psi' & \mathbf{1} \\ \mathbf{1} & -\dfrac{m\tau}{c\eta}\langle f/c-1\rangle^{m-1}\partial_{\mathfrak{p}} f \otimes \partial_{\mathfrak{p}} f \\ & -\dfrac{\tau}{\eta}\langle f/c-1\rangle^m \partial^2_{\mathfrak{p}\mathfrak{p}} f \end{bmatrix} \tag{118}$$

and also governs the closed-form representation of the coupled electro-magneto-mechanical tangent operator defined in (108). Then, evaluation of the potential equations (107) and (108) finally gives the generalized stresses and the symmetric moduli

$$\mathfrak{s}'^{\tau} := \partial_{\mathfrak{f}'} w'^{\tau}_{\rm red} = \partial_{\mathfrak{f}'}\psi' \quad \text{and} \quad \mathfrak{c}'^{\tau} := \partial^2_{\mathfrak{f}'\mathfrak{f}'} w'^{\tau}_{\rm red} = \partial^2_{\mathfrak{f}'\mathfrak{f}'}\psi' - \begin{bmatrix} \partial^2_{\mathfrak{f}'\mathfrak{q}}\psi' \\ \mathbf{0} \end{bmatrix}^{\rm T} \overline{\boldsymbol{a}}'^{-1} \begin{bmatrix} \partial^2_{\mathfrak{q}\mathfrak{f}'}\psi' \\ \mathbf{0} \end{bmatrix}. \tag{119}$$

4. THE IBVP OF QUASI-STATIC ELECTRO-MAGNETO-MECHANICS

After having outlined the local constitutive equations, we focus on the boundary-value problem of electro-magneto-mechanical continuum embedded into free space as depicted in Figure 1. The underlying goal is to construct a compact representation of the coupled field equations consistent with the constitutive formulations introduced above. Let $\mathscr{B} \subset \mathscr{R}^d$ be the reference configuration of a material body and $\partial\mathscr{B} \subset \mathscr{R}^{d-1}$ its surface. We study the response of the body under quasi-static electro-magneto-mechanical loading in the range $\mathscr{T} \subset \mathscr{R}_+$ of time.

4.1. Primary fields in dissipative electro-magneto-mechanics

The boundary-value problem of electro-magneto-mechanics is a coupled three-field problem. On the mechanical side, the primary variable field is the *displacement field*

$$\boldsymbol{u}: \begin{cases} \mathscr{B}\times\mathscr{T} \to \mathscr{R}^3, \\ (\boldsymbol{x}, t) \mapsto \boldsymbol{u}(\boldsymbol{x}, t). \end{cases} \tag{120}$$

Copyright © 2011 John Wiley & Sons, Ltd.

DOI: 10.1002/nme

$\boldsymbol{u}$ is the displacement of the material point $\boldsymbol{x} \in \mathscr{B}$ at time $t \in \mathscr{T}$. On the non-mechanical side, the classical choice of primary fields are the *electric and magnetic potential fields*

$$\phi^e : \begin{cases} \mathscr{B} \times \mathscr{T} \to \mathscr{R} \\ (\boldsymbol{x}, t) \mapsto \phi^e(\boldsymbol{x}, t) \end{cases} \quad \text{and} \quad \phi^m : \begin{cases} \mathscr{B} \times \mathscr{T} \to \mathscr{R} \\ (\boldsymbol{x}, t) \mapsto \phi^m(\boldsymbol{x}, t). \end{cases} \tag{121}$$

With regard to a compact notation, we assemble all three primary fields to a *generalized displacement vector*

$$\boxed{\mathfrak{u}' := [\boldsymbol{u}, -\phi^e, -\phi^m]^{\mathrm{T}} \in \mathscr{R}^{d+2}} \tag{122}$$

of the coupled electro-magnetic-mechanical problem. For the *dissipative* response under consideration, we have in addition the internal variables

$$\mathfrak{q} : \begin{cases} \mathscr{B} \times \mathscr{T} \to \mathscr{R}^m, \\ (\boldsymbol{x}, t) \mapsto \mathfrak{q}(\boldsymbol{x}, t) \end{cases} \tag{123}$$

introduced in the preceding Sections 2 and 3, which are now considered as local fields on the domain $\mathscr{B}$ of the solid. Figure 5 visualizes the four fields introduced above.

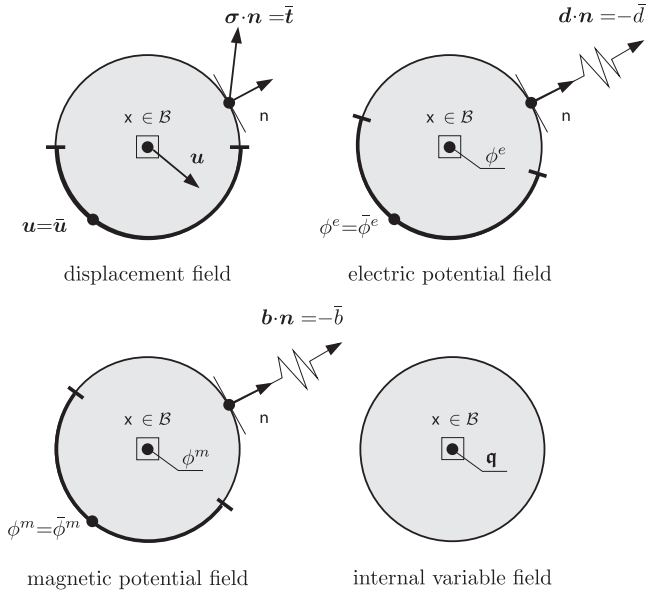

Figure 5. Multifield problem of dissipative electro-magneto-mechanics. The boundary $\partial\mathscr{B}$ of the solid is decomposed into three pairs of overlapping parts $\partial\mathscr{B} = \partial\mathscr{B}_u \cup \partial\mathscr{B}_t = \partial\mathscr{B}_{\phi^e} \cup \partial\mathscr{B}_d = \partial\mathscr{B}_{\phi^m} \cup \partial\mathscr{B}_b$ (a) *Mechanical boundary conditions* determine the displacement $\boldsymbol{u} = \bar{\boldsymbol{u}}$ on $\partial\mathscr{B}_u$ and the tractions $\boldsymbol{\sigma}\cdot\boldsymbol{n} = \bar{\boldsymbol{t}}$ on $\partial\mathscr{B}_t$ and (b) *Electric boundary conditions* determine the electric potential $\phi^e = \bar{\phi}^e$ on $\partial\mathscr{B}_{\phi^e}$ and the normal electric displacement $\boldsymbol{d}\cdot\boldsymbol{n} = -\bar{d}$ on $\partial\mathscr{B}_d$. (c) *Magnetic boundary conditions* determine the magnetic potential $\phi^m = \bar{\phi}^m$ on $\partial\mathscr{B}_{\phi^m}$ and the normal magnetic induction $\boldsymbol{b}\cdot\boldsymbol{n} = -\bar{b}$ on $\partial\mathscr{B}_b$. $\bar{\boldsymbol{\gamma}}$ is the mechanical body force and $\bar{\rho}^e$ the density of free changes.

Copyright © 2011 John Wiley & Sons, Ltd.

DOI: 10.1002/nme

4.2. Potential equations of primary variables

The first class of field equations concern the definition of gradient fields associated with the primary fields introduced above. Let $\boldsymbol{f}$ be the mechanical deformation field. This field is assumed to satisfy the *deformation compatibility condition*

$$\oint_{\mathscr{C}} \boldsymbol{f}\cdot \mathrm{d}\boldsymbol{s}=\boldsymbol{0}, \tag{124}$$

where $\mathscr{C}$ is an arbitrary curve in the solid domain $\mathscr{B}$. Using the Stokes theorem, this equation can be recast into the local field equation $\mathrm{Curl}[\boldsymbol{f}]=\boldsymbol{0}$ in $\mathscr{B}$ with $\mathrm{Curl}[\boldsymbol{f}]:=\boldsymbol{\epsilon}:\mathrm{Grad}^{\mathrm{T}(13)}[\boldsymbol{f}]=\epsilon_{ijk}f_{lk,j}$, where $\boldsymbol{\epsilon}=\epsilon_{ijk}$ is the skew third-order permutation tensor. Clearly, the mechanical compatibility condition is automatically satisfied by the definition of the deformation

$$\boldsymbol{f}=\mathrm{Grad}[\boldsymbol{u}] \tag{125}$$

in terms of the displacement field, due to the property $\mathrm{Curl}[\mathrm{Grad}[\boldsymbol{u}]]=\epsilon_{ijk}u_{l,kj}=\boldsymbol{0}$. We assume $\|\mathrm{Grad}[\boldsymbol{u}]\|<\epsilon$ in the small-strain theory under consideration. Furthermore, consider the electric and magnetic field strengths $\boldsymbol{e}$ and $\boldsymbol{h}$, respectively. For quasi-static problems, these two fields must satisfy the conditions

$$\oint_{\mathscr{C}} \boldsymbol{e}\cdot \mathrm{d}\boldsymbol{s}=\boldsymbol{0} \quad \text{and} \quad \oint_{\mathscr{C}} \boldsymbol{h}\cdot \mathrm{d}\boldsymbol{s}=\int_{\mathscr{S}} \bar{\boldsymbol{j}}\cdot \mathrm{d}\boldsymbol{a}. \tag{126}$$

Here, $\mathscr{S}$ is an arbitrary surface bounded by the curve $\mathscr{C}$ in the solid $\mathscr{B}$. The first equation is the quasi-static version of *Faraday's law*, often called the second Maxwell equation. The second statement is the quasi-static version of the *Amperes law*, often called the fourth Maxwell equation, where $\bar{\boldsymbol{j}}$ is the current vector that is considered to be *given* in our treatment. Using again Stokes's theorem, we find the associated field equations in the solid domain $\mathrm{Curl}[\boldsymbol{e}]=\boldsymbol{0}$ and $\mathrm{Curl}[\boldsymbol{h}]=\bar{\boldsymbol{j}}$ in $\mathscr{B}$, with $\mathrm{Curl}[\boldsymbol{e}]:=\boldsymbol{\epsilon}:\mathrm{Grad}^{\mathrm{T}}[\boldsymbol{e}]=\epsilon_{ijk}e_{k,j}$. Assuming a given vector $\bar{\boldsymbol{h}}$ such that the prescribed current may be expressed in the form $\bar{\boldsymbol{j}}=\mathrm{Curl}[\bar{\boldsymbol{h}}]$, we may recast the second equation in the form $\mathrm{Curl}[\boldsymbol{h}-\bar{\boldsymbol{h}}]=\boldsymbol{0}$. Hence, the quasi-static versions of Faraday's and Amperes laws are automatically satisfied by their definitions

$$\boldsymbol{e}=-\mathrm{Grad}[\phi^{e}] \quad \text{and} \quad \boldsymbol{h}=-\mathrm{Grad}[\phi^{m}]+\bar{\boldsymbol{h}} \tag{127}$$

in terms of the electric and magnetic potentials, due to the property $\mathrm{Curl}[\mathrm{Grad}[\phi]]=\epsilon_{ijk}\phi_{,kj}=0$. Taking into account the definition (122) of the generalized displacement $\mathfrak{u}'$ and the generalized deformation $\mathfrak{f}'$ introduced in (82) in context with the free enthalpy formulation, we assemble the three field equations (125) and (127) in the compact form

$$\boxed{\mathfrak{f}'=\mathrm{GRAD}[\mathfrak{u}']+\bar{\mathfrak{f}}'} \tag{128}$$

in terms of a generalized gradient operator whose evaluation gives (125) and (127). Here,

$$\bar{\mathfrak{f}}':=[\boldsymbol{0},\boldsymbol{0},\bar{\boldsymbol{h}}]^{\mathrm{T}}\in\mathscr{R}^{d\times d+2d} \tag{129}$$

is given.

4.3. Balance equations for secondary variables

The second class of field equations is governed by the secondary variable fields. On the mechanical side, let $\boldsymbol{\sigma}$ be the total stress field. The stresses are governed by the static versions of the *balances of linear and angular momentum*. These mechanical equilibrium conditions read as

$$\int_{\partial\mathscr{P}} \boldsymbol{\sigma}\cdot \mathrm{d}\boldsymbol{a}+\int_{\mathscr{P}} \bar{\boldsymbol{\gamma}}\,\mathrm{d}v=\boldsymbol{0} \quad \text{and} \quad \int_{\partial\mathscr{P}} \boldsymbol{x}\times\boldsymbol{\sigma}\cdot \mathrm{d}\boldsymbol{a}+\int_{\mathscr{P}} \boldsymbol{x}\times\bar{\boldsymbol{\gamma}}\,\mathrm{d}v=\boldsymbol{0} \tag{130}$$

Copyright © 2011 John Wiley & Sons, Ltd.

DOI: 10.1002/nme

for an arbitrary part $\mathscr{P}\subset\mathscr{B}$ of the solid with surface $\partial\mathscr{P}$. Here, $\bar{\boldsymbol{\gamma}}$ is a given mechanical body force field. Recall that the total stress tensor includes electro-magnetic body forces and couples as emphasized in the footnote of Section 2.1. Using the Gauss theorem, we recast these equations into the field form

$$\mathrm{Div}[\boldsymbol{\sigma}]+\bar{\boldsymbol{\gamma}}=\mathbf{0} \quad \text{and} \quad \boldsymbol{\sigma}^{\mathrm{T}}=\boldsymbol{\sigma} \tag{131}$$

in the domain $\mathscr{B}$. As pointed out in the subsequent statement, the symmetry of the total stress is automatically satisfied by the constitutive equations that satisfy the principle of material frame invariance. On the electro-magnetic side, consider fields for the electric displacement and the magnetic induction fields $\boldsymbol{d}$ and $\boldsymbol{b}$, respectively. These vector fields govern the *Gauss law* for the conservation of electric charge, often called the first Maxwell equation, and the *Gauss–Faraday law* of magnetic induction, often called the third Maxwell equation. The quasi-static versions of these statement read as

$$\int_{\partial\mathscr{P}}\boldsymbol{d}\cdot d\boldsymbol{a}-\int_{\mathscr{P}}\bar{\rho}^{e}\,\mathrm{d}v=0 \quad \text{and} \quad \int_{\partial\mathscr{P}}\boldsymbol{b}\cdot d\boldsymbol{a}=0 \tag{132}$$

for an arbitrary part $\mathscr{P}\subset\mathscr{B}$ of the solid. Here, $\bar{\rho}^{e}$ is a *given* density of free charge in the solid. Using the Gauss theorem, these equations can be recast into the field equations

$$\mathrm{Div}[\boldsymbol{d}]-\bar{\rho}^{e}=0 \quad \text{and} \quad \mathrm{Div}[\boldsymbol{b}]=0 \tag{133}$$

in the domain $\mathscr{B}$. With the generalized stress $\mathfrak{s}'$ defined in (82), we assemble the three field equations $(131)_1$ and (133) in the compact form

$$\boxed{\mathrm{DIV}[\mathfrak{s}']+\bar{\mathfrak{g}}'=\mathbf{0}} \tag{134}$$

in terms of generalized divergence operators and an array of generalized body forces

$$\bar{\mathfrak{g}}':=[\bar{\boldsymbol{\gamma}},-\bar{\rho}^{e},0]^{\mathrm{T}}\in\mathscr{R}^{d+2} \tag{135}$$

Note that the generalized vectors $\mathfrak{u}'$, $\mathfrak{f}'$ and $\mathfrak{s}'$ introduced in (122) and (82) assemble $2d\times d+5d+2$ *unknown scalar fields*. For their determination, the generalized field equations (128) and (134) of the coupled electro-magneto-mechanical problem provide $d\times d+3d+2$ scalar component equations. Thus $d\times d+2d$ component equations are missing in order to solve a particular problem of electro-magneto-mechanics. These equations are the constitutive equations that characterize the individual mechanical response.

4.4. Objective, locally dissipative material of the grade one

We consider *locally* dissipative electro-magneto-mechanical materials of the grade one consistent with our local treatment in Section 2. To this end, consider a constitutive function for the *mixed energy–enthalpy storage* of the coupled problem by the functional dependence

$$\psi'=\tilde{\psi}'(\mathfrak{u}',\mathrm{GRAD}[\mathfrak{u}']+\bar{\mathfrak{f}}',\mathfrak{q};\boldsymbol{x}) \tag{136}$$

on the generalized displacement $\mathfrak{u}'$, its first gradient and the internal variables $\mathfrak{q}$ at a typical position $\boldsymbol{x}\in\mathscr{B}$. Clearly, this function must satisfy certain invariance conditions. On the mechanical side, a small strain version of the principle of material frame invariance may be based on a time-dependent *infinitesimal rigid rotation* superimposed onto the displaced solid $\boldsymbol{u}^{+}(\boldsymbol{x},t):=\boldsymbol{u}(\boldsymbol{x},t)+\boldsymbol{w}(t)\boldsymbol{x}+\boldsymbol{c}(t)$. Here, $\boldsymbol{w}(t)$ is a skew second-order tensor with $\boldsymbol{w}^{\mathrm{T}}=-\boldsymbol{w}$ and $\|\boldsymbol{w}\|<\epsilon$, representing an *infinitesimal rotation*. The vector $\boldsymbol{c}(t)$ characterizes a *translation*. On the electro-magnetic side, consider a time-dependent shift of the electric and magnetic potentials $\phi^{e+}(\boldsymbol{x},t):=\phi^{e}(\boldsymbol{x},t)+c^{e}(t)$ and $\phi^{m+}(\boldsymbol{x},t):=\phi^{m}(\boldsymbol{x},t)+c^{m}(t)$ in terms of the time-dependent functions c^{e} and c^{m}. In our compact notation, this yields the modification of the generalized displacement vector

$$\mathfrak{u}'^{+}:=[\boldsymbol{u}'(\boldsymbol{x},t)+\boldsymbol{w}(t)\boldsymbol{x}+\boldsymbol{c}(t),-\phi^{e}(\boldsymbol{x},t)-c^{e}(t),-\phi^{m}(\boldsymbol{x},t)-c^{m}(t)]^{\mathrm{T}}. \tag{137}$$

Copyright © 2011 John Wiley & Sons, Ltd.

DOI: 10.1002/nme

With this notion at hand, we postulate an invariance principle

$$\tilde{\psi}'(\mathbf{u}'^{+}, \mathrm{GRAD}[\mathbf{u}'^{+}]+\bar{\mathfrak{f}}', \mathfrak{q}; \boldsymbol{x}) = \tilde{\psi}'(\mathbf{u}', \mathrm{GRAD}[\mathbf{u}']+\bar{\mathfrak{f}}', \mathfrak{q}; \boldsymbol{x}) \quad \text{for all} \quad \boldsymbol{w}, \boldsymbol{c}, c^e, c^m \tag{138}$$

that must be satisfied by the free enthalpy function $\tilde{\psi}'$. It is clear due to the arbitrary shifts $\boldsymbol{c}$, c^e and c^m, that $\tilde{\psi}'$ must not depend on the generalized displacement $\mathbf{u}'$. Furthermore, due to the arbitrary infinitesimal rotation $\boldsymbol{w}$, $\tilde{\psi}'$ must depend only on the symmetric part of the deformation. As a consequence, we end up with the *reduced form representation*

$$\psi'(\mathfrak{f}', \mathfrak{q}; \boldsymbol{x}) = \tilde{\psi}'(\boldsymbol{\varepsilon}, \boldsymbol{e}, \boldsymbol{h}, \mathfrak{q}; \boldsymbol{x}) \quad \text{with} \quad \boldsymbol{\varepsilon} := \tfrac{1}{2}(\boldsymbol{f}+\boldsymbol{f}^{\mathrm{T}}) \tag{139}$$

i.e. depending on the symmetric strain tensor $\boldsymbol{\varepsilon}$, the electric and magnetic field strengths $\boldsymbol{e}$ and $\boldsymbol{h}$ as well as the internal variables $\mathfrak{q}$ according to the *local* formulations in Sections 2 and 3. The reduced enthalpy function ψ' then defines, according to our derivation of Equation (97) in Section 3.2, the generalized stress

$$\boxed{\mathfrak{s}' = \partial_{\mathfrak{f}'}\psi'(\mathfrak{f}', \mathfrak{q}; \boldsymbol{x})} \tag{140}$$

in terms of the generalized deformation $\mathfrak{f}'$ and the internal variables $\mathfrak{q}$. Note that the latter are defined *locally* by the evolution equations discussed in Sections 2 and 3. A typical representation of an evolution equation is the Biot equation (98), i.e.

$$\boxed{\mathbf{0} \in \partial_{\mathfrak{q}}\psi'(\mathfrak{f}', \mathfrak{q}; \boldsymbol{x}) + \partial_{\dot{\mathfrak{q}}}\phi(\dot{\mathfrak{q}}; \boldsymbol{x}) \quad \text{with} \quad \mathfrak{q}(0, \boldsymbol{x}) = \mathfrak{q}_0(\boldsymbol{x}).} \tag{141}$$

The total stress $\boldsymbol{\sigma}$ turns out to be symmetric due to the dependence of the objective free enthalpy on the symmetric part of the deformation $\boldsymbol{f}$. Hence, the objectivity demand (138) implies automatically the local form of the balance of angular momentum $(131)_2$. The above constitutive equation provides $d \times d + 2d$ component equations which in combination with Equations (128) and (134) characterizes an individual problem of quasi-static electro-magneto-mechanics.

4.5. Boundary conditions of the coupled problem

Insertion of (128) and (140) into (134) finally yields the coupled system of quasi-static electro-magneto mechanics

$$\mathrm{DIV}[\partial_{\mathfrak{f}'}\psi'(\mathrm{GRAD}[\mathbf{u}']+\bar{\mathfrak{f}}', \mathfrak{q}; \boldsymbol{x})]+\bar{\mathfrak{g}}' = \mathbf{0} \tag{142}$$

providing $d+2$ coupled scalar differential equations for the determination of the generalized displacement vector $\mathbf{u}' \in \mathscr{R}^{d+2}$ in the solid domain $\mathscr{B}$ under consideration. Note again that the internal variables are considered to be determined by accompanying *local* evolution equation, such as (141). Depending on the choice of the constitutive function, the above coupled system of differential equations is in general non-linear. Only for a *quadratic* choice of the enthalpy in the *non-dissipative case*, the above differential equation attains the linear form $\mathrm{DIV}[\mathfrak{c}'(\boldsymbol{x}) \cdot (\mathrm{GRAD}[\mathbf{u}']+\bar{\mathfrak{f}}')]+\bar{\mathfrak{g}}' = \mathbf{0}$. The coupled system (142) of electro-magneto-mechanical differential equations must be subjected to specific boundary conditions. *On the mechanical side*, the boundary of the solid is decomposed according to $\partial\mathscr{B} = \partial\mathscr{B}_u \cup \partial\mathscr{B}_t$, where the displacement is prescribed on $\partial\mathscr{B}_u$ by a Dirichlet-type condition and the traction vector on $\partial\mathscr{B}_t$ by a Neumann-type condition

$$\boldsymbol{u} = \bar{\boldsymbol{u}}(\boldsymbol{x}, t) \ \text{ on } \partial\mathscr{B}_u \quad \text{and} \quad \boldsymbol{\sigma}\cdot\boldsymbol{n} = \bar{\boldsymbol{t}}(\boldsymbol{x}, t) \ \text{ on } \partial\mathscr{B}_t \tag{143}$$

in terms of the given functions for the displacement $\bar{\boldsymbol{u}}$ on the surface and the surface tractions $\bar{\boldsymbol{t}}$. Here, $\boldsymbol{n}(\boldsymbol{x})$ is the outward normal field on the surface $\partial\mathscr{B}$. *On the electric side*, the surface of the solid is decomposed according to $\partial\mathscr{B} = \partial\mathscr{B}_{\phi^e} \cup \partial\mathscr{B}_d$, where the electric potential is prescribed

Copyright © 2011 John Wiley & Sons, Ltd.

DOI: 10.1002/nme

on $\partial\mathscr{B}_{\phi^e}$ by a Dirichlet-type condition and the electric displacement on $\partial\mathscr{B}_d$ by a Neumann-type conditions

$$\phi^e = \bar{\phi}^e(\boldsymbol{x},t) \;\text{ on }\; \partial\mathscr{B}_{\phi^e} \quad\text{and}\quad \boldsymbol{d}\cdot\boldsymbol{n} = -\bar{d}(\boldsymbol{x},t) \;\text{ on }\; \partial\mathscr{B}_d \tag{144}$$

in terms of the given functions for the electric potential $\bar{\phi}^e$, $\bar{\phi}^m$ and the surface charge $\bar{q}$. *On the magnetic side*, the surface of the solid is decomposed according to $\partial\mathscr{B} = \partial\mathscr{B}_{\phi^m} \cup \partial\mathscr{B}_b$, where the magnetic potential is prescribed on $\partial\mathscr{B}_{\phi^m}$ by a Dirichlet-type condition and the magnetic induction on $\partial\mathscr{B}_b$ by a Neumann-type condition

$$\phi^m = \bar{\phi}^m(\boldsymbol{x},t) \;\text{ on }\; \partial\mathscr{B}_{\phi^m} \quad\text{and}\quad \boldsymbol{b}\cdot\boldsymbol{n} = -\bar{b}(\boldsymbol{x},t) \;\text{ on }\; \partial\mathscr{B}_b \tag{145}$$

in terms of the given functions for the magnetic potential $\bar{\phi}^e$, $\bar{\phi}^m$ and the magnetic surface induction $\bar{h}$. See Figure 5 for a visualization of the boundary conditions.

The simple expression (142) for the coupled system of partial differential equations of the electro-magneto-mechanical problem underlines the advantage of the compact notation introduced above. Consistent with this notation, we may also assemble the above outlined boundary conditions (143)–(145) in the compact array form

$$\mathfrak{u}' = \bar{\mathfrak{u}}'(\boldsymbol{x},t) \;\text{ on }\; \partial\mathscr{B}_{\mathfrak{u}'} \quad\text{and}\quad \mathfrak{s}'\cdot\mathfrak{n} = \bar{\mathfrak{t}}'(\boldsymbol{x},t) \;\text{ on }\; \partial\mathscr{B}_{\mathfrak{t}'}. \tag{146}$$

Here, $\bar{\mathfrak{u}}' := [\bar{\boldsymbol{u}}(\boldsymbol{x},t), -\bar{\phi}^e(\boldsymbol{x},t), -\bar{\phi}^m(\boldsymbol{x},t)]^{\mathrm{T}} \in \mathscr{R}^{d+2}$ assembles the prescribed primary variables on Dirichlet boundaries $\partial\mathscr{B}_{\mathfrak{u}'} := \{\partial\mathscr{B}_u, \partial\mathscr{B}_{\phi^e}, \partial\mathscr{B}_{\phi^m}\}$. Furthermore, $\bar{\mathfrak{t}}' := [\bar{\boldsymbol{t}}(\boldsymbol{x},t), -\bar{d}(\boldsymbol{x},t), -\bar{b}(\boldsymbol{x},t)]^{\mathrm{T}} \in \mathscr{R}^{d+2}$ assembles the prescribed variables on the Neumann boundaries $\partial\mathscr{B}_{\mathfrak{t}'} := \{\partial\mathscr{B}_t, \partial\mathscr{B}_d, \partial\mathscr{B}_b\}$. The generalized vector $\mathfrak{n} := [\boldsymbol{n},\boldsymbol{n},\boldsymbol{n}]^{\mathrm{T}}$ provides the outward surface normals for each partial field of the coupled problem.

5. ENTHALPY- AND ENERGY-BASED VARIATIONAL PRINCIPLES FOR IBVP

Finally, we outline *global* variational principles, which govern the boundary-value problems of coupled electro-magneto-mechanics by exploiting the *local* constitutive variational principles proposed in Sections 2 and 3.

5.1. Enthalpy-based variational principle for dissipative response

In what follows, we define a variational principle that governs the *incremental* coupled boundary value problem of dissipative electro-magneto-mechanics. In line with our treatment of the local constitutive response in Section 3, we consider a time increment $\tau := t - t_n$ and introduce the functional

$$I'^{\tau}(\mathfrak{u}',\mathfrak{q}) = \int_{\mathscr{B}} \{w'(\mathrm{GRAD}[\mathfrak{u}'] + \bar{\mathfrak{f}}', \mathfrak{q}) - \bar{\mathfrak{g}}'\cdot(\mathfrak{u}' - \mathfrak{u}'_n)\}\,\mathrm{d}v - \int_{\partial\mathscr{B}_{\mathfrak{t}'}} \bar{\mathfrak{t}}'\cdot(\mathfrak{u}' - \mathfrak{u}'_n)\,\mathrm{d}a \tag{147}$$

in terms of the generalized displacement field $\mathfrak{u}' = \mathfrak{u}'(\boldsymbol{x},t)$ defined in (122) and the internal variable field $\mathfrak{q} = \mathfrak{q}(\boldsymbol{x},t)$ at the *discrete* time t. Here, $\hat{w}'$ is the incremental work potential defined in (100) in terms of the mixed energy–enthalpy function ψ' and the dissipation function ϕ. Note that we used the compact notation introduced above. We may interpret the above expression as the difference between the incremental internal and external work of the coupled electro-magneto-mechanical problem at quasi-static conditions. With this definition at hand, we define the *incremental variational principle*

$$\boxed{(\mathfrak{u}',\mathfrak{q}) = \mathrm{Arg}\left\{\underset{\mathfrak{u}'\in\mathscr{W}',\,\mathfrak{q}}{\mathrm{stat}}\; I'^{\tau}(\mathfrak{u}',\mathfrak{q})\right\} = \mathrm{Arg}\left\{\inf_{\boldsymbol{u}}\sup_{-\phi^e}\sup_{-\phi^m}\inf_{\mathfrak{q}} I'^{\tau}(\boldsymbol{u},-\phi^e,-\phi^m,\mathfrak{q})\right\}} \tag{148}$$

Copyright © 2011 John Wiley & Sons, Ltd.

DOI: 10.1002/nme

Box 4: Variational principles in dissipative electro-magneto-mechanics.

1. *Energy-based Formulation.* The primary variables are the displacement $\boldsymbol{u}$, the electric displacement $\boldsymbol{d}$ and the magnetic induction $\boldsymbol{b}$. The generalized displacement vector

$$\mathfrak{u} := [\boldsymbol{u}, \boldsymbol{d}, \boldsymbol{b}]^{\mathrm{T}} \in \mathscr{R}^{3d}$$

and the internal variables $\mathfrak{q}$ are determined by the incremental *minimization principle*

$$\boxed{(\mathfrak{u}, \mathfrak{q}) = \operatorname{Arg}\left\{ \inf_{\boldsymbol{u}} \inf_{\boldsymbol{d}} \inf_{\boldsymbol{b}} \inf_{\mathfrak{q}} I_\epsilon^\tau(\mathfrak{u}, \mathfrak{q}) \right\}}$$

subject to $\boldsymbol{u} = \bar{\boldsymbol{u}}$ on $\partial\mathscr{B}_u$ with the functional

$$I_\epsilon^\tau := \int_{\mathscr{B}} w_\epsilon(\mathrm{GRAD}[\mathfrak{u}], \mathfrak{u}, \mathfrak{q})\,\mathrm{d}v + \int_{\partial\mathscr{B}_{\phi^e}} \bar{\phi}^e \boldsymbol{n}\cdot(\boldsymbol{d}-\boldsymbol{d}_n)\mathrm{d}a + \int_{\partial\mathscr{B}_{\phi^m}} \bar{\phi}^m \boldsymbol{n}\cdot(\boldsymbol{b}-\boldsymbol{b}_n)\mathrm{d}a$$

based on the extended incremental work potential

$$w_\epsilon := \psi(\nabla\boldsymbol{u}, \boldsymbol{d}, \boldsymbol{b}, \mathfrak{q}) - \psi_n + \tau\phi([\mathfrak{q}-\mathfrak{q}_n]/\tau) + \frac{\epsilon_e}{2}\,\mathrm{tr}^2[\nabla\boldsymbol{d}] + \frac{\epsilon_m}{2}\,\mathrm{tr}^2[\nabla\boldsymbol{b}]$$

2. *Enthalpy-based Formulation.* The primary variables are the displacement $\boldsymbol{u}$, the electric potential and magnetic potentials ϕ^e and ϕ^m. The generalized displacement vector

$$\mathfrak{u}' := [\boldsymbol{u}, -\phi^e, -\phi^m]^{\mathrm{T}} \in \mathscr{R}^{d+2}$$

and internal variables $\mathfrak{q}$ are determined by the incremental *saddle-point principle*

$$\boxed{(\mathfrak{u}', \mathfrak{q}) = \operatorname{Arg}\left\{ \inf_{\boldsymbol{u}} \sup_{-\phi^e} \sup_{-\phi^m} \inf_{\mathfrak{q}} I'^\tau(\mathfrak{u}', \mathfrak{q}) \right\}}$$

subject to $\boldsymbol{u} = \bar{\boldsymbol{u}}$ on $\partial\mathscr{B}_u$, $\phi^e = \bar{\phi}^e$ on $\partial\mathscr{B}_{\phi^e}$ and $\phi^m = \bar{\phi}^m$ on $\partial\mathscr{B}_{\phi^m}$ with

$$I'^\tau := \int_{\mathscr{B}} w'(\mathrm{GRAD}[\mathfrak{u}'], \mathfrak{q})\,\mathrm{d}v$$

based on the incremental work potential

$$w' := \psi'(\nabla\boldsymbol{u}, -\nabla\phi^e, -\nabla\phi^m, \mathfrak{q}) - \psi'_n + \tau\phi([\mathfrak{q}-\mathfrak{q}_n]/\tau)$$

which determines for given boundary-value data the primary variables of the electro-magneto-mechanical problem. Here, $\mathscr{W}'$ is the set of admissible primary variables that satisfy Dirichlet-type boundary conditions $(146)_1$, i.e.

$$\mathscr{W}' := \{\mathfrak{u}' \,|\, \mathfrak{u}' = \bar{\mathfrak{u}}'(\boldsymbol{x}, t) \text{ on } \partial\mathscr{B}_{\mathfrak{u}'}\}. \tag{149}$$

Note that the above variational principle defines a *saddle-point problem* with respect to the mechanical and the electro-magnetic fields. The stationary principle provides an infimum with respect to the mechanical displacement $\boldsymbol{u}$ and a supremum with respect to the electro-magnetic variable $-\phi^e$ and $-\phi^m$.

The solution of the above variational principle is achieved in *two steps* similar to the constitutive problem outlined in Section 3. Owing to the local nature of the evolution equations for the internal variables, see e.g (98), the *first solution step* is the incremental update of the internal variables at

Copyright © 2011 John Wiley & Sons, Ltd.

DOI: 10.1002/nme

Box 5: Reduced incremental variational principles.

1. *Energy-based Formulation.* The primary variables are the displacement $\boldsymbol{u}$, the electric displacement $\boldsymbol{d}$ and the magnetic induction $\boldsymbol{b}$. For known internal variables $\mathfrak{q}$ obtained by constitutive updates in Box 2 or 3, the generalized displacement

$$\mathfrak{u} := [\boldsymbol{u}, \boldsymbol{d}, \boldsymbol{b}]^{\mathrm{T}} \in \mathscr{R}^{3d}$$

is updated by the *reduced incremental minimization principle*

$$\boxed{\mathfrak{u} = \mathrm{Arg}\left\{ \inf_{\boldsymbol{u}} \inf_{\boldsymbol{d}} \inf_{\boldsymbol{b}} I^{\tau}_{\epsilon,\mathrm{red}}(\mathfrak{u}) \right\}}$$

subject to $\boldsymbol{u} = \bar{\boldsymbol{u}}$ on $\partial\mathscr{B}_u$, based on the functional

$$I^{\tau}_{\epsilon,\mathrm{red}} := \int_{\mathscr{B}} w_{\epsilon,\mathrm{red}}(\mathrm{GRAD}[\mathfrak{u}], \mathfrak{u})\,\mathrm{d}v + \int_{\partial\mathscr{B}_{\phi^e}} \bar{\phi}^e \boldsymbol{n}\cdot(\boldsymbol{d}-\boldsymbol{d}_n)\mathrm{d}a + \int_{\partial\mathscr{B}_{\phi^m}} \bar{\phi}^m \boldsymbol{n}\cdot(\boldsymbol{b}-\boldsymbol{b}_n)\mathrm{d}a$$

with incremental work potential $w_{\mathrm{red}}(\nabla\boldsymbol{u}, \boldsymbol{d}, \boldsymbol{b})$ from Box 2 or 3, extended by

$$w_{\epsilon,\mathrm{red}} := w_{\mathrm{red}}(\nabla\boldsymbol{u}, \boldsymbol{d}, \boldsymbol{b}) + \frac{\epsilon_e}{2}\,\mathrm{tr}^2[\nabla\boldsymbol{d}] + \frac{\epsilon_m}{2}\,\mathrm{tr}^2[\nabla\boldsymbol{b}]$$

2. *Enthalpy-based Formulation.* The primary variables are the displacement $\boldsymbol{u}$, the electric and magnetic potentials ϕ^e and ϕ^m. For known internal variables $\mathfrak{q}$ obtained by constitutive updates in Box 2 or 3, the generalized displacement

$$\mathfrak{u}' := [\boldsymbol{u}, -\phi^e, -\phi^m]^{\mathrm{T}} \in \mathscr{R}^{d+2}$$

is determined by the *reduced incremental saddle-point principle*

$$\boxed{\mathfrak{u}' = \mathrm{Arg}\left\{ \inf_{\boldsymbol{u}} \sup_{-\phi^e} \sup_{-\phi^m} I'^{\tau}_{\mathrm{red}}(\mathfrak{u}') \right\}}$$

subject to $\boldsymbol{u} = \bar{\boldsymbol{u}}$ on $\partial\mathscr{B}_u$, $\phi^e = \bar{\phi}^e$ on $\partial\mathscr{B}_{\phi^e}$ and $\phi^m = \bar{\phi}^m$ on $\partial\mathscr{B}_{\phi^m}$, based on

$$I'^{\tau}_{\mathrm{red}} := \int_{\mathscr{B}} w'_{\mathrm{red}}(\mathrm{GRAD}[\mathfrak{u}'])\,\mathrm{d}v$$

with incremental work potential $w'_{\mathrm{red}}(\nabla\boldsymbol{u}, -\nabla\phi^e, -\nabla\phi^m)$ from Box 2 or 3.

a local point of the solid, obtained by

$$(S1): \quad \mathfrak{q} = \mathrm{Arg}\left\{ \inf_{\mathfrak{q}} w'(\mathfrak{f}', \mathfrak{q}) \right\} \quad \text{at } \boldsymbol{x} \in \mathscr{B} \tag{150}$$

for given $\mathfrak{f}' = \mathrm{GRAD}[\mathfrak{u}'] + \bar{\mathfrak{f}}'$ as pointed out in (102). Recall that we outlined details of the numerical implementation of this local constitutive minimization problem in Section 2.4. This defines the condensed or reduced incremental work potential

$$w'_{\mathrm{red}}(\mathfrak{f}') = \inf_{\mathfrak{q}} \hat{w}'(\mathfrak{f}', \mathfrak{q}) \tag{151}$$

as introduced in (103). With this condensed incremental work potential *for updated internal variables* $\mathfrak{q}$ at hand, we introduce a reduced incremental functional

$$I'^{\tau}_{\mathrm{red}}(\mathfrak{u}') = \int_{\mathscr{B}} \{ w'_{\mathrm{red}}(\mathrm{GRAD}[\mathfrak{u}'] + \bar{\mathfrak{f}}') - \bar{\mathfrak{g}}'\cdot(\mathfrak{u}' - \mathfrak{u}'_n) \}\,\mathrm{d}v - \int_{\partial\mathscr{B}_{\mathfrak{t}'}} \bar{\mathfrak{t}}'\cdot(\mathfrak{u}' - \mathfrak{u}'_n)\mathrm{d}a \tag{152}$$

Copyright © 2011 John Wiley & Sons, Ltd.

DOI: 10.1002/nme

that depends only on the generalized displacement vector $\mathbf{u}'$ at the current time t. The *second solution step* then considers the reduced stationary principle

$$(S2): \quad \mathbf{u}' = \mathrm{Arg}\left\{ \operatorname*{stat}_{\mathbf{u}' \in \mathscr{W}'} I'^{\tau}_{\mathrm{red}}(\mathbf{u}') \right\}. \tag{153}$$

The variation of this principle gives the necessary condition

$$\delta I'^{\tau}_{\mathrm{red}} = \int_{\mathscr{B}} \{ \partial_{\mathbf{f}'} w'_{\mathrm{red}} \cdot \mathrm{GRAD}[\delta \mathbf{u}'] - \bar{\mathbf{g}}' \cdot \delta \mathbf{u}' \} \, \mathrm{d}v - \int_{\partial \mathscr{B}_{\mathrm{t}'}} \bar{\mathbf{t}}' \cdot \delta \mathbf{u}' \mathrm{d}a = 0. \tag{154}$$

Taking into account $\delta \mathbf{u} \in \mathscr{W}_0 := \{ \delta \mathbf{u} | \delta \mathbf{u} = \mathbf{0} \text{ on } \partial \mathscr{B}_{\mathrm{u}} \}$, and using the Gauss theorem in terms of the generalized displacement field, we end up with

$$\delta I'^{\tau}_{\mathrm{red}} = - \int_{\mathscr{B}} \{ \mathrm{DIV}[\partial_{\mathbf{f}'} \psi'] + \bar{\mathbf{g}}' \} \cdot \delta \mathbf{u}' \, \mathrm{d}v + \int_{\partial \mathscr{B}_{\mathrm{t}'}} \{ [\partial_{\mathbf{f}'} \psi'] \cdot \mathfrak{n} - \bar{\mathbf{t}}' \} \cdot \delta \mathbf{u}' \mathrm{d}a = 0, \tag{155}$$

where we inserted (114) or (119). The Euler equations of the reduced variational principle outlined above are the balance equations (134) of coupled electro-magneto-mechanics, including the constitutive equations (140), along with the Neumann-type boundary conditions $(146)_2$ for the coupled fields, i.e.

$$\begin{aligned} \mathrm{Div}[\partial_{\boldsymbol{f}} \psi'] + \bar{\gamma} = \mathbf{0} \quad & \text{in } \mathscr{B}, \quad \partial_{\boldsymbol{f}} \psi' \cdot \boldsymbol{n} = \bar{\boldsymbol{t}} \quad \text{on } \partial \mathscr{B}_t, \\ \mathrm{Div}[-\partial_{\boldsymbol{e}} \psi'] + \bar{\rho}^e = 0 \quad & \text{in } \mathscr{B}, \quad \partial_{\boldsymbol{e}} \psi' \cdot \boldsymbol{n} = \bar{d} \quad \text{on } \partial \mathscr{B}_d, \\ \mathrm{Div}[-\partial_{\boldsymbol{h}} \psi'] = 0 \quad & \text{in } \mathscr{B}, \quad \partial_{\boldsymbol{h}} \psi' \cdot \boldsymbol{n} = \bar{b} \quad \text{on } \partial \mathscr{B}_b. \end{aligned} \tag{156}$$

Note again the compactness of the notation introduced above. The variational functional (147) of coupled electro-magneto-mechanics has formally the same structure as the classical variational functional of elastostatics. It extends the classical principle of minimum potential energy of elastostatics to a stationarity principle for the fully coupled problem. With regard to the subclass of electro-mechanical problems, the principle is in line with the variational framework of Allik and Hughes [51] for *non-dissipative* piezoelectricity. Note that the above enthalpy-based principle has a saddle-point property for the coupled problem. A distinct energy-based minimization principle of coupled electro-magneto-mechanics is constructed below.

5.2. Energy-based variational principles for dissipative response

5.2.1. Lagrange-type variational principle. We now construct an energy-based minimization principle for the coupled electro-magneto-mechanical response. To this end, we proceed in the following steps. First, we consider the mixed energy–enthalpy function ψ' in work potential w' defined in (100) as a function of the energy ψ through the Legendre–Fenchel transformation of the form (83), which we write in context with the potential relationships (127) in the form

$$\psi' = \inf_{\boldsymbol{d}, \boldsymbol{b}} [\psi(\mathrm{Grad}[\boldsymbol{u}], \boldsymbol{d}, \boldsymbol{b}, \mathbf{q}; \boldsymbol{x}) + \boldsymbol{d} \cdot \mathrm{Grad}[\phi^e] + \boldsymbol{b} \cdot (\mathrm{Grad}[\phi^m] - \bar{\boldsymbol{h}})]. \tag{157}$$

This equation is used to eliminate the mixed energy–enthalpy ψ' in the incremental variational principle (148). Insertion of the expression in the bracket of (157) into the functional I'^{τ} defined in (147), using integration by parts based on the relationships $\boldsymbol{d} \cdot \mathrm{Grad}[\phi^e] = \mathrm{Div}[\phi^e \boldsymbol{d}] - \phi^e \mathrm{Div}[\boldsymbol{d}]$ and $\boldsymbol{b} \cdot \mathrm{Grad}[\phi^m] = \mathrm{Div}[\phi^m \boldsymbol{b}] - \phi^m \mathrm{Div}[\boldsymbol{b}]$ and taking into account the boundary conditions $(144)_1$ and $(145)_1$ for the electric and magnetic potentials $\bar{\phi}^e$ and $\bar{\phi}^e$ on $\partial \mathscr{B}_{\phi^e}$ and $\partial \mathscr{B}_{\phi^m}$, we end up with the *energy-based incremental functional*

$$\begin{aligned} I^{\tau}_{\lambda}(\mathbf{u}, \phi^e, \phi^m, \mathbf{q}) = & \int_{\mathscr{B}} \{ w(\mathrm{Grad}[\boldsymbol{u}], \boldsymbol{d}, \boldsymbol{b}, \mathbf{q}; \boldsymbol{x}) - \phi^e (\mathrm{Div}[\boldsymbol{d}] - \bar{\rho}^e) - \phi^m \mathrm{Div}[\boldsymbol{b}] \} \, \mathrm{d}v \\ & - \int_{\mathscr{B}} \bar{\mathbf{g}} \cdot (\mathbf{u} - \mathbf{u}_n) \, \mathrm{d}v - \int_{\partial \mathscr{B}_{\mathrm{t}}} \bar{\mathbf{t}} \cdot (\mathbf{u} - \mathbf{u}_n) \mathrm{d}a \end{aligned} \tag{158}$$

Copyright © 2011 John Wiley & Sons, Ltd.

DOI: 10.1002/nme

in terms of the incremental work potential w defined in (46). Here, we introduced the *modified* generalized displacement vector

$$\boxed{\mathfrak{u} := [\boldsymbol{u}, \boldsymbol{d}, \boldsymbol{b}]^{\mathrm{T}} \in \mathscr{R}^{3d}} \tag{159}$$

dual to (122) and a *modified* generalized body force vector

$$\bar{\mathfrak{g}} := [\bar{\gamma}, \mathbf{0}, \bar{\boldsymbol{h}}]^{\mathrm{T}} \in \mathscr{R}^{3d} \tag{160}$$

dual to (135). Thus, in the energy-based variational formulation, we use the electric displacement $\boldsymbol{d}$ and the magnetic induction $\boldsymbol{b}$ as primary variables and consider the boundary condition for these fields as the Dirichlet-type conditions. As a consequence, we interchanged (144) and (145) by considering $\boldsymbol{d}\cdot\boldsymbol{n} = -\bar{d}(\boldsymbol{x}, t)$ on $\partial\mathscr{B}_d$ and $\phi^e = \bar{\phi}^e(\boldsymbol{x}, t)$ on $\partial\mathscr{B}_{\phi^e}$ as the electric Dirichlet- and Neumann-type conditions, respectively, and $\boldsymbol{b}\cdot\boldsymbol{n} = -\bar{b}(\boldsymbol{x}, t)$ on $\partial\mathscr{B}_b$ and $\phi^m = \bar{\phi}^m(\boldsymbol{x}, t)$ on $\partial\mathscr{B}_{\phi^m}$ as the magnetic Dirichlet- and Neumann-type conditions, respectively. The functional (158) was obtained by assuming the Dirichlet-type conditions to be *a priori satisfied*. Similar to (146), we write in the energy formulation the boundary conditions in the array format

$$\mathfrak{u} = \bar{\mathfrak{u}}(\boldsymbol{x}, t) \text{ on } \partial\mathscr{B}_{\mathrm{u}} \quad \text{and} \quad \mathfrak{s}\cdot\mathfrak{n} = \bar{\mathfrak{t}}(\boldsymbol{x}, t) \text{ on } \partial\mathscr{B}_{\mathrm{t}}, \tag{161}$$

where, $\bar{\mathfrak{u}} := [\bar{\boldsymbol{u}}(\boldsymbol{x}, t), -\bar{d}(\boldsymbol{x}, t)\boldsymbol{n}, -\bar{b}(\boldsymbol{x}, t)\boldsymbol{n}]^{\mathrm{T}} \in \mathscr{R}^{3d}$ assembles the prescribed primary variables on the complementary Dirichlet boundaries $\partial\mathscr{B}_{\mathrm{u}} := \{\partial\mathscr{B}_u, \partial\mathscr{B}_d, \partial\mathscr{B}_b\}$. Furthermore, $\bar{\mathfrak{t}} := [\bar{\boldsymbol{t}}, -\bar{\phi}^e\boldsymbol{n}, -\bar{\phi}^e\boldsymbol{n}]^{\mathrm{T}} \in \mathscr{R}^{3d}$ assembles the prescribed variables on the complementary Neumann boundaries $\partial\mathscr{B}_{\mathrm{t}} := \{\partial\mathscr{B}_t, \partial\mathscr{B}_{\phi^e}, \partial\mathscr{B}_{\phi^m}\}$. The generalized vector $\mathfrak{n} := [\boldsymbol{n}, \boldsymbol{n}, \boldsymbol{n}]^{\mathrm{T}}$ provides the outward surface normals for each partial field of the coupled problem. $\mathfrak{s}$ is the canonical generalized stress vector defined in (3).

With the above Lagrange-type functional (158) at hand, we define the incremental *energy-based variational principle*

$$\boxed{\{\mathfrak{u}, \phi^e, \phi^m, \mathfrak{q}\} = \mathrm{Arg}\left\{\inf_{\boldsymbol{u},\boldsymbol{d},\boldsymbol{b}} \sup_{\phi^e,\phi^m} \inf_{\mathfrak{q}} I_\lambda^\tau(\boldsymbol{u}, \boldsymbol{d}, \boldsymbol{b}, \phi^e, \phi^m, \mathfrak{q})\right\}} \tag{162}$$

subject to the complementary Dirichlet-type boundary conditions

$$\mathscr{W} := \{\mathfrak{u} | \mathfrak{u} = \bar{\mathfrak{u}}(\boldsymbol{x}, t) \text{ on } \partial\mathscr{B}_{\mathrm{u}}\}. \tag{163}$$

Note that this energy-based variational principle includes the mechanical displacement $\boldsymbol{u}$, the electric potential $\boldsymbol{d}$, the magnetic induction $\boldsymbol{b}$ and the internal variable $\mathfrak{q}$ as variables, but in addition still the electric and magnetic potentials ϕ^e and ϕ^m, respectively. The latter two are viewed as *Lagrangian multiplier fields*, which enforce the electric Gauss and the magnetic Gauss–Faraday laws (133) as constraints. The solution of the above variational principle is achieved in *two steps* similar to the constitutive problem outlined in Section 2. Owing to the local nature of the evolution equations for the internal variables, see e.g (39), the *first solution step* is the incremental update of the internal variables at a local point of the solid, obtained by

$$(S1): \quad \mathfrak{q} = \mathrm{Arg}\left\{\inf_{\mathfrak{q}} w(\mathfrak{f}, \mathfrak{q})\right\} \quad \text{at } \boldsymbol{x} \in \mathscr{B} \tag{164}$$

for given $\mathfrak{f} = \{\mathrm{Grad}[\boldsymbol{u}], \boldsymbol{d}, \boldsymbol{b}\}$ as pointed out in (48). Recall that we outlined details of the numerical implementation of this local constitutive minimization problem in Section 2.4. This defines the condensed or reduced incremental work potential

$$w_{\mathrm{red}}(\mathfrak{f}) = \inf_{\mathfrak{q}} w(\mathfrak{f}, \mathfrak{q}) \tag{165}$$

Copyright © 2011 John Wiley & Sons, Ltd.

DOI: 10.1002/nme

as introduced in (49). With this condensed incremental work potential *for updated internal variables* $\mathbf{q}$ at hand, we introduce a reduced incremental functional

$$I^{\tau}_{\lambda,\mathrm{red}}(\mathbf{u},\phi^e,\phi^m)=\int_{\mathscr{B}}\{w_{\mathrm{red}}(\mathrm{Grad}[\boldsymbol{u}],\boldsymbol{d},\boldsymbol{b};\boldsymbol{x})-\phi^e(\mathrm{Div}[\boldsymbol{d}]-\bar{\rho}^e)-\phi^m\mathrm{Div}[\boldsymbol{b}]\}\,\mathrm{d}v$$
$$-\int_{\mathscr{B}}\bar{\mathbf{g}}\cdot(\mathbf{u}-\mathbf{u}_n)\,\mathrm{d}v-\int_{\partial\mathscr{B}_{\mathrm{t}}}\bar{\mathbf{t}}\cdot(\mathbf{u}-\mathbf{u}_n)\mathrm{d}a \tag{166}$$

that depends only on the generalized displacement vector $\mathbf{u}$ and the Lagrange parameters ϕ^e and ϕ^m at the current time t. The *second solution step* then considers the reduced stationary principle

$$(S2):\quad \{\mathbf{u},\phi^e,\phi^m\}=\mathrm{Arg}\left\{\inf_{\boldsymbol{u},\boldsymbol{d},\boldsymbol{b}}\sup_{\phi^e,\phi^m} I^{\tau}_{\lambda,\mathrm{red}}(\boldsymbol{u},\boldsymbol{d},\boldsymbol{b},\phi^e,\phi^m)\right\}. \tag{167}$$

The variation of the functional $I_{\lambda\mathrm{red}}$ gives the necessary condition

$$\delta I^{\tau}_{\lambda,\mathrm{red}}=\int_{\mathscr{B}}\{-(\mathrm{Div}[\partial_f w_{\mathrm{red}}]+\bar{\boldsymbol{\gamma}})\cdot\delta\boldsymbol{u}+(\partial_d w_{\mathrm{red}}+\mathrm{Grad}[\phi^e])\cdot\delta\boldsymbol{d}$$
$$+(\partial_b w_{\mathrm{red}}+\mathrm{Grad}[\phi^m]-\bar{\boldsymbol{h}})\cdot\delta\boldsymbol{b}-(\mathrm{Div}[\boldsymbol{d}]-\bar{\rho}^e)\delta\phi^e-(\mathrm{Div}[\boldsymbol{b}])\delta\phi^m\}\,\mathrm{d}v$$
$$+\int_{\partial\mathscr{B}_t}(\partial_f w\cdot\boldsymbol{n}-\bar{\boldsymbol{t}})\cdot\delta\boldsymbol{u}\mathrm{d}a-\int_{\partial\mathscr{B}_{\phi^e}}(\phi^e-\bar{\phi}^e)\boldsymbol{n}\cdot\delta\boldsymbol{d}\mathrm{d}a-\int_{\partial\mathscr{B}_{\phi^m}}(\phi^m-\bar{\phi}^m)\boldsymbol{n}\cdot\delta\boldsymbol{b}\mathrm{d}a=0. \tag{168}$$

yielding with (71) or (81) the Euler equations

$$\begin{aligned}
\mathrm{Div}[\partial_f\psi]+\bar{\boldsymbol{\gamma}}=\mathbf{0}\quad&\text{in }\mathscr{B},\qquad \mathrm{Div}[\boldsymbol{b}]=0\quad\text{in }\mathscr{B},\\
\partial_d\psi=-\mathrm{Grad}[\phi^e]\quad&\text{in }\mathscr{B},\qquad \partial_f\psi\cdot\boldsymbol{n}=\bar{\boldsymbol{t}}\quad\text{on }\partial\mathscr{B}_t,\\
\partial_b\psi-\bar{\boldsymbol{h}}=-\mathrm{Grad}[\phi^m]\quad&\text{in }\mathscr{B},\qquad \phi^e=\bar{\phi}^e\quad\text{on }\partial\mathscr{B}_{\phi^e},\\
\mathrm{Div}[\boldsymbol{d}]=\bar{\rho}^e\quad&\text{in }\mathscr{B},\qquad \phi^m=\bar{\phi}^m\quad\text{on }\partial\mathscr{B}_{\phi^m}.
\end{aligned} \tag{169}$$

These are the electro-magneto-mechanical balance equations (131) and (133), the electro-magnetic potential Equations (127) and the boundary conditions for the mechanical traction as well as the electric and magnetic potentials.**

**The Canonical Minimization Principle.* With the interpretation of the electric and magnetic potentials ϕ^e and ϕ^m in (158) as Lagrangian multiplier fields, we may define a *pure minimization principle of electro-magneto-mechanics*

$$\{\mathbf{u},\mathbf{q}\}=\mathrm{Arg}\left\{\inf_{\mathbf{u}\in\mathscr{W}_{ext},\mathbf{q}} I^{\tau}(\mathbf{u},\mathbf{q})\right\}=\mathrm{Arg}\left\{\inf_{\boldsymbol{u},\boldsymbol{d},\boldsymbol{b},\mathbf{q}} I^{\tau}(\boldsymbol{u},\boldsymbol{d},\boldsymbol{b},\mathbf{q})\right\} \tag{170}$$

based on the energy-based incremental functional

$$I^{\tau}(\mathbf{u},\mathbf{q})=\int_{\mathscr{B}}\{w(\mathrm{Grad}[\boldsymbol{u}],\boldsymbol{d},\boldsymbol{b},\mathbf{q})-\bar{\mathbf{g}}\cdot(\mathbf{u}-\mathbf{u}_n)\}\,\mathrm{d}v-\int_{\partial\mathscr{B}_{\mathrm{t}}}\bar{\mathbf{t}}\cdot(\mathbf{u}-\mathbf{u}_n)\mathrm{d}a. \tag{171}$$

Note that this energy-based functional I^{τ} is formally dual to the enthalpy-based functional I'^{τ} defined in (147). However, its variation is subject to the complementary Dirichlet-type boundary conditions *and additional constraints* on the dielectric displacement $\boldsymbol{d}$ and the magnetic induction $\boldsymbol{b}$ such that they satisfy *a priori* the Gauss-law and the Gauss–Faraday law, respectively. That is

$$\mathscr{W}_{ext}:=\{\mathbf{u}|\mathbf{u}=\bar{\mathbf{u}}(\boldsymbol{x},t)\text{ on }\partial\mathscr{B}_{\mathrm{u}},\mathrm{Div}[\boldsymbol{d}]=\bar{\rho}^e\text{ and }\mathrm{Div}[\boldsymbol{b}]=0\text{ in }\mathscr{B}\}. \tag{172}$$

We consider the minimization principle (170) as the *canonical energy-based variational principle of electro-magneto-mechanics*. It extends a suggestion of Mielke and Timofte [71] from electro-mechanics to electro-magneto-mechanics. Hence, when looking backward from our current state of development, we may consider the above derived variational principle (162) based on the Lagrange functional I_λ as a technical realization of the minimization principle (170) based on a *Lagrangian multiplier method* for the enforcement of the electro-magnetic constraints.

Copyright © 2011 John Wiley & Sons, Ltd.

DOI: 10.1002/nme

5.2.2. Penalty-type variational principle. We now suggest a simpler technical realization of an energy-based minimization principle

$$\boxed{\{\mathfrak{u},\mathfrak{q}\}=\mathrm{Arg}\left\{\inf_{\mathfrak{u}\in\mathscr{W},\mathfrak{q}} I_\epsilon^\tau(\mathfrak{u},\mathfrak{q})\right\}=\mathrm{Arg}\left\{\inf_{\boldsymbol{u},\boldsymbol{d},\boldsymbol{b},\mathfrak{q}} I_\epsilon^\tau(\boldsymbol{u},\boldsymbol{d},\boldsymbol{b},\mathfrak{q})\right\}} \tag{173}$$

subject to (163) in terms of the *penalty functional*

$$I_\epsilon^\tau(\mathfrak{u},\mathfrak{q})=\int_{\mathscr{B}}\{w_\epsilon(\mathrm{Grad}[\boldsymbol{u}],\boldsymbol{d},\boldsymbol{b},\mathfrak{q};\boldsymbol{x})-\bar{\mathfrak{g}}\cdot(\mathfrak{u}-\mathfrak{u}_n)\}\,\mathrm{d}v-\int_{\partial\mathscr{B}_\mathrm{t}}\bar{\mathfrak{t}}\cdot(\mathfrak{u}-\mathfrak{u}_n)\mathrm{d}a, \tag{174}$$

formulated in terms of an *extended penalty-type work potential*

$$w_\epsilon=w(\mathrm{Grad}[\boldsymbol{u}],\boldsymbol{d},\boldsymbol{b},\mathfrak{q})+\frac{\epsilon_e}{2}(\mathrm{tr}(\mathrm{Grad}[\boldsymbol{d}])-\bar{\rho}^e)^2+\frac{\epsilon_m}{2}\mathrm{tr}^2(\mathrm{Grad}[\boldsymbol{b}]), \tag{175}$$

which relaxes the Gauss- and Gauss–Faraday law constraints on $\boldsymbol{d}$ and $\boldsymbol{b}$, respectively. ϵ_e and ϵ_m are constant penalty parameters. Problem (173) gives the exact result of (170) for the limits $\epsilon_e\to\infty$ and $\epsilon_m\to\infty$. The solution of the above variational principle is achieved in *two steps*, where the *first solution step* is the incremental update (164) of the internal variables and the definition (165) of the condensed incremental work potential $w_\mathrm{red}(\mathfrak{f})$. We introduce a reduced incremental functional

$$I_{\epsilon,\mathrm{red}}^\tau(\mathfrak{u})=\int_{\mathscr{B}}\{w_{\epsilon,\mathrm{red}}(\mathrm{Grad}[\boldsymbol{u}],\boldsymbol{d},\boldsymbol{b})-\bar{\mathfrak{g}}\cdot(\mathfrak{u}-\mathfrak{u}_n)\}\,\mathrm{d}v-\int_{\partial\mathscr{B}_\mathrm{t}}\bar{\mathfrak{t}}\cdot(\mathfrak{u}-\mathfrak{u}_n)\mathrm{d}a \tag{176}$$

that depends only on the generalized displacement vector $\mathfrak{u}$ at the current time t. The *second solution step* then considers the reduced minimization principle

$$(S2):\quad \{\mathfrak{u}\}=\mathrm{Arg}\left\{\inf_{\boldsymbol{u},\boldsymbol{d},\boldsymbol{b}} I_{\epsilon,\mathrm{red}}^\tau(\boldsymbol{u},\boldsymbol{d},\boldsymbol{b})\right\}. \tag{177}$$

The variation of the functional $I_{\epsilon,\mathrm{red}}$ gives the necessary condition

$$\begin{aligned}\delta I_{\epsilon,\mathrm{red}}^\tau=&\int_{\mathscr{B}}\{-(\mathrm{Div}[\partial_{\boldsymbol{f}}w_\mathrm{red}]+\bar{\boldsymbol{\gamma}})\cdot\delta\boldsymbol{u}+(\partial_d w_\mathrm{red}+\mathrm{Grad}[\phi_\epsilon^e])\cdot\delta\boldsymbol{d}+(\partial_b w_\mathrm{red}+\mathrm{Grad}[\phi_\epsilon^m]-\bar{\boldsymbol{h}})\cdot\delta\boldsymbol{b}\}\,\mathrm{d}v\\&+\int_{\partial\mathscr{B}_t}(\partial_{\boldsymbol{f}}w_\mathrm{red}\cdot\boldsymbol{n}-\bar{\boldsymbol{t}})\cdot\delta\boldsymbol{u}\mathrm{d}a-\int_{\partial\mathscr{B}_{\phi^e}}(\phi_\epsilon^e-\bar{\phi}^e)\boldsymbol{n}\cdot\delta\boldsymbol{d}\mathrm{d}a-\int_{\partial\mathscr{B}_{\phi^m}}(\phi_\epsilon^m-\bar{\phi}^m)\boldsymbol{n}\cdot\delta\boldsymbol{b}\mathrm{d}a=0,\end{aligned} \tag{178}$$

yielding with (71) or (81) the Euler equations

$$\begin{aligned}\mathrm{Div}[\partial_{\boldsymbol{f}}\psi]+\bar{\boldsymbol{\gamma}}=\boldsymbol{0}\quad&\text{in }\mathscr{B},\quad \partial_{\boldsymbol{f}}\psi\cdot\boldsymbol{n}=\bar{\boldsymbol{t}}\quad\text{on }\partial\mathscr{B}_t,\\ \partial_d\psi=-\mathrm{Grad}[\phi_\epsilon^e]\quad&\text{in }\mathscr{B},\quad \phi_\epsilon^e=\bar{\phi}^e\quad\text{on }\partial\mathscr{B}_{\phi^e},\\ \partial_b\psi-\bar{\boldsymbol{h}}=-\mathrm{Grad}[\phi_\epsilon^m]\quad&\text{in }\mathscr{B},\quad \phi_\epsilon^m=\bar{\phi}^m\quad\text{on }\partial\mathscr{B}_{\phi^m}.\end{aligned} \tag{179}$$

In contrast to (169), where the electric and magnetic fields ϕ^e and ϕ^m appear as Lagrangian multipliers, they are in the above representation *defined by the expressions*

$$\phi_\epsilon^e:=-\epsilon_e(\mathrm{Div}[\boldsymbol{d}]-\bar{\rho}^e)\quad\text{and}\quad\phi_\epsilon^m:=-\epsilon_m\mathrm{Div}[\boldsymbol{b}] \tag{180}$$

in terms of the penalizations of violations of the Gauss- and Gauss–Faraday laws, respectively. Thus, for $\epsilon_e\to\infty$ and $\epsilon_m\to\infty$, the Euler equations of the variational principle (173) are the mechanical balance equations (131) along with Faraday's and Ampere's laws (127), which postulate the potential character of $\partial_d\psi$ and $\partial_b\psi-\bar{\boldsymbol{h}}$, respectively. The electro-mechanical balances, i.e. the Gauss and Gauss–Faraday laws (133), are incorporated by the penalty terms. Clearly, for large but

Copyright © 2011 John Wiley & Sons, Ltd.

DOI: 10.1002/nme

finite values of ϵ_e and ϵ_m used in practical applications such as outlined in the subsequent finite element treatment, the penalty-type minimization principle (173) satisfies these equations only in an approximative manner.[††]

5.3. FE discretization of enthalpy-based variational principle

An approximative numerical solution of the variational problem (153) associated with the *second solution step* can be obtained by a finite element method. We consider a monolithic discretization of the coupled electro-magneto-mechanical problem by a generalized displacement-type finite element method with mechanical, electric and magnetic degrees of freedom at the nodes. For a given finite element triangulation, the discrete variables of the coupled problem are assembled in the global generalized displacement vector

$$\mathfrak{d}' := [\boldsymbol{d}, -d^e, -d^m]^{\mathrm{T}} \in R^{N\cdot(d+2)}, \tag{185}$$

which assembles the coupled degrees at the M nodes of the mesh. It contains all nodal displacements $\boldsymbol{d}$, the *negative* electric nodal potential $-d^e$ and the *negative* magnetic nodal potential $-d^m$ of the finite element mesh at the current time t. With this notion at hand, we discretize the generalized displacement vector of the coupled problem and its gradient by

$$\mathfrak{u}'^h = \mathfrak{N}'\mathfrak{d}' \quad \text{and} \quad \mathrm{GRAD}[\mathfrak{u}'^h] = \mathfrak{B}'\mathfrak{d}' \tag{186}$$

in terms of N finite elements $\mathscr{B}^e \subset \mathscr{B}^h$ in the discretized solid domain $\mathscr{B}^h$. Here, $\mathfrak{N}'(\boldsymbol{x})$ is the matrix of finite element interpolation functions, $\mathfrak{B}'(\boldsymbol{x})$ the associated gradient matrix. With these shapes at hand, the finite element discretization of the above variational functional (152) appears in the form

$$I'^h_{\mathrm{red}}(\mathfrak{d}') = \int_{\mathscr{B}} \{w'(\mathfrak{B}'\mathfrak{d}' + \bar{\mathfrak{f}}'; \boldsymbol{x}) - \bar{\mathfrak{g}}' \cdot \mathfrak{N}'(\mathfrak{d}' - \mathfrak{d}'_n)\}\,\mathrm{d}v - \int_{\partial\mathscr{B}_{t'}} \bar{\mathfrak{t}}' \cdot \mathfrak{N}'(\mathfrak{d}' - \mathfrak{d}'_n)\mathrm{d}a \tag{187}$$

[††] *Vector-Potential-Type Variational Principle.* A third possibility for the technical realization of the variational principle (170) is the so-called *vector-potential method*. Examples are formulations in electro-mechanics proposed by Landis [56] and Semenov *et al*. [57]. Here, the basic idea is to substitute the electric and magnetic variables $\boldsymbol{d}$ and $\boldsymbol{b}$ in (170) by the expressions

$$\boldsymbol{d}(\boldsymbol{D}) = \mathrm{Curl}[\boldsymbol{D}] + \bar{\boldsymbol{d}} \quad \text{and} \quad \boldsymbol{b}(\boldsymbol{B}) = \mathrm{Curl}[\boldsymbol{B}] \tag{181}$$

in terms of the new vector fields $\boldsymbol{D}$ and $\boldsymbol{B}$, denoted as the *electric and magnetic vector potentials*, respectively. In $(181)_1$, $\bar{\boldsymbol{d}}$ is some given vector that satisfies $\mathrm{Div}[\bar{\boldsymbol{d}}] = \bar{\rho}^e$, accounting for the free charges in the domain. Note that the above ansatz satisfies a priori the Gauss- and Gauss–Faradays laws $\mathrm{Div}[\boldsymbol{d}] - \bar{\rho}^e = 0$ and $\mathrm{Div}[\boldsymbol{b}] = 0$ due to the property $\mathrm{Div}(\mathrm{Curl}[\boldsymbol{v}]) = \epsilon_{ijk} v_{k,ji} = 0$ of the curl-operator. Thus, the transformation is consistent with the admissible set $\mathscr{W}_{ext}$ of fields $\boldsymbol{d}$ and $\boldsymbol{b}$ defined in (173). However, note that the relationships between $\boldsymbol{D}$ and $\boldsymbol{d}$ as well as between $\boldsymbol{B}$ and $\boldsymbol{b}$ defined in (181) are *not unique*, because they are also satisfied for the transformed vector potentials $\boldsymbol{D} \to \boldsymbol{D} + \mathrm{Grad}[\delta]$ and $\boldsymbol{B} \to \boldsymbol{B} + \mathrm{Grad}[\mu]$ with the *arbitrary* scalar gauge functions δ and μ. This is a consequence of the property $\mathrm{Curl}(\mathrm{Grad}[s]) = \epsilon_{ijk} s_{,kj} = 0$ of the curl-operator. Hence, subsequent variational formulations based on the vector potentials $\boldsymbol{D}$ and $\boldsymbol{B}$ must be regularized by enforcing *additional gauge conditions*, such as the Coulomb-type constraints

$$\mathrm{Div}[\boldsymbol{D}] = 0 \quad \text{and} \quad \mathrm{Div}[\boldsymbol{B}] = 0, \tag{182}$$

which *determine* the abovementioned gauge functions by $\Delta\delta = 0$ and $\Delta\mu = 0$. Substituting the transformations (181) into (171), we obtain the incremental vector potential functional depending on the generalized displacement field

$$\mathfrak{U} := [\boldsymbol{u}, \boldsymbol{D}, \boldsymbol{B}]^{\mathrm{T}} \in \mathscr{R}^{3d}, \tag{183}$$

which assembles the displacement vector $\boldsymbol{u}$ and the electric and magnetic vector potentials $\boldsymbol{D}$ and $\boldsymbol{B}$, respectively. Similar to (175), we define an extended penalty-type incremental work potential

$$\hat{w}_v = \hat{w}(\mathrm{Grad}[\boldsymbol{u}], \mathrm{Curl}[\boldsymbol{D}] + \bar{\boldsymbol{d}}, \mathrm{Curl}[\boldsymbol{B}], \mathfrak{q}; \boldsymbol{x}) + \frac{\alpha_e}{2}\,\mathrm{tr}^2(\mathrm{Grad}[\boldsymbol{D}]) + \frac{\alpha_m}{2}\,\mathrm{tr}^2(\mathrm{Grad}[\boldsymbol{B}]), \tag{184}$$

which accounts exactly for the gauge constraints (182) in the limit $\alpha_e \to \infty$ and $\alpha_m \to \infty$ of the penalty parameters α_e and α_m, respectively.

Copyright © 2011 John Wiley & Sons, Ltd.

DOI: 10.1002/nme

and the discrete version of the variational principle (153) reads as

$$(S2): \quad \mathfrak{d}' = \mathrm{Arg}\left\{ \underset{\mathfrak{d}' \in \mathscr{W}'^h}{\mathrm{stat}} I'^h_{\mathrm{red}}(\mathfrak{d}') \right\} \tag{188}$$

in terms of the admissible generalized nodal displacements. Here, $\mathscr{W}'^h$ is the set of admissible nodal variables that satisfy the discrete version of the Dirichlet-type boundary conditions

$$\mathscr{W}'^h := \{\mathfrak{d}' | \mathfrak{d}' = \bar{\mathfrak{d}}' \text{ on } \partial\mathscr{B}^h_{\mathrm{u}'}\}. \tag{189}$$

The necessary condition of the above discrete variational principle (188)

$$I'^h_{\mathrm{red},\mathfrak{d}'}(\mathfrak{d}') = \mathbf{0} \tag{190}$$

provides a non-linear algebraic system for the determination of the generalized displacement vector $\mathfrak{d}'$ of the coupled electro-magneto-mechanical problem. This problem might be highly non-linear. It can be solved by a Newton–Raphson iteration, yielding the update equations

$$\mathfrak{d}' \Leftarrow \mathfrak{d}' - [I'^h_{\mathrm{red},\mathfrak{d}'\mathfrak{d}'}(\mathfrak{d}')]^{-1}[I'^h_{\mathrm{red},\mathfrak{d}'}(\mathfrak{d}')] \tag{191}$$

performed by some solver of linear equations. Observe carefully the *symmetry of the coupled tangent matrix* $\mathfrak{K}' := I'^h_{\mathrm{red},\mathfrak{d}'\mathfrak{d}'}$ resulting form the variational structure of the electro-magneto-mechanical problem. The iteration is terminated for

$$\| I'^h_{\mathrm{red},\mathfrak{d}'}(\mathfrak{d}') \| < \mathrm{tol} \tag{192}$$

if the residual $\mathfrak{r}' := I'^h_{\mathrm{red},\mathfrak{d}'}$ is less than a certain tolerance. Based on the variational structure of the coupled problem, the basic finite element arrays are determined by the first and second derivatives of the discrete variational functional (187). The *finite element residual vector array*

$$\mathfrak{R}' := I'^h_{\mathrm{red},\mathfrak{d}'} = \int_{\mathscr{B}} \{\mathfrak{B}'^T \mathfrak{s}'^h - \mathfrak{N}'^T \bar{\mathfrak{g}}'\}\, \mathrm{d}v - \int_{\partial\mathscr{B}_{\mathrm{t}'}} \mathfrak{N}'^T \bar{\mathfrak{t}}'\, \mathrm{d}a \tag{193}$$

and the *finite element tangent matrix array*

$$\mathfrak{K}' := I'^h_{\mathrm{red},\mathfrak{d}'\mathfrak{d}'} = \int_{\mathscr{B}} \mathfrak{B}'^T \mathfrak{c}'^h \mathfrak{B}'\, \mathrm{d}v \tag{194}$$

are governed by the generalized stresses and moduli

$$\mathfrak{s}'^h := \partial_{\mathfrak{f}'^h} w'(\mathfrak{B}'\mathfrak{d}' + \bar{\mathfrak{f}}'; \boldsymbol{x}) \quad \text{and} \quad \mathfrak{c}'^h := \partial^2_{\mathfrak{f}'^h \mathfrak{f}'^h} w'(\mathfrak{B}'\mathfrak{d}' + \bar{\mathfrak{f}}'; \boldsymbol{x}) \tag{195}$$

of the coupled problem. For the solution technique outlined above, these two arrays provide the interface to an individual local material model as outlined in Section 3.3, see Equations (114) and (119). These constitutive expressions contain for the linearized setting all coupling effects. Clearly, due to the variational structure of the coupled constitutive problem, the coupled moduli $\mathfrak{c}'^h$ is *symmetric*. However, recall, that due to saddle-point structure of the coupled variational principle, these moduli are *not positive definite*. As a consequence, the finite element tangent matrix $\mathfrak{K}'$ of the coupled problem defined in (194) is also not positive definite. This excludes the application of certain solvers for the linearized coupled problem. We therefore show below a variational structure based on a minimization structure.

5.4. FE discretization of energy-based variational principles

The finite element implementation of the penalty-type reduced incremental variational problem (177) is based on a generalized finite element method with mechanical, electric and magnetic degrees at the nodes. For a given finite element triangulation, the discrete variables of the coupled problem are assembled in the global generalized displacement vector

$$\mathfrak{d} := [\boldsymbol{d}, \boldsymbol{d}^e, \boldsymbol{d}^m]^{\mathrm{T}} \in R^{N\cdot(d+2)} \tag{196}$$

Copyright © 2011 John Wiley & Sons, Ltd.

DOI: 10.1002/nme

dual to (185). It contains all nodal displacements $\boldsymbol{d}$, the electric nodal displacement $\boldsymbol{d}^e$ and the magnetic nodal induction $\boldsymbol{d}^m$ of the finite element mesh at the current time t. With this notion at hand, we discretize the generalized displacement vector of the coupled problem and its gradient by

$$\mathbf{u}^h = \mathfrak{N}\mathfrak{d} \quad \text{and} \quad \text{GRAD}[\mathbf{u}^h] = \mathfrak{B}\mathfrak{d} \tag{197}$$

in terms of N finite elements $\mathscr{B}^e \subset \mathscr{B}^h$ in the discretized solid domain $\mathscr{B}^h$. Here, $\mathfrak{N}(\boldsymbol{x}) = [\boldsymbol{N}(\boldsymbol{x}), \boldsymbol{N}^e(\boldsymbol{x}), \boldsymbol{N}^m(\boldsymbol{x})]$ is the matrix of finite element interpolation functions, $\mathfrak{B}(\boldsymbol{x}) = [\boldsymbol{B}(\boldsymbol{x}), \boldsymbol{B}^e(\boldsymbol{x}), \boldsymbol{B}^m(\boldsymbol{x})]$ the associated gradient matrix. In what follows we drop the subscript that indicates the current time. With these shapes at hand, the finite element discretization of the above variational functional (176) appears in the form

$$I^h_{\epsilon,\text{red}}(\mathfrak{d}) = \int_{\mathscr{B}} \{w_\epsilon(\boldsymbol{B}_\epsilon \mathfrak{d}; \boldsymbol{x}) - \bar{\mathfrak{g}} \cdot \mathfrak{N}(\mathfrak{d} - \mathfrak{d}_n)\} \, \mathrm{d}v - \int_{\partial \mathscr{B}_\mathfrak{t}} \bar{\mathfrak{t}} \cdot \mathfrak{N}(\mathfrak{d} - \mathfrak{d}_n) \mathrm{d}a, \tag{198}$$

where we have introduced the finite element arrays $\boldsymbol{B}_\epsilon := [\boldsymbol{B}, \boldsymbol{N}^e, \boldsymbol{N}^m]$, $\boldsymbol{B}^e_\epsilon := [\boldsymbol{0}, \boldsymbol{B}^e, \boldsymbol{0}]$ and $\boldsymbol{B}^m_\epsilon := [\boldsymbol{0}, \boldsymbol{0}, \boldsymbol{B}^m]$. Then the discrete version of the variational principle (177) reads as

$$(S2): \quad \mathfrak{d} = \text{Arg}\{\inf_{\mathfrak{d} \in \mathscr{W}^h} I^h_{\epsilon,\text{red}}(\mathfrak{d})\} \tag{199}$$

in terms of the admissible generalized nodal displacements. Here, $\mathscr{W}^h$ is the set of admissible nodal variables which satisfy the discrete version of the Dirichlet-type boundary conditions

$$\mathscr{W}^h := \{\mathfrak{d} | \mathfrak{d} = \bar{\mathfrak{d}} \text{ on } \partial \mathscr{B}^h_\mathfrak{u}\}. \tag{200}$$

The necessary condition of the above discrete variational principle

$$I^h_{\epsilon,\text{red},\mathfrak{d}}(\mathfrak{d}) = \boldsymbol{0} \tag{201}$$

provides a non-linear algebraic system for the determination of the generalized displacement vector $\mathfrak{d}$ of the non-linear incremental electro-magneto-mechanical problem. It can be solved by a Newton–Raphson iteration, yielding the update equations

$$\mathfrak{d} \Leftarrow \mathfrak{d} - [I^h_{\epsilon,\text{red},\mathfrak{d}\mathfrak{d}}(\mathfrak{d})]^{-1} [I^h_{\epsilon,\text{red},\mathfrak{d}}(\mathfrak{d})] \tag{202}$$

performed by some solver of linear equations. Observe carefully the *symmetry of the coupled tangent matrix* $\mathfrak{K} := I^h_{\epsilon,\text{red},\mathfrak{d}\mathfrak{d}}$ resulting from the variational structure of the electro-magneto-mechanical problem. The iteration is terminated for

$$\| I^h_{\epsilon,\text{red},\mathfrak{d}}(\mathfrak{d}) \| < \text{tol} \tag{203}$$

if the residual $\mathfrak{R} := I^h_{\epsilon,\text{red},\mathfrak{d}}$ is less than a certain tolerance. Based on the variational structure of the coupled problem, the basic finite element arrays are determined by the first and second derivatives of the discrete variational functional (198). For the penalty method under consideration, the *finite element residual and tangent arrays* can be partitioned by

$$\mathfrak{R} = \mathfrak{R}_\epsilon + \mathfrak{R}^e_\epsilon + \mathfrak{R}^m_\epsilon \quad \text{and} \quad \mathfrak{K} = \mathfrak{K}_\epsilon + \mathfrak{K}^e_\epsilon + \mathfrak{K}^m_\epsilon. \tag{204}$$

The ground state contributions

$$\mathfrak{R}_\epsilon := \int_{\mathscr{B}} \{\mathfrak{B}^{\mathrm{T}}_\epsilon \mathfrak{s}^h - \mathfrak{N}^{\mathrm{T}} \bar{\mathfrak{g}}\} \mathrm{d}v - \int_{\partial \mathscr{B}_\mathfrak{t}} \mathfrak{N}^T \bar{\mathfrak{t}} \mathrm{d}a \quad \text{and} \quad \mathfrak{K}_\epsilon := \int_{\mathscr{B}} \mathfrak{B}^{\mathrm{T}}_\epsilon \mathfrak{c}^h \mathfrak{B}_\epsilon \, \mathrm{d}v \tag{205}$$

are governed by the generalized stresses and moduli

$$\mathfrak{s}^h := \partial_{\mathfrak{f}^h} \psi(\mathfrak{B}_\epsilon \mathfrak{d}; \boldsymbol{x}) \quad \text{and} \quad \mathfrak{c}^h := \partial^2_{\mathfrak{f}^h \mathfrak{f}^h} \psi(\mathfrak{B}_\epsilon \mathfrak{d}; \boldsymbol{x}) \tag{206}$$

of the coupled problem. For the solution technique outlined above, these two arrays provide the interface to an individual local material model as outlined in Section 2.3, see Equations (10) and

Copyright © 2011 John Wiley & Sons, Ltd.

DOI: 10.1002/nme

(21). These constitutive expressions contain for the linearized setting all coupling effects. Note carefully that due to minimization structure of the energy-based variational setting, these moduli are *positive definite*. As a consequence, the finite element tangent matrix $\mathfrak{K}$ of the coupled problem defined in (204) is also positive definite. This allows the application of efficient solvers like the conjugate gradient methods to the linearized coupled problem. The penalty contributions take the form

$$\mathfrak{R}^i_\epsilon := \int_{\mathscr{B}} \mathfrak{B}^{i\mathrm{T}}_\epsilon \phi^{ih}_\epsilon \, \mathrm{d}v \quad \text{and} \quad \mathfrak{K}^i_\epsilon := \int_{\mathscr{B}} \mathfrak{B}^{i\mathrm{T}}_\epsilon \epsilon_i \mathfrak{B}^i_\epsilon \, \mathrm{d}v \tag{207}$$

for $i = e, m$ are determined by the electric and magnetic potentials

$$\phi^{eh}_\epsilon := \epsilon_e(\mathrm{tr}(\boldsymbol{B}^e_\epsilon \mathfrak{d}) - \bar{\rho}^e) \quad \text{and} \quad \phi^{mh}_\epsilon := \mathrm{tr}\boldsymbol{B}^m_\epsilon \mathfrak{d}. \tag{208}$$

The penalty contributions (207) to the tangent *must be singular* in order to be successful. This is achieved by a *reduced integration* of these finite element arrays.

6. RESPONSE OF A THREE-PHASE MULTIFERROIC COMPOSITE

We now consider a numerical example which applies the above outlined formulations to a model problem: the modeling of the response of a *multiferroic composite* with full electro-magneto-mechanical coupling. The ME coupling effect, inherent in these composites, has recently attracted attention and opens important perspectives for the future design of new functional materials. Large ME coupling effects may be achieved in three-phase composite materials consisting of *electro-elastic, magneto-elastic and elastic phases*. Here, the ME coupling is achieved through the elastic matrix phase in which the electro-elastic and magneto-elastic particles are embedded. *Such a composite exhibits an ME coupling that is absent in each of the individual phases*. We refer to Fiebig [3], Eerenstein *et al*. [4] and Nan *et al.* [5] for a review of the ME effect and the associated materials. Lee *et al.* [2] performed a numerical investigation of the effective properties of a three-phase electro-magneto-elastic composite; however, restricted to linear response. In what follows, we outline a conceptual simulation of the fully dissipative, hysteretic macroscopic response of a multiferroic composite. To this end, we consider a three-phase electro-magneto-elastic composite material with a microstructure depicted in Figure 6, consisting of an elastic matrix with ferroelectric ($BaTiO_3$) and ferromagnetic ($Fe_{0.81}Ga_{0.19}$) inclusions of spherical shape. The elastic matrix is indicated in green, the ferroelectric inclusion in yellow and the ferromagnetic one in red color. The constitutive functions and inherent material parameters are specified below.

6.1. Ferroelectric and ferromagnetic constitutive functions of phases

For the model problem, we focus on the *enthalpy-based constitutive variational principles* for rate-dependent, dissipative response of the phases as outlined in Section 3, see Box 1 for a guideline and Box 3 for the definition of the incremental potentials. The constitutive functions for the *mixed energy–enthalpy function* ψ' of the composite phases are specifications of the energetic

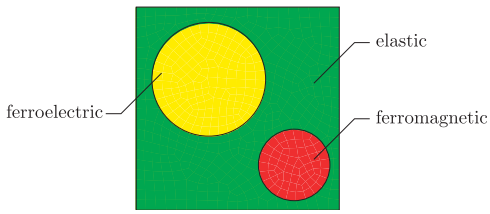

Figure 6. Microstructure of a three-phase multiferroic composite, allowing for electro-magneto-elastic coupling, consisting of an elastic matrix (green color) with ferroelectric $BaTiO_3$ (yellow) and ferromagnetic $Fe_{0.81}Ga_{0.19}$ (red) inclusions of spherical shape.

Copyright © 2011 John Wiley & Sons, Ltd.

DOI: 10.1002/nme

Table I. Material parameters adopted for the epoxy elastic matrix.

No.	Param.	Unit	Name	Value
1	λ	N/mm^2	Lamé parameter	2.97×10^3
2	μ	N/mm^2	Lamé parameter	1.28×10^3
3	μ_e	$mC/(kV\,m)$	Electric permittivity	0.1×10^{-3}
4	μ_m	N/A^2	Magnetic permeability	1×10^{-6}

formulations (32)–(37), subsequently being processed by the partial Legendre transformation (83). The *dual dissipation function* ϕ^* for a rate-dependent evolution of the electric polarization and the magnetization assumes the constitutive structure (75) in terms of the simple switching function f defined in (63). We choose idealized representations which contain on a simple level all relevant ferroelectric or ferromagnetic coupling effects. These functions will be specified in terms of the structural tensors

$$\begin{aligned}\mathbb{C}' &:= 2\mu\mathbb{I}+\lambda\mathbf{1}\otimes\mathbf{1},\\ \boldsymbol{\mu}_i' &:= \mu_i\mathbf{1},\\ \mathbb{h}'(\boldsymbol{a}) &:= \overset{12}{\mathrm{sym}}[\alpha_0^i\boldsymbol{a}\otimes\boldsymbol{a}\otimes\boldsymbol{a}+\alpha_\perp^i\mathbf{1}\otimes\boldsymbol{a}+\alpha_=^i\boldsymbol{a}\otimes\mathbf{1}].\end{aligned} \tag{209}$$

$\mathbb{C}'$ is an isotropic elasticity tensor, expressed in terms of the Lamé parameters λ and μ. $\boldsymbol{\mu}_i'$ are for $i=e,m$ isotropic electric permittivity and magnetic permeability tensors, respectively, with dielectric permittivity μ_e and magnetic permeability μ_m. Finally, $\mathbb{h}'(\boldsymbol{a})$ are for $i=e,m$ transversely isotropic, piezoelectric or a piezomagnetic coupling tensors, respectively. They are described in terms of the three coupling parameters $\alpha_\parallel^i$, $\alpha_\perp^i$, and $\alpha_=^i$, with $\alpha_0^i := \alpha_\parallel^i-\alpha_\perp^i-\alpha_=^i$.

6.1.1. Elastic phase. The elastic matrix phase is assumed to be epoxy. Its non-dissipative response is fully characterized by the mixed energy–enthalpy function

$$\psi'(\boldsymbol{\varepsilon},\boldsymbol{e},\boldsymbol{h}) = \tfrac{1}{2}\boldsymbol{\varepsilon}:\mathbb{C}':\boldsymbol{\varepsilon}-\tfrac{1}{2}\boldsymbol{e}\cdot\boldsymbol{\mu}_e'\cdot\boldsymbol{e}-\tfrac{1}{2}\boldsymbol{h}\cdot\boldsymbol{\mu}_m'\cdot\boldsymbol{h} \tag{210}$$

with structural tensors specified in 209 and the material parameters specified in Table I.

6.1.2. Ferroelectric phase. The dissipative ferroelectric phase is described by the internal variable vector $\mathfrak{q} := \{\boldsymbol{p}\}\in\mathscr{R}^3$ with dual force $\mathfrak{p} := \{\boldsymbol{\pi}^e\}\in\mathscr{R}^3$, according to the reduced setting (36), where $\boldsymbol{p}$ is the *remanent electric polarization* at a local material point. We assume the mixed energy–enthalpy and dual dissipation functions

$$\begin{aligned}\psi'(\boldsymbol{\varepsilon}^e,\boldsymbol{e},\boldsymbol{h},\boldsymbol{p}) &= \frac{1}{2}\boldsymbol{\varepsilon}^e:\mathbb{C}':\boldsymbol{\varepsilon}^e-\boldsymbol{\varepsilon}^e:\frac{|\boldsymbol{p}|}{p_s}\mathbb{h}'(\boldsymbol{a}^e)\cdot\boldsymbol{e}-\frac{1}{2}\boldsymbol{e}\cdot\boldsymbol{\mu}_e'\cdot\boldsymbol{e}-\boldsymbol{e}\cdot\boldsymbol{p}\\ &\quad -h_0^e\,p_s^2\left[\ln\left(1-\frac{|\boldsymbol{p}|}{p_s}\right)+\frac{|\boldsymbol{p}|}{p_s}\right]-\frac{1}{2}\boldsymbol{h}\cdot\boldsymbol{\mu}_m'\cdot\boldsymbol{h},\\ \phi^*(\boldsymbol{\pi}^e) &= \frac{e_c}{\eta^e(1+m^e)}\left\langle\frac{|\boldsymbol{\pi}^e|}{e_c}-1\right\rangle^{1+m^e}\end{aligned} \tag{211}$$

as specifications of (34), (37) and (75). Here, we use a kinematic assumption of the form (35) for the coupling of the remanent strain $\boldsymbol{\varepsilon}_e^r$ with the polarization $\boldsymbol{p}$, i.e.

$$\boldsymbol{\varepsilon}^e := \boldsymbol{\varepsilon}-\boldsymbol{\varepsilon}_e^r \quad\text{with}\quad \hat{\boldsymbol{\varepsilon}}_e^r(\boldsymbol{p}) := \frac{3}{2}\varepsilon_s^e\frac{|\boldsymbol{p}|}{p_s}\mathrm{dev}[\boldsymbol{a}^e\otimes\boldsymbol{a}^e] \tag{212}$$

and the polarization director $\boldsymbol{a}^e := \boldsymbol{p}/|\boldsymbol{p}|$. e_c is the coercive electric field, p_s the saturation polarization, ε_s^e the electric saturation strain, h_0^e a hysteresis shape parameter for the ferroelectric hystereses,

Copyright © 2011 John Wiley & Sons, Ltd.

DOI: 10.1002/nme

Table II. Material parameters adopted for $BaTiO_3$.

No.	Param.	Unit	Name	Value
1	λ	N/mm^2	Lamé parameter	76.6×10^3
2	μ	N/mm^2	Lamé parameter	44.7×10^3
3	α_0^e	$N/(kV\,mm)$	Piezoelectric coefficient	-0.2
4	$\alpha_\perp^e$	$N/(kV\,mm)$	Piezoelectric coefficient	-4.4
5	$\alpha_=^e$	$N/(kV\,mm)$	Piezoelectric coefficient	23.2
6	μ_e	$mC/(kV\,m)$	Electric permittivity	11.2×10^{-3}
7	μ_m	N/A^2	Magnetic permeability	5×10^{-6}
8	e_c	kV/mm	Coercive electric field	1.0
9	p_s	C/m^2	Saturation polarization	2.6×10^{-3}
10	ε_s^e	—	Elec. saturation remanent strain	0.1%
11	h_0^e	$(kV\,m)/C$	Elec. hysteresis shape parameter	3.8×10^3
12	η^e	$(mm^2)/(Cs)$	Elec. viscosity coefficient	10^{-2}
13	m^e	—	Elec. viscosity exponent	2

η^e the viscosity of the polarization and finally m^e the viscosity shape exponent. The assumed ferroelectric material parameters for $BaTiO_3$ are listed in Table II.

6.1.3. Ferromagnetic phase. The dissipative ferromagnetic phase is described by the internal variable vector $\mathfrak{q}:=\{\boldsymbol{m}\}\in\mathscr{R}^3$ with dual force $\mathfrak{p}:=\{\boldsymbol{\pi}^m\}\in\mathscr{R}^3$ in an analogous structure to the above specified ferroelectric phase, i.e. according to the reduced setting (36), where $\boldsymbol{m}$ is the *remanent magnetization vector* at a local material point. Hence, we assume the mixed energy–enthalpy and dual dissipation functions

$$\begin{aligned}\psi'(\boldsymbol{\varepsilon}^e,\boldsymbol{e},\boldsymbol{h},\boldsymbol{m}) &= \frac{1}{2}\boldsymbol{\varepsilon}^e:\mathbb{C}':\boldsymbol{\varepsilon}^e-\boldsymbol{\varepsilon}^e:\frac{|\boldsymbol{m}|}{m_s}\mathbb{h}'(\boldsymbol{a}^m)\cdot\boldsymbol{h}-\frac{1}{2}\boldsymbol{h}\cdot\boldsymbol{\mu}_m'\cdot\boldsymbol{h}-\boldsymbol{h}\cdot\boldsymbol{m}\\ &\quad -h_0^m m_s^2\left[\ln\left(1-\frac{|\boldsymbol{m}|}{m_s}\right)+\frac{|\boldsymbol{m}|}{m_s}\right]-\frac{1}{2}\boldsymbol{e}\cdot\boldsymbol{\mu}_e'\cdot\boldsymbol{e},\\ \phi^*(\boldsymbol{\pi}^m) &= \frac{h_c}{\eta^m(1+m^m)}\left\langle\frac{|\boldsymbol{\pi}^m|}{h_c}-1\right\rangle^{1+m^m}\end{aligned}\tag{213}$$

dual to (211). Similar to (211), we make a kinematic assumption for the coupling of the remanent strain $\boldsymbol{\varepsilon}_m^r$ with the magnetization $\boldsymbol{m}$, i.e.

$$\boldsymbol{\varepsilon}^e:=\boldsymbol{\varepsilon}-\boldsymbol{\varepsilon}_m^r\quad\text{with}\quad\hat{\boldsymbol{\varepsilon}}_m^r(\boldsymbol{m}):=\frac{3}{2}\varepsilon_s^m\frac{|\boldsymbol{m}|}{m_s}\mathrm{dev}[\boldsymbol{a}^m\otimes\boldsymbol{a}^m]\tag{214}$$

and the magnetization director $\boldsymbol{a}^m:=\boldsymbol{m}/|\boldsymbol{m}|$. h_c is the coercive magnetic field, m_s the saturation magnetization, ε_s^m the magnetic saturation strain, h_0^m a hysteresis shape parameter for the ferromagnetic hystereses, η^m the viscosity of the magnetization, and finally m^m the viscosity shape exponent. The assumed ferromagnetic material parameters for $Fe_{0.81}Ga_{0.19}$ are specified in Table III.

6.2. Simulation of polarization, magnetization and overall response

For the subsequent investigation of the overall response, we discretize the multiferroic composite depicted in Figure 6 by the finite element method outlined in Section 5. Here, we use the *enthalpy-based variational structure of the incremental BVP* outlined in Section 5.1 and its space-discrete counterpart in Section 5.3. Box 5 summarizes the reduced variational principle based on the incremental constitutive potentials specified in Box 3, which governs the local update algorithms at typical integration points of the finite element mesh. As already highlighted in Section 5.3,

Copyright © 2011 John Wiley & Sons, Ltd.

DOI: 10.1002/nme

Table III. Material parameters adopted for $Fe_{0.81}Ga_{0.19}$ (Galfenol).

No.	Param.	Unit	Name	Value
1	λ	N/mm^2	Lamé parameter	15.0×10^3
2	μ	N/mm^2	Lamé parameter	10.0×10^3
3	α_0^m	N/(A mm)	Piezomagnetic coefficient	0.0733
4	$\alpha_\perp^m$	N/(A mm)	Piezomagnetic coefficient	0.1800
5	$\alpha_=^m$	N/(A mm)	Piezomagnetic coefficient	−0.1218
6	μ_e	mC/(kV m)	Electric permittivity	0.08×10^{-3}
7	μ_m	N/A^2	Magnetic permeability	4.5×10^{-6}
8	h_c	A/mm	Coercive magnetic field	2.0
9	m_s	N/(A mm)	Saturation magnetization	1.48×10^{-3}
10	ε_s^m	—	Mag. saturation remanent strain	0.025%
11	h_0^m	A^2/N	Mag. hysteresis shape parameter	5.0×10^3
12	η^m	(A mm)/(N s)	Mag. viscosity coefficient	10^{-3}
13	m^m	—	Mag. viscosity exponent	2

the finite element ansatz (186) of the proposed variational setting results in a fully *symmetric monolithic structure* of the coupled three-field problem.

6.2.1. Ferroelectric and ferromagnetic response of composite. As already mentioned, the material response of the two inclusions is dissipative in nature. By applying a cyclic electric field to the pure ferroelectric material beyond the coercive value e_c, the typical dielectric and butterfly hystereses shown in Figures 7(a) and (b) are observed. On the other hand, by loading the pure ferromagnetic material with a periodic magnetic field of magnitude above the coercive magnetic field h_c, the magnetization and total strain hysteresis curves of Figures 7(c) and (d) are obtained. *None of the phases of the composite exhibits an intrinsic magneto-electric coupling*. If we apply to the composite a cyclic electric potential jump $[\![\phi^e]\!](t) := \phi^e_+ - \phi^e_-$ or a cyclic magnetic potential jump $[\![\phi^m]\!](t) := \phi^m_+ - \phi^m_-$ as shown in Figure 9, the hystereses reported in Figure 8 are observed. Here, we made use of *averaged quantities* $\bar{s}$ of the heterogeneous composite, which are defined by the homogenization

$$\bar{s} := \frac{1}{\mathrm{vol}(\mathscr{B})}\int_{\mathscr{B}} s\,\mathrm{d}v \tag{215}$$

of a local variable s over the composite domain $\mathscr{B}$. The hystereses in Figure 8 are slim and the averaged remanent polarization and magnetization $\bar{\boldsymbol{p}}$ and $\bar{\boldsymbol{m}}$ reached after unloading are relatively small compared to the saturation values. The reason for this behavior is the polarization-induced electric field and magnetization-induced magnetic field generated by the poled ferroelectric and magnetized ferromagnetic phases, respectively, which tend to depolarize and demagnetize these phases.

6.2.2. Demonstration of the ME coupling effect. In order to demonstrate the ability of the multi-ferroic composite in Figure 6 to show ME coupling, we perform a numerical experiment consisting of the following three steps:

1. *Polarization step*: The ferroelectric material is poled by a strong external electric field, going beyond the coercive value within the ferroelectric inclusion region. Later, for small applied electro-mechanical loading, the material response of the inclusion is piezoelectric.
2. *Magnetization step*: The ferromagnetic material is magnetized by a strong external magnetic field, going beyond the coercive value within the ferromagnetic inclusion region. By applying successively small magneto-mechanical loadings, the material response of the inclusion turns to be piezomagnetic.

Copyright © 2011 John Wiley & Sons, Ltd.

DOI: 10.1002/nme

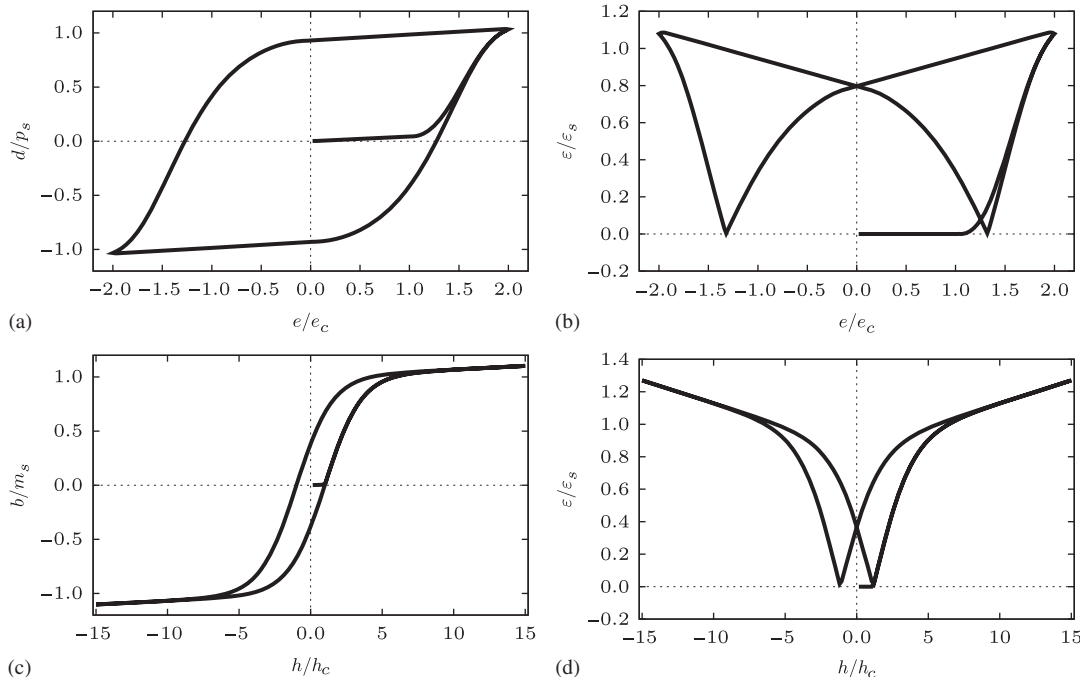

Figure 7. Hystereses in the pure ferroelectric ($BaTiO_3$) and ferromagnetic (Galfenol) phases. (a) Dielectric and (b) butterfly hystereses obtained under cyclic electric field. (c) Magnetic induction and (d) total strain hysteresis curves under cyclic magnetic field.

3. *Magneto-electric step*: An electric field is applied to the composite material and a variation of the magnetic induction is observed. This proves the magneto-electric coupling of the composite consisting of an elastic matrix with a poled ferroelectric inclusion and a magnetized ferromagnetic inclusion.

1. Polarization Step. In order to simulate a ferroelectric poling process, an electric potential jump $[\![\phi^e(t)]\!]$ is prescribed between two electrodes on the left and the right sides of the composite as triangular loading in the following manner: first $[\![\phi^e(t)]\!]$ is increased from 0 to 1500 kV until $t_1 = 100$ s and then reduced to zero at $t_2 = 200$ s, cf. Figure 9. Thus, an electric field greater than the coercive value e_c is reached in the ferroelectric inclusion region, inducing the poling. A high electric potential is needed because of the inhomogeneous composition of the material. In Figures 10(a) and (b), we report the electric potential distribution at the instant $t_1 = 100s$, when the highest voltage is applied, and $t_2 = 200$ s, after electric unloading, respectively. In the same Figures, the distribution of the remanent polarization $\boldsymbol{p}$ is reported. Note that the polarization is not homogeneously distributed within the ferroelectric phase. This is a consequence of the heterogeneity of the composite. Figure 10(c) and (d) show that the poling process leads to a deformation which affects the full composite.

2. Magnetization Step. Once the ferroelectric inclusion is poled, we magnetize the ferromagnetic phase. To this end, a magnetic potential jump $[\![\phi^m(t)]\!]$ is prescribed between the left and right boundaries of the composite as a pulse loading in the following manner: first $[\![\phi^m(t)]\!]$ is increased from 0 to 600 A until $t_1 = 100$ s and then reduced to zero at $t_2 = 200$ s, cf. Figure 9. Here, a magnetic field greater than the coercive value h_c is reached in the ferromagnetic inclusion region, inducing a full magnetization of the phase. A high magnetic potential is needed because of the inhomogeneity of the composite. Figures 11(a) and (b) report the magnetic potential distribution at the instant $t_1 = 100$ s, when the highest magnetic potential difference is applied, and $t_2 = 200$ s, after unloading. They also contain the distribution of the remanent magnetization $\boldsymbol{m}$. Similar to the electric polarization, the magnetization is not homogeneously distributed within the ferromagnetic

Copyright © 2011 John Wiley & Sons, Ltd.

DOI: 10.1002/nme

inclusion region. Figure 11(c) and (d) show the additional deformation in the composite implied by the magnetization.

3. ME Coupling Effect. After the above two steps, the ferroelectric and ferromagnetic inclusions are poled and magnetized. Thus, for small applied electric or magnetic fields below the coercive values, they show *linear piezoelectric or piezomagnetic behavior*, respectively. However, since the piezoelectric and piezomagnetic phases are joined by an elastic matrix, a *coupling between the electric, magnetic and strain fields of the composite is achieved*. Although the elastic matrix is neither piezoelectric nor piezomagnetic, the strain field in the matrix couples the electric field of the piezoelectric phase to the magnetic field of the piezomagnetic phase. Indeed, if the piezoelectric

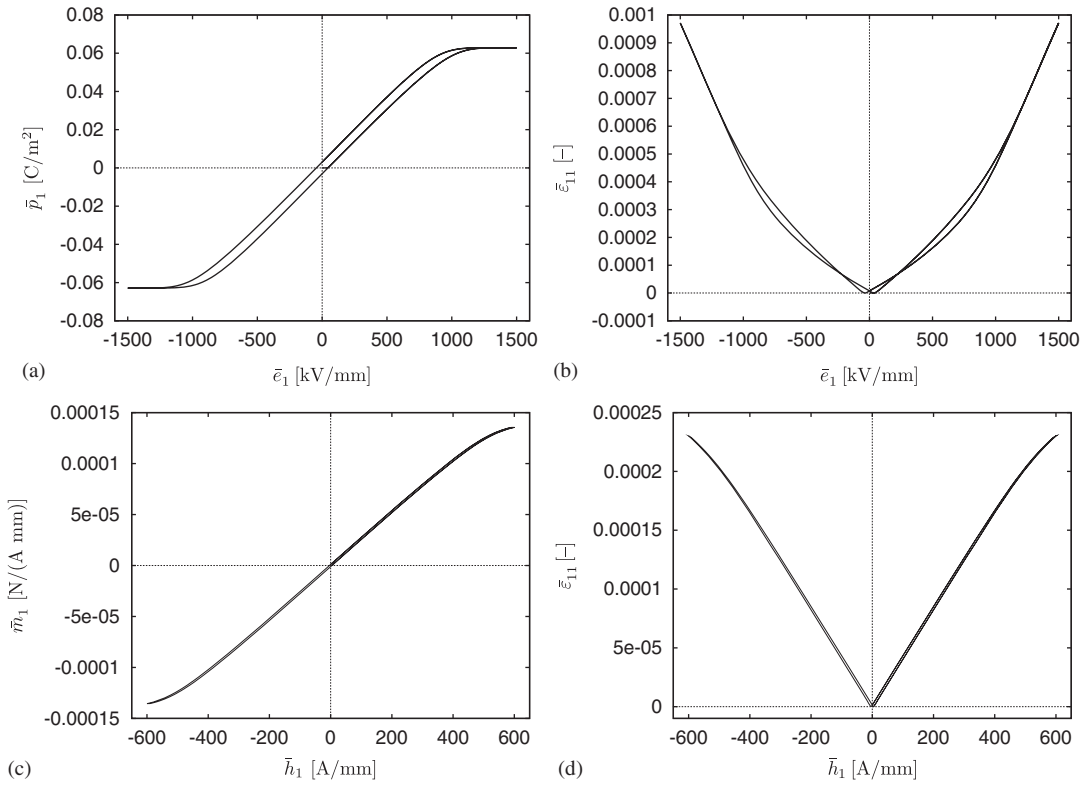

Figure 8. Hysteresis curves for three-phase composite. Hystereses of (a) $\bar{p}_1$ vs $\bar{e}_1$ and (b) $\bar{\boldsymbol{\varepsilon}}_{11}$ vs $\bar{e}_1$ under cyclic electric potential jump $[\![\phi^e(t)]\!]$ applied between the left and right electrodes (cf. Figure 9). Hystereses of (a) $\bar{m}_1$ vs $\bar{h}_1$ and (b) $\bar{\boldsymbol{\varepsilon}}_{11}$ vs $\bar{h}_1$ under cyclic magnetic potential jump $[\![\phi^m(t)]\!]$ applied between the left and right sides (cf. Figure 9).

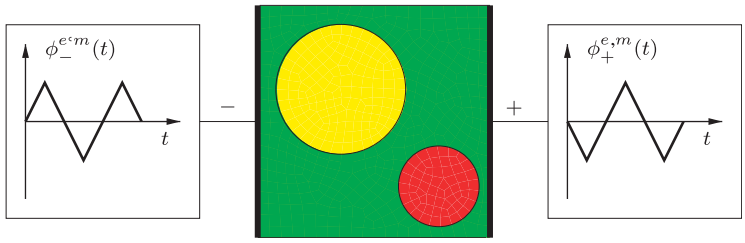

Figure 9. Loading conditions for the polarization and magnetization of the composite. Between the right (+) and left (−) sides, an electric potential jump $[\![\phi^e(t)]\!]$ is applied during the polarization. The composite is then loaded by a magnetic potential jump $[\![\phi^m(t)]\!]$ during subsequent magnetization. The specimen is left free to expand in both cases.

Copyright © 2011 John Wiley & Sons, Ltd.

DOI: 10.1002/nme

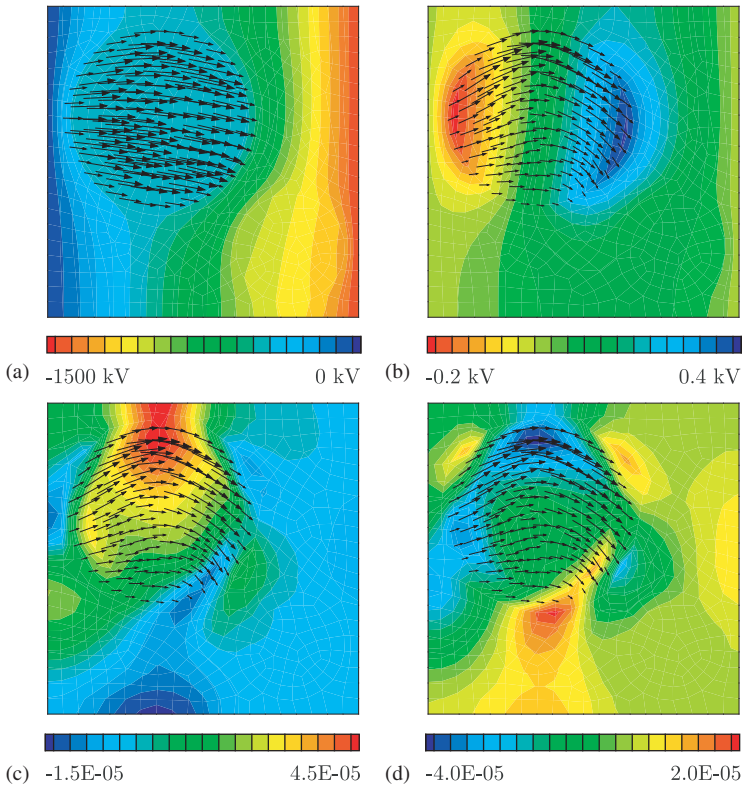

Figure 10. Polarization step 1. Polarization and electric potential (a) for the maximum electric potential jump $[\![\phi^e = 1500]\!]$ kV and (b) after unloading. A non-zero polarization remains in the ferroelectric phase after unloading, accompanied by a residual electric potential. As a consequence of the polarization process of the ferroelectric phase, a deformation remains after the electric unloading. The strain components ε_{11} and ε_{22} are plotted in (c) and (d), respectively.

phase deforms under the influence of an applied electric field, the deformation is transmitted to the piezomagnetic phase through the elastic matrix and the ferromagnetic particle generates a change in the magnetic induction. Conversely, a change in the electric displacement arises in the piezoelectric phase due to an elastic strain generated by the piezomagnetic phase under the influence of a magnetic field. Hence, the *multiferroic composite exhibits ME coupling*, though it is absent in each of the phases.

In order to demonstrate this coupling, we apply between the right and left electrodes a linearly increasing electric potential jump $[\![\phi^e(t)]\!]$ till a maximum value of 150 kV, which produces an electric field $\boldsymbol{e}$ in the ferroelectric phase much smaller than the coercive value e_c, i.e. $|\boldsymbol{e}| \ll e_c$. In order to ensure that the averaged strain $\bar{\boldsymbol{\varepsilon}}$ and magnetic field $\bar{\boldsymbol{h}}$ are zero, we set on the boundary $\partial\mathscr{B}$ of the composite jumps of the displacement $[\![\boldsymbol{u}(t)]\!]$ and the magnetic potential $[\![\phi^m(t)]\!]$ to zero. As a consequence, changes in the average secondary variables $\bar{\boldsymbol{\sigma}}$, $\bar{\boldsymbol{d}}$ and $\bar{\boldsymbol{b}}$ depend only on the changes of $\bar{\boldsymbol{e}}$. Applying a negative potential jump $[\![\phi^e(t)]\!]<0$, we observe an averaged electric field $\bar{\boldsymbol{e}}$, with 1-(horizontal)- and 2-(vertical-coordinates $|\bar{e}_1|>|\bar{e}_2|$ and $\bar{e}_1>0$. In particular, $|\bar{e}_2|$ is approximately 10% of $|\bar{e}_1|$. Hence, the averaged electric field is not completely oriented along the horizontal direction, because of the heterogeneity of the composite. Since we have $|\bar{p}_1|>|\bar{p}_2|$ with $\bar{p}_1>0$ and $|\bar{m}_1|>|\bar{m}_2|$ with $\bar{m}_1>0$, *such an electric field produces an elongation of the ferroelectric phase in the horizontal direction*. This deformation is then transferred to the ferromagnetic phase through the elastic matrix and *generates a contraction of the ferromagnetic phase in the horizontal direction*, because of the imposed stiff mechanical boundary conditions. As a consequence of this contraction, we observe a *decrease of the averaged magnetic induction* $\Delta\bar{b}_1$ *for an increase of the averaged electric field* $\Delta\bar{e}_1$. Figure 12 reports on this ME coupling by plotting changes of

Copyright © 2011 John Wiley & Sons, Ltd.

DOI: 10.1002/nme

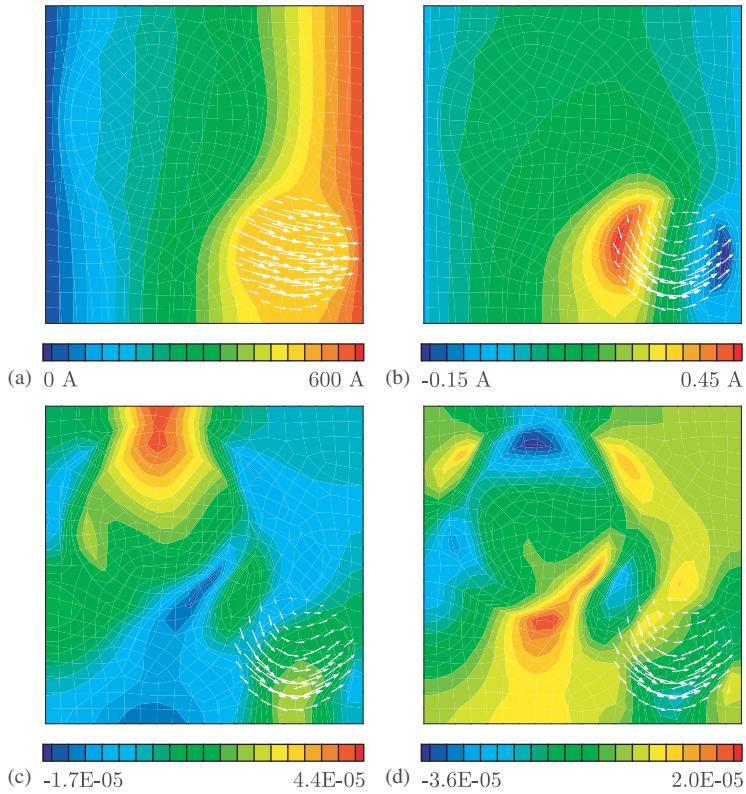

Figure 11. Magnetization step 2. Magnetization and magnetic potential (a) for the maximum magnetic potential jump $[\![\phi^m]\!] = 1500$ A and (b) after unloading. A non-zero magnetization remains in the ferromagnetic phase after unloading, accompanied by a residual magnetic potential. As a consequence of the magnetization process, a deformation remains after magnetic unloading, which is added to those which remained after the polarization-step. The strain components ε_{11} and ε_{22} are shown in (c) and (d), respectively.

the averaged components of the magnetic induction $\Delta\bar{b}_1$ and $\Delta\bar{b}_2$ as functions of the change in the homogenized electric field components $\Delta\bar{e}_1$ and $\Delta\bar{e}_2$. Note that an ME coupling is already evident after the electric polarization step 1. This can be observed in Figure 13 by plotting $\bar{d}_1$ as a function $\bar{h}_1$ during the magnetization step 2. Here, due to the large applied magnetic field, a *non-linear* ME coupling is observed. The presented types of numerical investigations provide a basis for future investigations on multiferroic sensors and actuators, which allow to control a magnetic field through an electric field and vice versa.

7. CONCLUSION

A general framework for the modeling of dissipative functional materials with electro-magneto-mechanical couplings based on *incremental variational principles* was developed. It focused on quasi-static problems, where mechanical inertia effects and time-dependent electro-magnetic couplings are *a priori* neglected and a time-dependence enters the formulation only through a possible rate-dependent dissipative material response. It was shown that the proposed variational structure of the coupled problem has consequences with respect to all aspects of the continuum-based modeling in electro-magneto-mechanics. At first, the *local constitutive modeling* of the coupled dissipative response, i.e. stress, electric and magnetic fields versus strain, electric displacement and magnetic induction, was based on incremental potentials. Next, the implications to the formulation of *boundary-value-problems* were shown, which appeared in energy-based

Copyright © 2011 John Wiley & Sons, Ltd.

DOI: 10.1002/nme

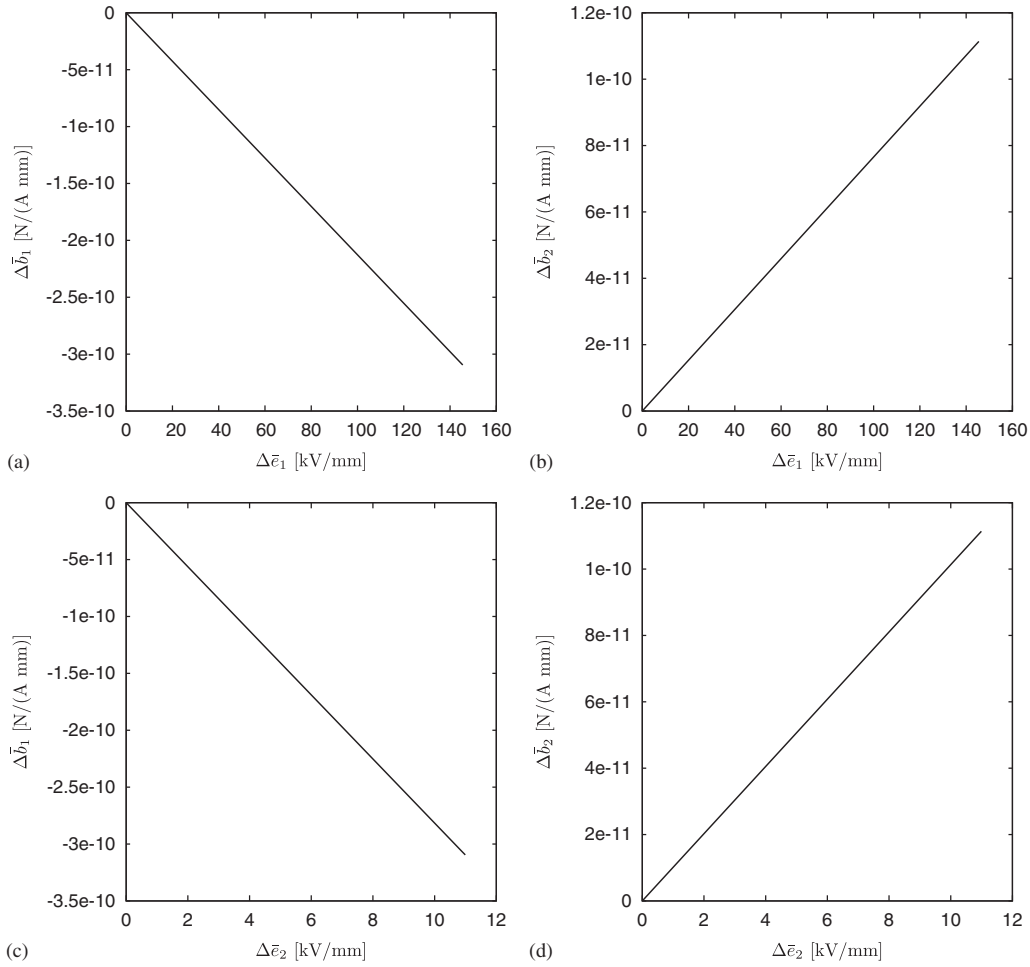

Figure 12. Magneto-electric coupling. After polarizing the ferroelectric phase and magnetizing the ferromagnetic phase, the application of an electric potential jump $[\![\phi^e(t)]\!]$ results in an ME coupling effect, i.e. a variation $\Delta\bar{\boldsymbol{b}}$ of the averaged magnetic induction $\bar{\boldsymbol{b}}$ as function of the variation $\Delta\bar{\boldsymbol{e}}$ of the homogenized electric field $\bar{\boldsymbol{e}}$.

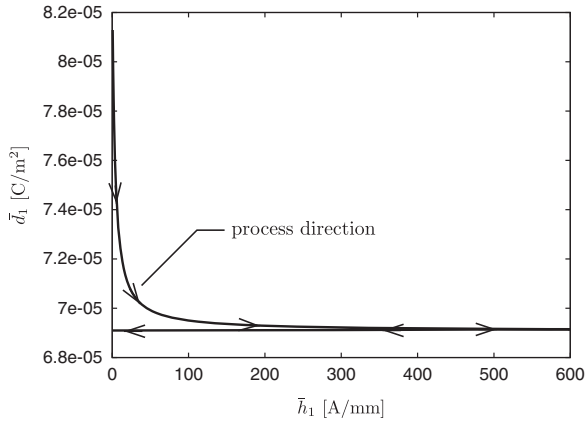

Figure 13. Magneto-electric coupling. After the polarization step, a coupling between magnetic and electric fields is already evident. Plotted is the component $\bar{d}_1$ of the averaged electric displacement versus the averaged electric field $\bar{h}_1$ during the magnetization process.

Copyright © 2011 John Wiley & Sons, Ltd.

DOI: 10.1002/nme

formulations as minimization problems and in enthalpy-based formulations as saddle-point problems. Furthermore, the *material stability* of dissipative electro-magneto-mechanical problems was defined in terms of the convexity/concavity of the incremental potentials. We outlined a spectrum of alternative variational principles and discussed implications with regard to their computational implementation, such as the formulation of constitutive update algorithms and finite element solvers. Form the viewpoint of the constitutive modeling, including the understanding of the stability in coupled electro-magneto-mechanics, an *energy-based formulation* was shown to be the canonical setting. From the viewpoint of the computational convenience, an *enthalpy-based formulation* is the most convenient setting. A numerical investigation of a *multiferroic composite* with full electro-magneto-mechanical coupling demonstrated perspectives of the proposed framework with regard to the future design of new functional materials.

ACKNOWLEDGEMENTS

A support for this research was provided by the German Research Foundation (DFG) for the Cluster of Excellence Exc 310 *Simulation Technology* at the University of Stuttgart.

REFERENCES

1. Bar-Cohen Y. *Electroactive Polymer* (*EAP*) *Actuators as Artificial Muscles—Reality*, *Potential and Challenges*. SPIE Press: Bellingham, 2004.
2. Lee J, Boyd IV JG, Lagoudas DC. Effective properties of three-phase electro-magneto-elastic composites. *International Journal of Engineering Science* 2005; **43**:790–825.
3. Fiebig M. Revival of the magnetoelectric effect. *Journal of Physics D*: *Applied Physics* 2005; **38**:R123–R152.
4. Eerenstein W, Mathur ND, Scott JF. Multiferroic and magnetoelectirc materials. *Nature* 2006; **442**:759–765.
5. Nan CW, Bichurin MI, Dong S, Viehland D, Srinivasan G. Multiferroic magnetoelectric composites: historical perspective, status, and future directions. *Journal of Applied Physics* 2008; **103**:031101-1-35.
6. Landau LD, Lifshitz EM. *Electrodynamics of Continuous Media*. Pergamon Press: Oxford, 1960.
7. Guggenheim EA. On magnetic and electrostatic energy. *Proceedings of the Royal Society of London A* 1936; **155**:49–70.
8. Guggenheim EA. The thermodynamics of magnetization. *Proceedings of the Royal Society of London A* 1936; **155**:70–101.
9. Tiersten HF. Coupled magnetomechanical equations for magnetically saturated insulators. *Journal of Mathematical Physics* 1964; **5**:1298–1318.
10. Tiersten HF, Tsai CF. On the interaction of the electromagnetic field with heat conducting deformable insulators. *Journal of Mathematics and Physics* 1972; **13**:361–378.
11. Brown Jr WF. Magnetoelastic interactions. *Tracts in Natural Philosophy*, vol. 9. Springer: New York, 1966;
12. Penfield Jr P, Haus HA. *Electrodynamics of Moving Media*. MIT Press: Cambridge MA, 1967.
13. Coleman BD, Dill EH. Thermodynamic restrictions on the constitutive equations of electromagnetic theory. *Zeitschrift für Angewandte Mathematik und Physik* 1971; **22**:691–702.
14. Coleman BD, Dill EH. On the thermodynamics of electromagnetic fields in materials with memory. *Archive for Rational Mechanics and Analysis* 1971; **41**:132–162.
15. Truesdell C, Toupin R. The classical field theories. In *Principles of Classical Mechanics and Field Theory*, *Encyclopedia of Physics*, Flügge S (ed.), vols. III/I. Springer: Berlin, 1960; 226–795.
16. Pao YH, Hutter K. Electrodynamics for moving elastic solids and viscous fluids. *Proceedings of the IEEE* 1975; **63**:1011–1021.
17. Hutter K, Van de Ven AAF, Urescu A. *Electromagnetic Field Matter Interactions in Thermoelastic Solids and Viscous Fluids*. Springer: Berlin, 2006.
18. Maugin GA, Eringen AC. On the equations of the electrodynamics of deformable bodies of finite extent. *Journal de Mécanique* 1977; **16**:101–147.
19. Eringen AC, Maugin GA. *Electrodynamics of Continua. Foundations and Solid Media*, vol. 1. Springer: Berlin, 1990.
20. Eringen AC, Maugin GA. *Electrodynamics of Continua. Fluid and Complex Media*, vol. 2. Springer: Berlin, 1990.
21. Maugin GA. *Continuum Mechanics of Electromagnetic Solids*. Elsevier: Amsterdam, 1988.
22. Nowacki W. Foundations of linear piezoelectricity. In *Electromagnetic Interactions in Elastic Solids*, Parkus H (ed.), vol. 257. Springer: Wien, 1979; 105–157.
23. Kovetz A. *Electromagnetic Theory*. Oxford University Press: Oxford, 2000.
24. Smith RC. *Smart Material Systems. Model Development*. SIAM Frontiers in Applied Mathematics: Philadelphia, 2005.
25. Ikeda T. *Fundamentals of Piezoelectricity*. Oxford University Press: Oxford, 1990.

Copyright © 2011 John Wiley & Sons, Ltd.

DOI: 10.1002/nme

26. Bassiouny E, Ghaleb AF, Maugin GA. Thermodynamical formulation for coupled electromechanical hysteresis effects. I. Basic equations. *International Journal of Engineering Science* 1988; **26**:1279–1295.
27. Bassiouny E, Ghaleb AF, Maugin GA. Thermodynamical formulation for coupled electromechanical hysteresis effects. II. Poling of ceramics. *International Journal of Engineering Science* 1988; **26**:1297–1306.
28. Bassiouny E, Maugin GA. Thermodynamical formulation for coupled electromechanical hysteresis effects. III. Parameter identification. *International Journal of Engineering Science* 1989; **27**:975–987.
29. Bassiouny E, Maugin GA. Thermodynamical formulation for coupled electromechanical hysteresis effects. IV. Combined electromechanical loading. *International Journal of Engineering Science* 1989; **27**:989–1000.
30. Cocks ACF, McMeeking RM. A phenomenological constitutive law for the behaviour of ferroelectric ceramics. *Ferroelectrics* 1999; **228**:219–228.
31. Kamlah M, Tsakmakis C. Phenomenological modeling of the non-linear electro-mechanical coupling in ferroelectrics. *International Journal of Solids and Structures* 1999; **36**:669–695.
32. Kamlah M, Böhle U. Finite element analysis of piezoceramic components taking into account ferroelectric hysteresis behavior. *International Journal of Solids and Structures* 2001; **38**:605–633.
33. Kamlah M, Wang Z. A thermodynamically and microscopically motivated constitute model for piezoceramics. *Computational Materials Science* 2003; **28**:409–418.
34. Landis CM. Fully coupled, multi-axial, symmetric constitutive laws for polycrystalline ferroelectric ceramics. *Journal of Mechanics and Phyiscs of Solids* 2002; **50**:127–152.
35. Landis CM. Non-linear constitutive modelling of ferroelectrics. *Current Opinion in Solid State and Materials Science* 2004; **8**:59–69.
36. Huber JE, Fleck NA. Multi-axial electrical switching of a ferroelectric: theory versus experiment. *Journal of Mechanics and Physics of Solids* 2001; **49**:785–811.
37. McMeeking RM, Landis CM. A phenomenological multi-axial constitutive law for switching in polycrystaline ferroelectric ceramics. *International Journal of Engineering Science* 2002; **40**:1553–1577.
38. Schröder J, Romanowski H. A thermodynamically consistent mesoscopic model for transversely isotropic ferroelectric ceramics in a coordinate-invariant setting. *Archive of Applied Mechanics* 2005; **74**:863–877.
39. Klinkel S. A phenomenological constitutive model for ferroelastic and ferroelectric hysteresis effects in ferroelectric ceramics. *International Journal of Solids and Structures* 2006; **43**:7197–7222.
40. Zhang W, Bhattacharya K. A computational model of ferroelectric domains. Part I: model formulation and domain switching. *Acta Materialia* 2005; **53**:185–198.
41. Zhang W, Bhattacharya K. A computational model of ferroelectric domains. Part II: grain boundaries and defect pinning. *Acta Materialia* 2005; **53**:199–209.
42. Su Y, Landis CM. Continuum thermodynamics of ferroelectric domain evolution: theory, finite element implementation, and application to domain wall pinning. *Journal of the Mechanics and Physics of Solids* 2007; **55**:280–305.
43. Schrade D, Müller R, Gross D. Domain evolution in ferroelectric materials: a continuum phase field model and finite element implementation. *Computational Methods in Applied Mechanics and Engineering* 2007; **196**: 4365–4374.
44. Smith RC, Dapino MJ, Seelecke S. Free energy model for hysteresis in magnetostrictive transducers. *Journal of Applied Physics* 2003; **93**:458–466.
45. Linnemann K, Klinkel S. A constitutive model for magnetostrictive materials—theory and finite element implementation. *PAMM Proceedings in Applied Mathematics and Mechanics*, Berlin, vol. 6, 2006; 393–394.
46. James RD, Wuttig M. Magnetostriction of martensite. *Philosophical Magazine A* 1998; **77**:1273–1299.
47. O'Handley RC. Model for strain and magnetization in magnetic shape-memory alloys. *Journal of Applied Physics* 1998; **83**:3263–3270.
48. Likhachev AA, Ullakko K. Magnetic-field-controlled twin boundaries motion and giant magneto-mechanical effects in Ni–Mn–Ga shape memory alloy. *Physics Letters A* 2000; **275**:142–151.
49. Hirsinger L, Lexcellent C. Modelling eetwinning of martensite platelets under magnetic and (or) stress actions on NiMnGa alloys. *Journal of Magnetism and Magnetic Materials* 2003; **254–255**:275–277.
50. Kiefer B, Lagoudas DC. Magnetic field-induced martensitic variant reorientation in magnetic shape memory alloys. *Philosophical Magazine*, *Special Issue*: *Recent Advances in Theoretical Mechanics* 2005; **85**:4289–4329.
51. Allik H, Hughes TJR. Finite element method for piezoelectric vibration. *International Journal for Numerical Methods in Engineering* 1970; **2**:151–157.
52. Benjeddou A. Advaces in piezoelectric finite element modeling of adaptive structural elements: a survey. *Journal of Computers and Structures* 2000; **76**:347–363.
53. Klinkel S, Wagner W. A piezoelectric solid shell element based on a mixed variational formulation for geometrically linear and nonlinear applications. *Computers and Structures* 2008; **86**:38–46.
54. Kamlah M, Liskowsky CA, McMeeking RM, Balke H. Finite element simulation of a polycrystalline ferroelectric based on a multidomain single crystal switching model. *International Journal of Solids and Structures* 2005; **42**:2949–2964.
55. Elhadrouz M, Zineb BT, Patoor E. Finite element analysis of a multilayer piezoelectric actuator taking into account the ferroelectric and ferroelastic behaviours. *International Journal of Engineering Science* 2006; **44**:996–1006.
56. Landis CM. A new Finite elemnt formulation for electromechanical boundary value problems. *International Journal for Numerical Methods in Engineering* 2002; **55**:613–628.

Copyright © 2011 John Wiley & Sons, Ltd.

DOI: 10.1002/nme

57. Semenov AS, Kessler H, Liskowsky A, Balke H. On a vector potential formulation for 3D electromechanical finite element analysis. *Communication in Numerical Methods in Engineering* 2006; **22**:357–375.
58. Ghandi K, Hagood NW. A hybrid finite-element model for phase transition in nonlinear electro-mechanically coupled material. *Mathematics and Control in Smart Structures*, *Proceedings*, vol. 3039. SPIE: Bellingham, 1997; 97–112.
59. Semenov AS, Liskowsky AC, Balke H. Return mapping algorithms and consistent tangent operators in ferroelectroelasticity. *International Journal for Numerical Methods in Engineering* 2009; **81**:1298–1340.
60. DeSimone A, James RD. A constrained theory of magnetoelasticity. *Journal of the Mechanics and Physics of Solids* 2002; **50**:283–320.
61. Simó JC, Honein T. Variational formulation, discrete conservation laws, and path-domain independent integrals for elasto-viscoplasticity. *Journal of Applied Mechanics* 1990; **57**:488–497.
62. Ortiz M, Stainier L. The variational formulation of viscoplastic constitutive updates. *Computer Methods in Applied Mechanics and Engineering* 1999; **171**:419–444.
63. Miehe C. Strain-driven homogenization of inelastic microstructures and composites based on an incremental variational formulation. *International Journal for Numerical Methods in Engineering* 2002; **55**:1285–1322.
64. Carstensen C, Hackl K, Mielke A. Non-convex potentials and microstructures in finite-strain plasticity. *Proceedings of the Royal Society London A* 2002; **458**:299–317.
65. Miehe C, Schotte J, Lambrecht M. Homogenization of inelastic solid materials at finite strains based on incremental minimization principles. Application to the texture analysis of polycrystals. *Journal of the Mechanics and Physics of Solids* 2002; **50**:2123–2167.
66. Miehe C, Lambrecht M, Gürses E. Analysis of material instabilities in inelastic solids by incremental energy minimization and relaxation methods: evolving deformation microstructures in finite plasticity. *Journal of the Mechanics and Physics of Solids* 2004; **52**:2725–2769.
67. Biot MA. *Mechanics of Incremental Deformations*. Wiley: New York, 1965.
68. Ziegler H. Some extremum principles in irreversible thermodynamics with application to continuum mechanics. In *Progress in Solid Mechanics*, Sneddon IN, Hill R (eds), vol. IV. Springer: Berlin, Heidelberg, 1963.
69. Germain P. *Cours de Mécanique des Milieux Continus*. Masson et Cie: Paris, 1973.
70. Halphen B, Nguyen QS. Sur les matéraux standards généralisés. *Journal de Mécanique* 1975; **14**:39–63.
71. Mielke A, Timofte AM. An energetic material model for time-dependent ferroelectric behavior: existence and uniqueness. *Mathematical Methods in the Applied Sciences* 2006; **29**:1393–1410.
72. Hill R. A general theory of uniqueness and stability in elastic-plastic solids. *Journal of the Mechanics and Physics of Solids* 1958; **6**:236–249.
73. Petryk H. Material instability and strain-rate discontinuities in incrementally nonlinear continua. *Journal of the Mechanics and Physics of Solids* 1992; **40**:1227–1250.
74. Nguyen QS. *Stability and Nonlinear Solid Mechanics*. Wiley: New York, 2000.
75. Miehe C, Lambrecht M. Analysis of microstructure development in shearbands by energy relaxation of incremental stress potentials: large-strain theory for standard dissipative solids. *International Journal for Numerical Methods in Engineering* 2003; **58**:1–41.
76. Hill R. *The Mathematical Theory of Plasticity*. Oxford University Press: Oxford, 1950.
77. Maugin GA. *The Thermomechanics of Plasticity and Fracture*. Cambridge University Press: Cambridge, 1992.
78. Han W, Reddy BD. *Plasticity*: *Mathematical Theory and Numerical Analysis*. Springer: New York, 1999.
79. Simó JC. Numerical analysis of classical plasticity. In *Handbook for Numerical Analysis*, Ciarlet PG, Lions JJ (eds). Elseiver: Amsterdam, 1998; 183–499.
80. Simó JC, Hughes TJR. *Computational Inelasticity*. Springer: New York, 1998.
81. Armero F, Perez-Foguet A. On the formulation of closest-point projection algorithms in elastoplasticity. Part I: the variational structure. *International Journal for Numerical Methods in Engineering* 2002; **53**:297–329.
82. Boehler JP. Applications of tensor functions in solid mechanics. *CISM Courses and Lectures*, vol. 292. Springer: Berlin, 1987.
83. Kamlah M. Ferroelectric and ferroelastic piezoceramics- modelling of electromechanical hysteresis phenomena. *Continuum Mechanics and Thermodynamics* 2001; **13**:219–268.
84. Perzyna P. Fundamental problems in viscoplasticity. *Advances in Applied Mechanics* 1966; **9**:243–377.
85. Rockafellar RT. A genaral correspondence between dual minimax problems and convex programs. *Pacific Journal of Mathematics* 2003; **25**:597–611.

Copyright © 2011 John Wiley & Sons, Ltd.

DOI: 10.1002/nme